DOCTORAL THESIS

Assessment of Electroencephalographic Measures Applied in the Detection of Depression

Laura Päeske

TALLINNA TEHNIKAÜLIKOOL
TALLINN UNIVERSITY OF TECHNOLOGY
TALLINN 2021

TALLINN UNIVERSITY OF TECHNOLOGY
DOCTORAL THESIS
17/2021

Assessment of Electroencephalographic Measures Applied in the Detection of Depression

LAURA PÄESKE

TAL TECH PRESS

TALLINN UNIVERSITY OF TECHNOLOGY
School of Information Technologies, Department of Health Technologies
Curriculum: School of Science
This dissertation was accepted for the defence of the degree 22/02/2021

Supervisor: Prof. Maie Bachmann, PhD
School of Information Technologies
Tallinn University of Technology
Tallinn, Estonia

Co-supervisor: Prof. Jaan Raik, PhD
School of Information Technologies
Tallinn University of Technology
Tallinn, Estonia

Opponents: Dr. Milena Čukić Radenković, PhD
Institute of Knowledge Technology
Complutense University of Madrid
Madrid, Spain

Prof. Lauri Parkkonen, PhD
Department of Neuroscience and Biomedical Engineering
Aalto University
Espoo, Finland

Defence of the thesis: 23/03/2021, Tallinn

Declaration:
Hereby I declare that this doctoral thesis, my original investigation and achievement, submitted for the doctoral degree at Tallinn University of Technology has not been submitted for doctoral or equivalent academic degree.
Laura Päeske

---
signature

European Union
European Regional
Development Fund

Investing
in your future

ISSN 2585-6898 (publication)
ISBN 978-9949-83-676-5 (publication)
ISSN 2598-6901 (PDF)
ISBN 978-9949-83-677-2 (PDF)
Printed by Auratrükk

TALLINNA TEHNIKAÜLIKOOL
DOKTORITÖÖ
17/2021

Depressiooni avastamiseks kasutatavate elektroentsefalograafilise signaali mõõdikute analüüs

LAURA PÄESKE

TAL TECH KIRJASTUS

Contents

List of Publications

The current thesis is based on the following publications referred to in the text by their Roman numerals I–III:

I Bachmann, M., **Päeske, L**., Kalev, K., Aarma, K., Lehtmets, A., Ööpik, P., Lass, J., & Hinrikus, H. (2018). Methods for classifying depression in single channel EEG using linear and nonlinear signal analysis. *Computer Methods and Programs in Biomedicine, 155*, 11−17. doi: 10.1016/j.cmpb.2017.11.023

II **Päeske, L.**, Hinrikus, H., Lass, J., Raik, J., & Bachmann, M. (2020). Negative correlation between functional connectivity and small-worldness in the alpha frequency band of a healthy brain. *Frontiers in Physiology, 11*, 910. doi: 10.3389/fphys.2020.00910

III **Päeske, L.**, Bachmann, M., Põld, T., de Oliveira, S. P. M., Lass, J., Raik, J., & Hinrikus, H. (2018). Surrogate Data Method Requires End-Matched Segmentation of Electroencephalographic Signals to Estimate Non-linearity. *Frontiers in Physiology, 9*, 1350. doi: 10.3389/fphys.2018.01350

Author's Contribution to the Publications

The contribution by the author to the papers included in the thesis is as follows (Publications I–III):

I Participating in the electroencephalography (EEG) recordings, partly processing the data with MATLAB, advising and partly writing the code for statistical analysis, participating in analyzing and interpreting the results, and moderately revising the manuscript.

II Idea of the study, participating in the EEG recordings, entire data processing with MATLAB, entire statistical analysis, major part in analyzing and interpreting the results, and writing the entire manuscript.

III Partly idea of the study, participating in the EEG recordings, entire data processing with MATLAB, entire statistical analysis, major part in analyzing and interpreting the results, and a major part in writing the manuscript.

Introduction

Depression is the leading cause of disability worldwide and a major contributor to the global burden of disease (WHO, 2020). Moreover, the burden of depression and other mental disorders is rising globally (WHO, 2019; WHO, 2020). The current COVID-19 pandemic has further increased depression symptoms in the general population (Ettman et al., 2020; Salari et al., 2020; Bäuerle et al., 2020). The long-term impact of the pandemic on mental health is yet unknown and can possibly have even more severe consequences (Troyer et al., 2020).

Currently, the diagnosis of depression is based on an evaluation of the intensity of subjective symptoms using clinical interviews and psychiatric questionnaires. The subjective assessment has led to remarkably frequent over- and underdiagnosis of depression (Aragonès et al., 2006; Mitchell et al., 2009; Rettew et al., 2009; WHO, 2020).

Objective markers in routine testing could imply signs of depression in an early stage to assist doctors in the early detection of depression or in the depression diagnosis. The US Preventive Services Task Force has recommended screening for depression in the general population, bringing out that the benefits overweigh the downsides (Siu et al., 2016). Furthermore, a scientific objective assessment of depression can help in clustering subjects for the development of specific therapeutics or track antidepressant efficiency (Bilello, 2016). Therefore, an inexpensive and easy methodology based on objective measures is required.

The current thesis provides novel knowledge about the objective electroencephalography (EEG) measures applied in the classification between subjects with depression and healthy subjects. I compare EEG measures in depression detection, taking into account that EEG measures in clinical practice should accurately discriminate depression, be simple, and have a low computational load. In **Publication I**, three linear and three nonlinear single-channel EEG measures are compared in the classification between major depressive disorder (MDD) and healthy subjects. To the best of my knowledge, **Publication I** is the first to investigate the applicability of the EEG single-channel analysis in the classification between subjects with depression and healthy subjects compared to the EEG multi-channel analysis in previous studies. In addition, I examine whether nonlinear measures provide higher accuracy in the classification compared to linear EEG measures and compare the EEG channel regions in the classification between MDD and healthy subjects.

As MDD has been associated with disruptions in brain neural networks (Wang et al., 2012), the complex network analysis is expected to provide valuable input to depression classification. Functional connectivity (FC) and small-worldness (SW) describe two different aspects of an EEG functional network and have been previously used in the classification between MDD and healthy subjects (Leuchter et al., 2012; Mumtaz et al., 2017; Orgo et al., 2017). However, the relationship between EEG FC and SW has not been studied before, neither for healthy nor for depressed subjects. Therefore, **Publication II** is the first study to analyze the relationship between resting-state EEG alpha FC and SW for healthy subjects. Furthermore, the current thesis presents novel results about the relationship between alpha FC and SW for subjects with MDD.

The surrogate data method was developed to estimate nonlinearity in time series and has been previously used in the EEG studies of depression (Lee et al., 2007; Zuchowicz et al., 2019; Puthankattil, 2020). However, false detection of nonlinearity may occur in

case the data are strongly cyclic and the data segment does not comprise full periods of the dominant cyclic component (Stam et al., 1998; Small & Tse, 2002). The influence of the EEG segment end-mismatch on the surrogate data has not been studied before and the dominant frequency component is not considered in segmentation. Therefore, **Publication III** is the first study to examine the extent of an EEG segment end-mismatch on the results of the surrogate data method. The impact of the EEG alpha frequency component on the results of the surrogate data method is clarified in the case of resting-state EEG signals.

Aims of the thesis

The thesis aims to assess different aspects of resting-state EEG measures for the purpose of an objective marker to discriminate between healthy and depressed subjects. More specifically, the aims of the thesis are:

1. Compare EEG measures in depression detection (**Publication I**).
2. Compare EEG channel regions in depression detection (**Publication I**).
3. Find the relationship between EEG alpha FC and SW for healthy subjects and subjects with MDD (**Publication II**).
4. Clarify the impact of an EEG alpha frequency component on the results of the surrogate data method (**Publication III**).

Other Related Publications

- Põld, T., **Päeske, L**., Hinrikus, H., Lass, J., & Bachmann, M. (2021). Long-term stability of resting state EEG-based linear and nonlinear measures. *International Journal of Psychophysiology, 159*, 83−87. doi: 10.1016/j.ijpsycho.2020.11.013
- Uudeberg, T., **Päeske, L**., Põld, T., Lass, J., Hinrikus, H., & Bachmann, M. (2020). Long-Term Stability of EEG Spectral Asymmetry Index – Preliminary Study. In: Henriques J., Neves N., de Carvalho P. (eds) XV Mediterranean Conference on Medical and Biological Engineering and Computing – MEDICON 2019. MEDICON 2019. *IFMBE Proceedings, 76*. Springer, Cham. doi: 10.1007/978-3-030-31635-8_33
- Põld, T., **Päeske, L**., Bachmann, M., Lass, J., & Hinrikus, H. (2019). Assessment of Objective Symptoms of Depression in Occupational Health Examination. *Journal of Occupational and Environmental Medicine, 61*(7), 605−609. doi: 10.1097/JOM.0000000000001622
- **Päeske, L**., Bachmann, M., Raik, J., & Hinrikus, H. (2019). EEG Functional Connectivity Detects Seasonal Changes. In: Lhotska L., Sukupova L., Lacković I., Ibbott G. (eds) World Congress on Medical Physics and Biomedical Engineering 2018. *IFMBE Proceedings, 68/2*. Springer, Singapore. doi: 10.1007/978-981-10-9038-7_44
- Põld, T., Bachmann, M., **Päeske, L**., Kalev, K., Lass, J., & Hinrikus, H. (2019). EEG Spectral Asymmetry Is Dependent on Education Level of Men. In: Lhotska L., Sukupova L., Lacković I., Ibbott G. (eds) World Congress on Medical Physics and Biomedical Engineering 2018. *IFMBE Proceedings, 68/2*. Springer, Singapore. doi: 10.1007/978-981-10-9038-7_76

- Põld T., Bachman M., **Orgo L**., Kalev K., Lass J., & Hinrikus H. (2018). EEG Spectral Asymmetry Index Detects Differences Between Leaders and Non-leaders. In: Eskola H., Väisänen O., Viik J., Hyttinen J. (eds) EMBEC & NBC 2017. EMBEC 2017, NBC 2017. *IFMBE Proceedings, 65*. Springer, Singapore. doi: 10.1007/978-981-10-5122-7_5
- **Orgo, L**., Bachmann M., Kalev K., Järvelaid M., Raik J., & Hinrikus H. (2018). Dependence of the EEG Nonlinear Coupling on the Frequency Bands and the Segment Lengths. In: Eskola H., Väisänen O., Viik J., Hyttinen J. (eds) EMBEC & NBC 2017. EMBEC 2017, NBC 2017. *IFMBE Proceedings, 65*. Springer, Singapore. https://doi.org/10.1007/978-981-10-5122-7_200
- **Orgo, L**., Bachmann, M., Kalev, K., Järvelaid, M., Raik, J., & Hinrikus, H. (2017). Resting EEG Functional Connectivity and Graph Theoretical Measures for Discrimination of Depression. *2017 IEEE EMBS International Conference on Biomedical & Health Informatics*, Orlando, FL, 389−392. doi: 10.1109/BHI.2017.7897287
- **Orgo, L**., Bachmann, M., Kalev, K., Järvelaid, M., & Hinrikus, H. (2016). Brain Functional Connectivity in Depression: Gender Differences in EEG. *IEEE EMBS Conference on Biomedical Engineering and Science*, Kuala Lumpur, Malaysia, 270−273. doi: 10.1109/IECBES.2016.7843456
- **Orgo, L**., Bachmann, M., Lass, J., & Hinrikus, H. (2015). Effect of Negative and Positive Emotions on EEG Spectral Asymmetry. *Annu Int Conf IEEE Eng Med Biol Soc, 2015*, 8107-8110 . doi: 10.1109/EMBC.2015.7320275
- Kalev, K., Bachmann, M., **Orgo, L**., Lass, J., & Hinrikus, H. (2015). Lempel-Ziv and Multiscale Lempel-Ziv Complexity in Depression. *Annu Int Conf IEEE Eng Med Biol Soc, 2015*, 4158-4161. doi: 10.1109/EMBC.2015.7319310

Abbreviations

APV	alpha power variability
C	clustering coefficient
C_{norm}	normalized clustering coefficient
DEG	degree of nonlinearity
DFA	detrended fluctuation analysis
EBC	edge betweenness centrality
EC	eyes closed (recording condition)
EEG	electroencephalography
EO	eyes open (recording condition)
FAA	frontal alpha asymmetry
FC	functional connectivity
fMRI	functional magnetic resonance imaging
HFD	Higuchi fractal dimension
ICOH	imaginary part of coherency
KEFB-CSP	kernel eigen-filter-bank common spatial pattern
KFD	Katz fractal dimension
L	characteristic path length
L_{norm}	normalized characteristic path length
LZC	Lempel-Ziv complexity
MDD	major depressive disorder
MEG	magnetoencephalography
MRI	magnetic resonance imaging
MSC	magnitude-squared coherence
NBC	node betweenness centrality
PET	positron emission tomography
REST	reference electrode standardization technique
RGP	relative gamma power
SampEn	sample entropy
SASI	spectral asymmetry index
SL	synchronization likelihood
SW	small-worldness

1 Literature Review

1.1 Searching for objective markers

Several markers have been analyzed with the aim to objectively discriminate between subjects with depression and healthy subjects. I will be focusing on the most frequent and promising techniques. Firstly, discriminative biomarkers have been searched from omics such as genomics, transcriptomics, metabolomics, and proteomics (Bilello, 2016; Mora et al., 2018). Some previous studies have obtained good classification between MDD and healthy subjects (Papakostas et al., 2013; Bilello et al., 2015). However, no biomarker-based method has proven to have sufficiently high specificity, sensitivity, and reproducibility for clinical settings (Bilello, 2016; Mora et al., 2018). Omics data is noisy and often with low reproducibility, caused, for example, by data changes over time within a system and differences in sample preparation protocols between studies (Ning & Lo, 2010). Furthermore, because of invasive sampling, omics biomarkers are difficult to apply in depression screening.

Secondly, some studies have also analyzed audio-visual data to differentiate between subjects with depression and healthy subjects and although further research is needed, studies have found promising results (Williamson et al., 2014; Solomon et al., 2015). The shortcoming of audio-visual data is the dependence on ethnocultural characteristics, as well as gender (Wang et al., 2019a) and other possible characteristics such as smoking habits (Solomon et al., 2015). Another question is the deception-proofness of the system. Solomon et al. 2015 found that most acoustic features that were found to be significantly different between subjects with depression and healthy subjects during normal behavior remained so during concealed behavior. However, only 9 subjects with depression and 8 healthy subjects participated and multiple comparisons of 98 statistically tested features were not considered. Therefore, further research is needed.

Thirdly, neuroimaging techniques are most widely used in the classification between subjects with depression and healthy subjects. These techniques include EEG, magnetoencephalography (MEG), magnetic resonance imaging (MRI), and positron emission tomography (PET). EEG has been commonly used in the classification between depressed and control subjects with high classification accuracies (Table 4 in Appendix 1). Furthermore, the review by Gao et al. (2018) showed that MRI techniques, functional MRI (fMRI), structural MRI (sMRI), and diffusion tensor imaging (DTI) have also been widely studied and have shown high accuracy in the classification between healthy subjects and subjects with depression. Some studies have also used MEG (Lu et al., 2013; Lu et al., 2014) or PET (Kautzky et al., 2017), but those techniques have not been used as widely as MRI or EEG. Although MEG and MRI are non-invasive and have a good spatial resolution, these devices are expensive and non-portable (Parkkonen, 2014; Scarapicchia et al., 2017), and therefore unreasonable for screening depression in clinical applications. EEG is both non-invasive and cost-effective, being a promising neuroimaging technique for clinical settings. Furthermore, the long-term stability of EEG measures supports their reliability (Põld et al., 2021). Accordingly, EEG is used in the current thesis.

1.2 Classification between subjects with depression and healthy subjects using EEG

Several resting-state EEG studies have used machine learning methods to classify healthy subjects and subjects with depression (Table 4 in Appendix 1). EEG power has been used as the most frequent machine learning feature in different studies. While some studies have reported alpha power to give the best results (Mohammadi et al., 2015; Liao et al., 2017; Lee et al., 2018; Mahato & Paul, 2020), other studies have found delta, theta, beta, or gamma power to give better results than alpha power (Knott et al., 2001; Cai et al., 2018). Furthermore, Mohammadi et al. (2015) found the best results with eyes open (EO) delta power if linked mastoids was used as a reference and eyes closed (EC) alpha power if EEG channel CZ was used as a reference. This result shows that the choice of the reference and recording conditions can have great influence on the results. While some studies have found best results with the power of different frequency bands, other studies have found interhemispheric alpha asymmetry (Mumtaz et al., 2017) or detrended fluctuation analysis (DFA), Higuchi fractal dimension (HFD), correlation dimension, and Lyapunov exponent (Hosseinifard et al., 2013) to give higher accuracy compared to power in the classification between subjects with depression and healthy subjects. In addition, several other EEG measures have been reported to classify better between healthy and depressed subjects than other EEG measures analyzed in these studies: theta asymmetry (Mahato & Paul, 2020), sample entropy (SampEn) (Čukić et al., 2020b), network measures node betweenness centrality (NBC) and clustering coefficient (C) (Sun et al., 2019), absolute center frequency of the beta wave (Cai et al., 2018), synchronization likelihood (SL) (Mumtaz et al., 2018), spectral asymmetry index (SASI) (Bachmann et al., 2017), kernel eigen-filter-bank common spatial pattern (KEFB-CSP) (Liao et al., 2017), and HFD in the beta frequency band (Ahmadlou et al., 2012).

In addition to the EEG measures, the choice of EEG channels is also important in discriminating depression. Most significant results have been found from frontal (Knott et al., 2001; Ahmadlou et al., 2012; Mohammadi et al., 2015; Mumtaz et al., 2017; Acharya et al., 2018; Mumtaz et al., 2018), temporal (Hosseinifard et al., 2013; Liao et al., 2017; Mumtaz et al., 2018; Sun et al., 2019) and posterior (Hosseinifard et al., 2013; Mohammadi et al., 2015; Mumtaz et al., 2018) regions (Table 4 in Appendix 1). However, the comparisons between studies are complicated, because the most significant brain regions are dependent on the EEG measure, the results depend on the choice of the reference, and some studies do not include all brain regions in their analysis (Knott et al., 2001; Ahmadlou et al., 2012; Acharya et al., 2018; Cai et al., 2018).

Based on the previous resting-state EEG studies, it is unclear which measures and channels best discriminate between depressed and healthy subjects. A wide range of different EEG measures has been used across studies and therefore the comparison between the measures is complicated. Furthermore, there is a wide range of variables that could influence the results and cause inconsistencies between studies, such as the choice of the subjects, EEG acquisition, and signal preprocessing. Several studies have reported that a combination of different EEG measures gave the highest classification accuracy (Table 4 in Appendix 1). Interestingly, the measure combinations giving the highest accuracy may not coincide with the measures with the highest group differences (Knott et al., 2001), meaning that combining different measures may give new perspectives. Nevertheless, no EEG measure or a combination of measures has been

consistently reported to be the best in discriminating between healthy and depressed subjects.

For an EEG application for depression screening in clinical practice, simplicity is important. Firstly, the number of EEG channels should be as low as possible. Several EEG measures successfully applied in the classification between subjects with depression and healthy subjects are calculated for an EEG signal from a single EEG channel, such as EEG power, DFA, HFD, and correlation dimension (Table 4 in Appendix 1). On the other hand, some measures require multiple channels, such as inter- and intrahemispheric asymmetry, FC, and graph theoretical measures. Discrimination of depression based on a single-channel EEG signal analysis has been considered in a few studies (Bachmann et al., 2013; Bachmann et al., 2017; Acharya et al., 2018; Lee et al., 2018). However, it is unclear whether single-channel EEG measures can provide as good discrimination between healthy subjects and subjects with depression as multi-channel EEG measures and whether using a single EEG channel would be sufficient.

Secondly, the computational load of chosen EEG measures should be low. Generally, linear EEG measures are computationally less expensive. However, if nonlinear measures provide significantly better classification accuracy between healthy and depressed subjects, nonlinear measures should be chosen instead. On the one hand, previous studies have reported nonlinear properties of EEG signals (Rubinov et al., 2009; Bae et al., 2017; Lei et al., 2017; Puthankattil, 2020) and nonlinear measures can detect nonlinear information that linear measures cannot. On the other hand, linear measures are faster to compute, more robust to noise, and can perform as well as nonlinear measures in some cases (Netoff et al., 2006; Bastos & Schoffelen, 2016; Cai et al., 2018). Therefore, the comparison between linear and nonlinear EEG measures in the classification between healthy and depressed subjects is required.

1.3 Graph theoretical analysis

Over the last decade, EEG FC and functional network analysis have gained much interest, due to the ability to estimate interactions between signals from different brain regions and topological properties of an EEG functional network. As MDD has been associated with disruptions in brain neural networks (Wang et al., 2012), FC and graph theory are expected to provide valuable input to depression classification. Calculating FC requires at least two channels, while graph theory measures require full-head EEG. Therefore, FC and graph theory measures could be considered for discriminating depression in clinical practice if they provide significantly higher classification accuracy compared to single-channel EEG measures.

EEG signals can be analyzed using complex network analysis. A graph is constructed by computing FC between EEG signals, obtaining a connectivity matrix. Weak connections are removed by thresholding the FC values: an edge exists only if the value of FC is higher than the threshold. For proportional thresholds, a percentage of the highest FC values is kept. The small-world organization has been widely applied to study complex brain networks. A network has small-world properties when it has higher functional segregation and similar functional integration than a random network (Rubinov & Sporns, 2010). The measures of C and local efficiency are used to describe functional segregation and characteristic path length (L) and global efficiency are used to describe functional integration of an EEG network. A measure of SW estimates the trade-off between functional integration and segregation in a single statistic (Humphries & Gurney, 2008).

Previous EEG studies have shown that FC could be a promising marker to discriminate depression (Knott et al., 2001; Fingelkurts et al., 2007; Leuchter et al., 2012; Olbrich et al., 2014; Li et al., 2017; Zhang et al., 2018; Shim et al., 2018). MDD has been mostly characterized by increased FC in the theta and alpha frequency bands. Olbrich et al. (2014) reported increased prefrontal lagged phase synchronization for MDD patients in the alpha frequency band. Fingelkurts et al. (2007) found that EEG structural synchrony was positively correlated with the severity of depression in the alpha and theta frequency bands. According to Li et al. (2017), MDD subjects have increased coherence in the theta frequency band and Leuchter et al. (2012) found significantly increased coherence in the delta, theta, alpha, and beta frequency bands. However, some studies have also found a significant decrease in FC for subjects with MDD (Knott et al., 2001; Zhang et al., 2018; Shim et al., 2018). Knott et al. (2001) found decreased inter-hemispheric coherence in the delta, theta, alpha, and beta frequency bands. Shim et al. (2018) found a decrease in the phase-locking value (PLV) in the theta and alpha frequency bands. Zhang et al. (2018) also found a decrease in the FC, estimated by Pearson correlation coefficients of power spectral density, in the alpha frequency band.

Several studies have used topological measures describing small-world properties of an EEG functional network, as well as other functional network measures to study depression (Li et al., 2017; Orgo et al., 2017; Zhang et al., 2018; Shim et al., 2018; Sun et al., 2019). Mostly, randomization of functional networks is found for the subjects with depression. Li et al. (2017) calculated leaf fraction, the mean weight of the minimum spanning tree, and hierarchical clustering in the theta frequency band because the difference in coherence between MDD and control subjects was more evident in the theta band than in the alpha and beta bands. For the group of MDD subjects, they found increased leaf fraction and mean weight, indicating a more random functional network structure in MDD. They also found lower clustering in the frontal regions. Sun et al. (2019) calculated L, C, edge betweenness centrality, NBC, and modularity in the theta and alpha frequency bands. In the theta frequency band, they found significant differences in L, edge betweenness centrality (EBC), and NBC between subjects with MDD and healthy subjects. However, depending on the binarization technique, these measures were decreased or increased in MDD. In the alpha frequency band, they found decreased L, C, EBC, NBC, and modularity for MDD, revealing randomization in functional networks. Zhang et al. (2018) calculated C, normalized clustering coefficient ($\mathrm{C_{norm}}$), L, normalized characteristic path length ($\mathrm{L_{norm}}$), global and local efficiency, power law exponent, exponential cutoff, resilience, size of the largest component, and the rich-club coefficient for the alpha frequency band. Only the alpha band was chosen because the correlation matrix density was significantly different in that frequency band between MDD and control groups. They found that MDD subjects had decreased C, $\mathrm{L_{norm}}$, L, local efficiency, exponential cutoff, and rich-club coefficient and increased global efficiency, power law exponent, and the size of largest component. These alterations again indicate a shift towards a more random network topology. Shim et al. (2018) found decreased C in the theta and alpha frequency bands, decreased efficiency in the alpha band, and increased path length in the alpha band for MDD subjects. In our previous study, we investigated whether adding the EEG features of graph theoretical measures L, C, and SW to the features of coherence would increase the classification accuracy between healthy subjects and subjects with depression (Orgo et al., 2017). As a result, no significant increase was found.

FC and graph theory measures complement each other by describing different aspects of the functional network. When alterations in FC and graph theory measures in a mental disorder are analyzed, the relationship between FC and graph theory measures is also important to know. However, to the best of my knowledge, the relationship between EEG FC and graph theory measures has not been studied before, neither for healthy nor for depressed subjects.

1.4 Surrogate data method

The multivariate surrogate data method (Theiler et al., 1992; Prichard & Theiler, 1994) has been widely used for different EEG applications, including studying depression (Lee et al., 2007; Zuchowicz et al., 2019; Puthankattil, 2020). The surrogate data method was introduced by Theiler et al. (1992) for nonlinearity testing in time series and is therefore often used for nonlinearity testing in the EEG time series (Breakspear & Terry, 2002; Natarajan et al., 2004; Lee et al., 2007; Bae et al., 2017; Lei et al., 2017; Orgo et al., 2018; Puthankattil, 2020). The null hypothesis that data were generated by a linear process and therefore data can be fully explained by a linear model, is set. Surrogate data is generated from original data by taking the Fourier transform, rotating the phase of each frequency, and taking the inverse Fourier transform. The null hypothesis is rejected if the nonlinear statistics calculated for original and surrogate data are significantly different.

In addition to nonlinearity testing, the surrogate data method has been widely used to analyze different aspects of EEG signals. In the current thesis, I focus on studies where the surrogate data method is used in applications also applicable in classifying between depressed and healthy subjects. These applications include EEG preprocessing and the calculation of different measures. Firstly, Chavez et al. (2018) used the surrogate data method for artifact removal from an EEG signal. Secondly, some studies have used the surrogate data method to determine the statistical threshold of connectivity values in the network analysis. Dimitriadis et al. (2015) calculated global and local efficiency to compare subjects with mild traumatic brain injury and control subjects. Olejarczyk et al. (2017) used the surrogate data method in the network analysis to calculate degree, strength, local efficiency, betweenness centrality, density, L, C, and global efficiency to analyze the effects between eyes open and eyes closed conditions. Zuchowicz et al. (2018) calculated network strength and degree to study the effects of repetitive transcranial magnetic stimulation (rTMS) treatment on MDD and bipolar disorder patients. Thirdly, some studies have used EEG measures calculated for original and surrogate data to compare subject groups or different conditions. Nicolaou et al. (2017) removed insignificant imaginary part of coherency (ICOH) values using the surrogate data method before calculating average ICOH values to compare the EEG in response to music stimuli played at four different tempi. Wang et al. (2019b) calculated original and surrogate values of SampEn to compare subjects with Alzheimer's disease and healthy subjects. Alonso et al. (2010) compared cross mutual information for the surrogate data and the difference between the cross mutual information calculated for the original and surrogate data to evaluate the pharmacological effects of alprazolam.

Although the surrogate data method has been widely used for EEG analysis, these studies do not take into account the EEG segment end-mismatch while applying the surrogate data method. Stam et al. (1998) and Small and Tse (2002) brought out that a false detection of nonlinearity may occur with the surrogate data method if the data are strongly cyclic and the length of the analyzed signal segment does not comprise full periods of the dominant cyclic component. This problem can be explained by the spectral

leakage in the discrete Fourier transform. Thornhill (2005) showed that even a small segment end-mismatch could cause false detection of nonlinearity for sine waves. However, they showed that pseudoperiodic data with less regular cycles were more robust to small end-mismatches.

In the eyes-closed resting state, EEG is generally characterized by dominant alpha frequency rhythm, especially in the posterior regions. However, the influence of the EEG cyclic alpha component on the surrogate data method has not been studied before. Therefore, the impact of the EEG alpha frequency component on the results of the surrogate data method needs to be clarified.

2 Methods

2.1 Subjects

The study group of **Publication I** consisted of 13 subjects with MDD and 13 healthy subjects without any history of depression. Healthy subjects were chosen to match MDD subjects according to age, sex, and handedness. Both groups consisted of 5 male and 8 female subjects with a mean age of 38.7 years and a standard deviation of 15.8 years. Subjects with MDD were referred by psychiatrists or family physicians and EEG recordings were made before starting with the treatment.

The study group of **Publication II** and **Publication III** consisted of 80 healthy subjects**.** Out of all subjects, 38 were female and 42 were male. The mean age was 37.0 years and the standard deviation was 14.5 years. In addition, in the current thesis, the results of 13 subjects with MDD were added to the results of healthy subjects from **Publication II**.

The subjects were asked to abstain from alcohol 24 hours and from coffee two hours prior to the EEG recording. The studies were conducted in accordance with the Declaration of Helsinki and were approved by the Tallinn Medical Research Ethics Committee. Informed consent was obtained from each subject before participating in the study.

2.2 EEG recordings and preprocessing

EEG signals were recorded using the Neuroscan Synamps2 acquisition system (Compumedics, NC, USA) from 30 electrodes (Fp1, Fp2, F7, F3, Fz, F4, F8, FT7, FC3, FCz, FC4, FT8, T7, C3, Cz, C4, T8, TP7, CP3, CPz, CP4, TP8, P7, P3, Pz, P4, P8, O1, Oz, O2). EEG electrodes were positioned according to the extended international 10-20 system and linked mastoids was used as the reference. Furthermore, horizontal and vertical electrooculograms were recorded to monitor eye movements.

The duration of the resting-state EEG recordings was between 7 and 30 minutes and the sampling rate was 1000 Hz. During the recordings, the subjects were lying in a relaxed position with their eyes closed. The room was dimly lit and electrically shielded. In addition, earplugs were used to minimize any disturbances.

The data were analyzed using MATLAB (The Mathworks, Inc.) and MATLAB toolboxes Brain Connectivity Toolbox (Rubinov & Sporns, 2010) and HERMES (Niso et al., 2013). The EEG signals were digitally filtered at the cutoff frequencies of 0.5 Hz and 46 Hz in **Publication I**, 8 Hz and 12 Hz into alpha frequency band in **Publication II** and 1 Hz and 45 Hz in **Publication III**. The sampling frequency was reduced to 200 Hz in **Publication II** to reduce the computation time of FC measures. The length of data segments also differed between publications: 10 seconds (10 000 samples) in **Publication I**, 20.48 seconds (4096 samples) in **Publication II**, and 5.3 seconds (5300 samples) in **Publication III**. The actual length of segments in **Publication III** depended on the frequency of dominant alpha waves. All segments were visually inspected and segments with ocular, muscular, or other artefacts were removed.

In **Publications II** and **III**, the signals were re-referenced according to the reference electrode standardization technique (REST) (Yao, 2001). Previous studies have brought out that REST has a good performance even for low-density EEG montages and may be a good reference technique to compare results from different research labs. (Qin et al., 2010; Huang et al., 2017). In **Publication I**, the reference remained the average of mastoids, as initially recorded.

2.3 Measures of EEG

A wide selection of EEG measures was calculated throughout the publications presented in the current thesis. A summary of these measures is given in Table 1.

Table 1. EEG measures used in the thesis.

	Measure	Usage in publications	Estimates
Nonlinear measures	Higuchi fractal dimension (HFD)	Publications I and III	Complexity and self-similarity of time series
	Katz fractal dimension (KFD)	Publication III	Fractal dimension based on morphology
	Lempel-Ziv complexity (LZC)	Publications I and III	Randomness of finite sequences
	Sample entropy (SampEn)	Publication III	Signal irregularity
	Synchronization likelihood (SL)	Publications II and III	Functional connectivity
	Detrended fluctuation analysis (DFA)	Publication I	Quantifies long-range temporal correlations
Linear measures	Spectral asymmetry index (SASI)	Publication I	Balance of beta and theta band powers
	Alpha power variability (APV)	Publication I	Alpha power variability
	Relative gamma power (RGP)	Publication I	Relative gamma power
	Magnitude-squared coherence (MSC)	Publication II	Functional connectivity
	Imaginary part of coherency (ICOH)	Publication II	Functional connectivity

2.4 Classification between MDD and healthy subjects (Publication I)

Three nonlinear and three linear measures (Table 1), as well as combinations of these measures, were compared. The calculation of the EEG measures and more thorough explanations of the methods are presented in **Publication I**. Briefly, the classification was conducted using logistic regression with leave-one-out cross-validation. The statistical significance of classification accuracies was estimated by randomly rearranging the labels of MDD and healthy subjects and making a null distribution from the maximum classification accuracies of each permutation. The confidence level of $p<0.05$ from the maximum classification accuracies was considered statistically significant.

2.5 Correlation between functional connectivity and small-worldness (Publication II)

The calculation of the FC measures and SW, as well as more thorough explanations of the methods, are presented in **Publication II**. For each subject, the mean values of EEG alpha FC and SW were calculated over all channels and Pearson correlation between FC

and SW was calculated for healthy subjects and subjects with depression. The confidence level of $p < 0.05$ was used and the p-value was adjusted according to the number of statistical tests using Bonferroni correction to address the problem of multiple comparisons. As three different measures and nine different graph densities were used, the number of statistical tests was 27 and p-value was adjusted to $p < 0.05/27 = 0.0019$.

2.6 Degree of nonlinearity depending on the alpha period (Publication III)

To determine whether the surrogate data method significantly depends on the EEG alpha frequency component, the degree of nonlinearity (DEG) was calculated for gradually incremented EEG segments. We defined DEG as the percentage of segments where nonlinearity was detected. The starting EEG segment consisted of an integer number of alpha periods and was approximately 5 seconds long. The length of the starting EEG segment was gradually increased by 2, 4, 6, ..., 108 ms within one alpha period and DEG was calculated for each segment. The calculation of the surrogate data method, the DEG, and the incrementation process are more thoroughly explained in the methods of **Publication III.** One-way analysis of variance (ANOVA) was conducted to determine whether the value of DEG was influenced by the alpha frequency component for five nonlinear EEG measures (Table 1). The calculation of the EEG measures is briefly explained in **Publication III**.

3 Results

3.1 Classification between MDD and healthy subjects (Publication I)

The maximum classification accuracies of different EEG channels are presented in Table 2 and the classification accuracies of all analyzed measure combinations and channels are shown in Tables 1 and 2 in **Publication I.** Statistically significant classification accuracies (higher than 0.81) are marked with a gray background. The best classification accuracy between subjects with MDD and healthy subjects was obtained with the combinations of measures: 88% with SASI and RGP from linear measures, 88% with HFD, DFA, and LZC from nonlinear measures, and 92% with all measures combined. The highest classification accuracies for single EEG measures were obtained with the linear measures APV and RGP. Although classification accuracies of SASI, HFD, DFA, and LZC did not reach statistical significance after permutation testing, these measures gave high classification accuracies in different measure combinations. Therefore, the results obtained show that no superior EEG measure was found in the depression classification.

Nonlinear measures did not provide better classification accuracy compared to linear measures. When comparing single EEG measures, the highest classification accuracies were slightly higher for linear measures. However, when EEG measures were combined, slightly better results were obtained with nonlinear measures. The classification accuracies were not statistically compared and therefore these comparisons are conjectural.

The highest classification accuracies were found from central, temporal, and parietal regions. However, no EEG channel was found to be superior in the classification between MDD and healthy subjects.

*Table 2. Maximum classification accuracies between MDD and healthy subjects for each EEG measure combination as a summary of Tables 1 and 2 from **Publication I**. Grey background marks statistical significance (p<0.05) after permutation testing.*

Linear EEG measures	
	Accuracy
SASI	77%
APV	81%
RGP	81%
SASI & APV	77%
SASI & RGP	88%
APV & RGP	81%
SASI & APV & RGP	81%

Nonlinear EEG measures	
	Accuracy
HFD	77%
DFA	77%
LZC	69%
HFD & DFA	81%
HFD & LZC	85%
DFA & LZC	81%
HFD & DFA & LZC	88%

All 6 measures combined	Accuracy 92%

3.2 Correlation between functional connectivity and small-worldness (Publication II)

As a result of **Publication II**, a statistically significant negative correlation occurred for all three FC measures for healthy subjects (Fig. 1). MSC and ICOH resulted in statistically significant correlations for graph densities 15% ... 50% and SL 20% ... 50%. The highest correlations between FC and SW are shown in Fig. 3 in **Publication II**. Furthermore, novel results presented in the current thesis also show a negative correlation for all three FC

measures for MDD subjects (Fig. 2). Correlations calculated using MSC were significant for graph densities 30% ... 40%, using SL 35% ... 50%, and using ICOH 35%. The results for MDD subjects are novel and have not been previously published (Fig. 2). The negative correlation between FC and SW was similar for MDD and healthy subjects, but the level of statistical significance was different due to an unequal number of subjects in each group: 80 healthy subjects and 13 MDD subjects.

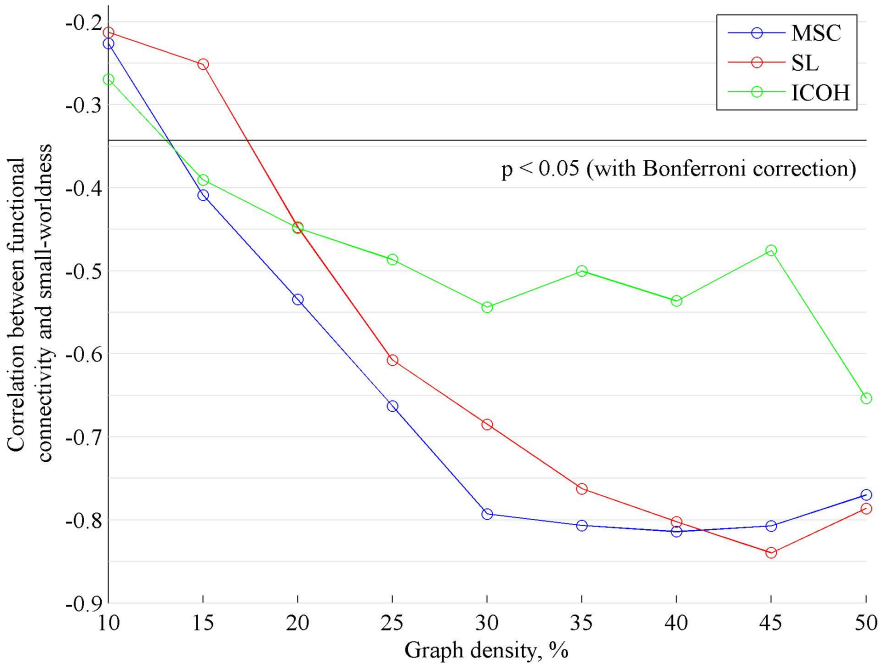

*Figure 1. The values of Pearson correlation coefficients for healthy subjects between measures of functional connectivity (MSC, SL, and ICOH) and small-worldness calculated from these measures (SW^{MSC}, SW^{SL}, and SW^{ICOH}) for different graph densities (**Publication II**). The black horizontal line corresponds to a correlation -0.34. Correlations below this line are statistically significant with a confidence level of 0.05 (p-value is adjusted according to the Bonferroni correction to p<0.0019).*

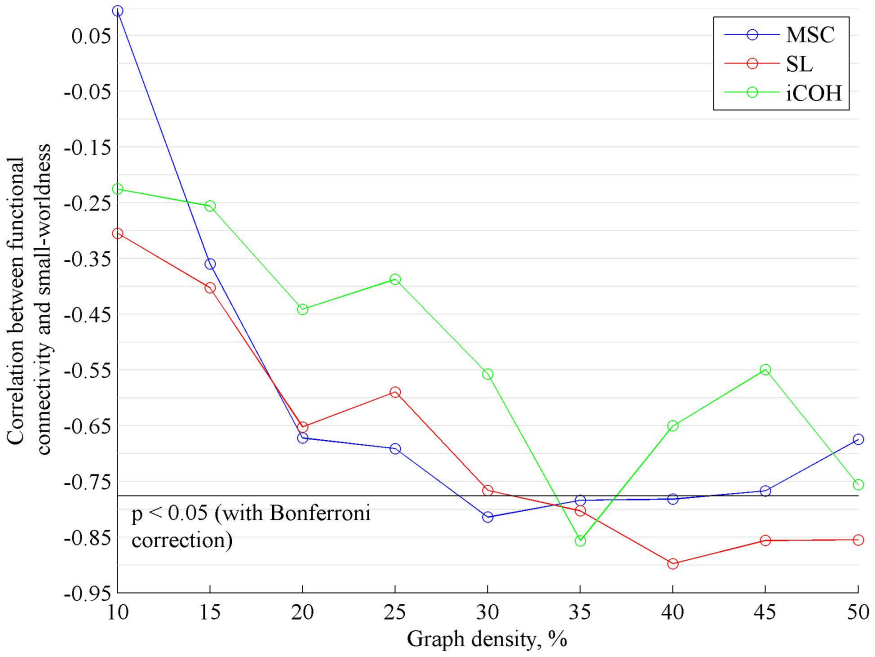

Figure 2. The values of Pearson correlation coefficients for major depressive disorder (MDD) subjects between measures of functional connectivity (MSC, SL, and ICOH) and small-worldness calculated from these measures (SW^{MSC}, SW^{SL}, and SW^{ICOH}) for different graph densities. The black horizontal line corresponds to a correlation -0.77. Correlations below this line are statistically significant with a confidence level of 0.05 (p-value is adjusted according to the Bonferroni correction to p<0.0019).

3.3 Degree of nonlinearity depending on the alpha period (Publication III)

The percentage of segments where nonlinearity was detected is presented in Table 3. HFD, KFD, and SampEn revealed significant nonlinearity within EEG signals (DEG>5%), but LZC and SL did not (DEG<5%). The value of DEG was statistically significantly influenced by the incrementation of the segment within one alpha period for every nonlinear statistic that indicated nonlinearity: HFD, KFD, and SampEn (Fig. 3). This result shows that the EEG DEG is influenced by the alpha cyclic component within the signal.

In addition, the dependence of DEG on the segment length increment in different channels (Fig. 2 in **Publication III**) and for different frequency bands (Fig. 3 in **Publication III)** are analyzed in **Publication III**. These results will not be discussed in the current thesis.

*Table 3. The degree of nonlinearity for 5-second EEG segments (**Publication III**).*

	HFD	KFD	LZC	SampEn	SL
DEG	45.7%	99.9%	0.4%	82.0%	4.4%

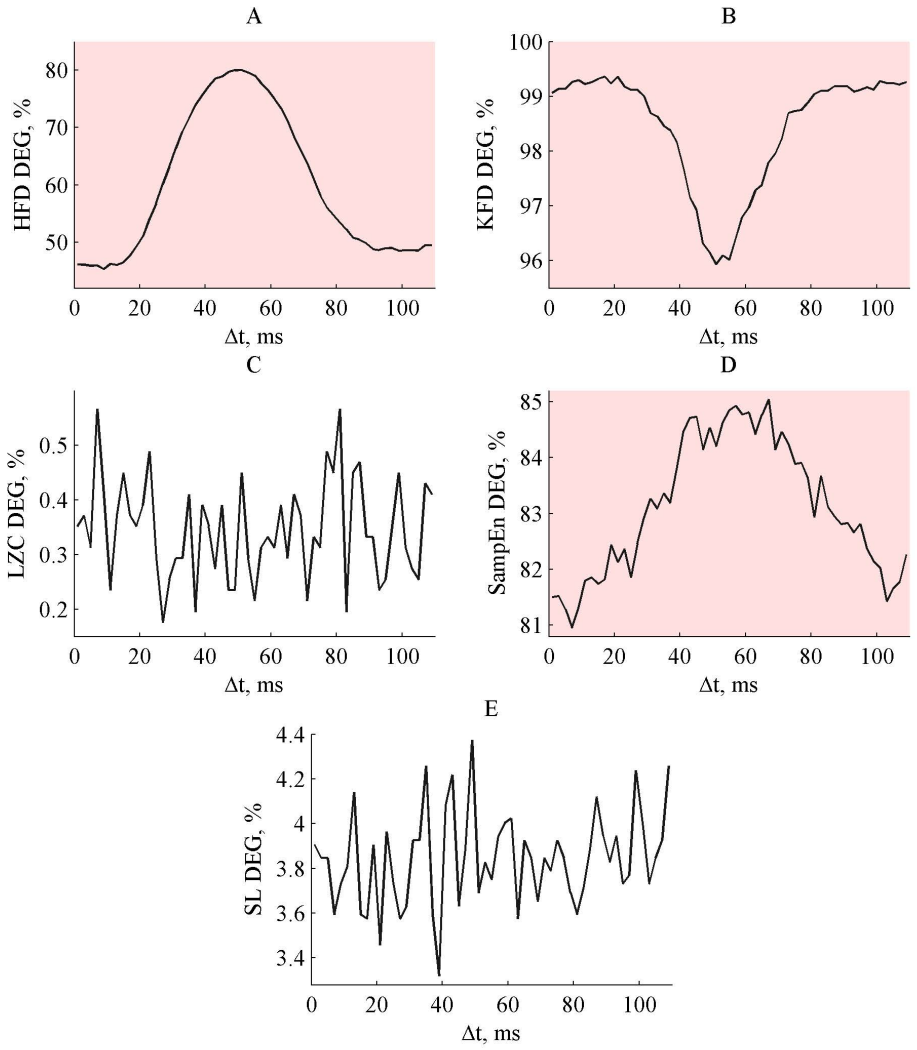

*Figure 3. The degree of nonlinearity DEG depending on the segment length increment Δt for (A) HFD, (B) KFD, (C) LZC, (D) SampEn, and (E) SL (**Publication III**). Statistically significant results are indicated with a pink background.*

4 Discussion

One purpose of the thesis was to find an easily measurable EEG marker to differentiate subjects with depression from control subjects. For a clinical application of discriminating depression, the simplicity and low computational load of EEG measures are important. Therefore, in **Publication I** we focused on EEG measures calculated from single EEG channels. On the one hand, the highest classification accuracies for single EEG measures were obtained for APV and RGP (81%). On the other hand, the combination of SASI and RGP and the combination of HFD, DFA, and LZC gave an even higher accuracy of 88%. Therefore, no specific EEG measure was concluded to be superior compared to other EEG measures, indicating that the choice of the EEG measures in discriminating depression is not strictly limited to certain measures. Therefore, other factors, such as the computational load, can be considered. The inconsistency of previous studies (Table 4 in Appendix 1) supports the conclusion of **Publication I** that currently there is no EEG measure that would be superior in depression classification. A review by de Aguiar Neto and Rosa (2019) included 42 EEG studies and also did not point out any superior EEG-based measures. They recommended using theta or gamma frequency band, HFD, and connectivity measures to discriminate between subjects with depression and healthy subjects and alpha frequency band for the detection of depression symptoms or for prognostics. In **Publication I**, we also found good results with RGP and HFD. However, it should be noted that the suggestions by de Aguiar Neto and Rosa (2019) were also influenced by the results of **Publication I**. The review by Čukić et al. (2020a) suggested using nonlinear EEG features and another review by Mahato and Paul (2019) suggested using band powers and relative wavelet energy.

De Aguiar Neto and Rosa (2019) suggested using connectivity measures among others to classify between healthy subjects and subjects with depression, as was done in some previous studies (Knott et al., 2001; Leuchter et al., 2012). However, FC and other multi-channel EEG measures are computationally more complex and require more EEG electrodes than single-channel measures analyzed in **Publication I**. The highest classification accuracy obtained in **Publication I** using single-channel EEG measures was 92%. Obtained accuracy is not lower compared to previous EEG studies using multi-channel EEG measures (Table 4 in Appendix 1). Previous studies have found similar classification accuracies for single- and multi-channel EEG studies: 62-98% for FC (Leuchter et al., 2012; Mumtaz et al., 2018), 66-88% for graph theory measures (Sun et al., 2019), 74-98% for asymmetry in combination with power (Mumtaz et al., 2017; Mahato & Paul, 2020), and 66-98% for measures calculated from single channels (Ahmadlou et al., 2012; Hosseinifard et al., 2013; Bachmann et al., 2017; Mahato & Paul, 2020; Čukić et al., 2020b). These results show that multi-channel EEG measures are expected to provide only limited advantage in the classification between healthy subjects and subjects with depression compared to single-channel measures. This conclusion is in agreement with the previous studies (van der Vinne et al., 2017; Wan et al., 2019). One year after **Publication I**, Wan et al. (2019) also found that single-channel EEG analysis can discriminate MDD as accurately as multi-channel analysis. Furthermore, the meta-analysis by Vinne et al. (2017) included 16 studies and showed a limited diagnostic value of frontal alpha asymmetry. Therefore, single-channel EEG measures could be preferred for clinical application, as the calculation of both FC and asymmetry requires at least two EEG channels and graph theory measures require full-head scalp EEG recordings.

As a result of **Publication II** and the thesis, we found a negative correlation between alpha FC and SW for MDD and healthy subjects. Based on the results of **Publication II**, we suggested that decreased alpha small-world organization is compensated with increased connectivity of alpha oscillations in a healthy brain. Furthermore, results presented in the current thesis (Fig. 2) show that the suggested compensational mechanism is maintained in depression. The conclusion that FC and graph theory measures provide similar discrimination between MDD and healthy subjects compared to single-channel EEG measures supports the proposition that compensating decreased small-world organization with increased alpha connectivity works similarly for healthy and depressed subjects. This result is important for a better understanding of the mechanisms of functional networks of both MDD and healthy subjects. Furthermore, this result could be the reason why FC or graph theory measures have not been frequently used in classifying between healthy subjects and subjects with depression compared to other measures, such as band powers or HFD (Table 4 in Appendix 1).

Schizophrenia and Alzheimer's disease have been previously described with decreased FC in the alpha frequency band (Koenig et al., 2005; Jalili & Knyazeva, 2011; Wang et al., 2014; Di Lorenzo et al., 2015; Maran et al., 2016; Babiloni et al., 2016), but also decreased small-world measures (Micheloyannis et al., 2006; Rubinov et al., 2009; Wang et al., 2014; Babiloni et al., 2016). Therefore, based on the network analysis in the studies by other authors, the compensational mechanism suggested in **Publication II** may be disrupted in schizophrenia and Alzheimer's disease. Therefore, FC could be more valuable to discriminate schizophrenia or Alzheimer's disease compared to depression.

Generally, linear measures have a lower computational load than nonlinear measures. The results of **Publication I** demonstrated that linear EEG measures (SASI, APV, and RGP) provided similar classification accuracies compared to nonlinear EEG measures (HFD, LZC, and DFA) for discrimination of depression in resting state. This result is in line with previous studies because similar classification accuracies have been presented for both linear and nonlinear measures throughout different studies: 66% − 98% for linear measures (Knott et al., 2001; Leuchter et al., 2012; Hosseinifard et al., 2013; Bachmann et al., 2013; Mumtaz et al., 2017; Bachmann et al., 2017; Mumtaz et al., 2018; Lee et al., 2018; Mahato & Paul, 2020) and 70% - 98% for nonlinear measures (Ahmadlou et al., 2012; Hosseinifard et al., 2013; Bachmann et al., 2013; Bachmann et al., 2017; Mumtaz et al., 2018; Čukić et al., 2020b). Furthermore, while Hosseinifard et al. (2013) found that nonlinear measures provided better discrimination between subjects with depression and healthy subjects, Cai et al. (2018) found the opposite. Unfortunately, the classification accuracies were not statistically compared and therefore the comparisons are conjectural.

In **Publication III**, five nonlinear measures were analyzed: LZC, SL, HFD, KFD, and SampEn. As a result, HFD, KFD, and SampEn revealed a significant percentage of nonlinearity within the EEG signals (Table 3), indicating that the values of these measures were significantly altered if the phase information within the signal was lost. Although the values of HFD, KFD, and SampEn are influenced by nonlinear information within the EEG signals, the advantage of these measures compared to other measures in the classification between MDD and healthy subjects is not marginal (Table 4 in Appendix 1). LZC and SL did not reveal significant nonlinearity in the signal (Table 3), meaning that the values of these measures were not significantly influenced by nonlinear information within the EEG signals or the nonlinearity was not revealed by the surrogate data method. As a result of **Publication II**, we found similar results for nonlinear measure SL and linear measure MSC (Figs. 1 and 2 from **Publication II**). This result shows that

although SL is computationally much more demanding, MSC may work as well as SL. However, the same result may not apply to all EEG data. Lei et al. (2017) reported that 72% − 74% of EEG segments were identified as nonlinear using SL and Mumtaz et al. (2018) found that SL gave higher accuracy in the classification between MDD and healthy subjects compared to coherence.

In **Publication I**, the highest classification accuracies between MDD and healthy subjects were obtained using a combination of several EEG measures. Previous studies have also come to the same conclusion that the highest classification accuracy is obtained using a combination of different EEG measures (Knott et al., 2001; Hosseinifard et al., 2013; Cai et al., 2018; Mahato & Paul, 2020). The relationship between EEG measures gives information about the performance of combining different measures. Including highly correlated features in the classification may decrease the classification accuracy by overfitting the model. As an example, our previous study showed that adding graph theory features to FC features did not significantly increase accuracy in classifying between MDD and healthy subjects (Orgo et al., 2017). As a result of **Publication II** and the thesis, we found a negative correlation between alpha FC and SW for MDD and healthy subjects, conjointly explaining why combining these measures did not increase the classification accuracy in our previous study.

Another subject on the correlated EEG features is correlations between EEG channels. In **Publication I**, statistically significant classification accuracies were found from a range of EEG channels from central, temporal, and parietal regions. A result from a range of channels is expected due to the effects of volume conduction. Furthermore, previous studies have shown that depression affects brain activity across the whole cortex (Fingelkurts et al., 2006; Wang et al., 2012). Correlating EEG channels could be one reason why single-channel EEG measures give results comparable to multi-channel measures in the classification between subjects with depression and healthy subjects.

As a result of **Publication III**, EEG DEG was statistically significantly influenced by the alpha frequency component for every nonlinear EEG measure that indicated nonlinearity. This result indicates the importance of segmenting EEG signals according to the alpha component for eyes-closed resting-state EEG when using the surrogate data method. The surrogate data method has been widely used for EEG time series and is applicable in studies discriminating between subject groups (Dimitriadis et al., 2015; Wang et al., 2019b), including subjects with depression and healthy subjects (Lee et al., 2007; Zuchowicz et al., 2019; Puthankattil, 2020). However, to the best of my knowledge, previous studies have not considered the alpha component in EEG signal segmentation. Wang et al. (2019b) found that the EEG measures calculated for original data had better discrimination between subject groups compared to the EEG measures calculated for surrogate data. This result may be influenced by the EEG segment end-mismatch because random segmentation also randomizes surrogate data results (Fig. 3).

Although several studies have classified between subjects with depression and healthy subjects, presented accuracies are often obtained using the data on hand and are not extendable to unknown data. This is the case when testing is not performed on an independent data. Instead, data in EEG studies is often divided into training and validation sets and after that, the same data is divided into training and testing sets. In previous EEG studies, best performing EEG measures, frequency bands, or channels have been selected in a validation phase using either statistical tests to compare means of two groups such as ANOVA or t-test (Knott et al., 2001; Ahmadlou et al., 2012; Bachmann et al., 2013), correlation with a self-reported depression scale (Sun et al., 2019),

or feature selection (Hosseinifard et al., 2013; Cai et al., 2018; Mumtaz et al., 2018; Mahato & Paul, 2020). In **Publication I**, training and testing were conducted on data without any prior validation and therefore presented classification accuracies are not overfitted by the validation phase (Tables 1 and 2 in **Publication I**). The statistical significance of classification accuracies was estimated using a permutation test. Only a few depression EEG studies have used independent datasets for validating and testing (Mohammadi et al., 2015) or a statistical test to estimate the performance of the classifier (Sun et al., 2019). Independent subject groups are often not used due to the difficulty to find unmedicated volunteers with depression, resulting in a small number of subjects. Another obstacle is the individuality and complexity of depression: different subjects may exhibit different symptoms and comorbidity of disorders. Čukić et al. (2020a) brought out that a small number of subjects is one of the main problems in the EEG studies discriminating depression. They added that a larger number of subjects and independent testing would increase the prediction accuracy on unseen data and would decrease unwarranted optimism.

The current thesis focuses on classification between subjects with depression and healthy subjects and does not address the classification between various mental disorders. Markers for discriminating depression could assist doctors in the early detection of depression. Nevertheless, clinical diagnoses should be made by a medical doctor. Note that as a diagnosis of depression is based on subjective symptoms, the classification between healthy subjects and subjects with MDD is also based on detecting subjective symptoms of depression, because subjects for the studies are chosen based on clinical diagnoses. EEG measures addressed in the current thesis can also have applications in discriminating other psychiatric or degenerative disorders or between different disorders, but these areas are not covered in the current thesis.

Conclusions

The current thesis provides novel knowledge about the objective EEG measures applied in the classification between subjects with depression and healthy subjects. In accordance with the aims of the thesis, the following conclusions were made:

1. As a result of the thesis, no specific EEG measure was concluded to be superior compared to other EEG measures, indicating that the choice of the EEG measures in discriminating depression is not strictly limited to certain measures. Therefore, other factors, such as the computational load or simplicity, can be considered. The results of the thesis demonstrated that linear EEG measures provided similar classification accuracies compared to nonlinear EEG measures for discrimination of depression in resting state. Furthermore, **Publication I** was the first study to demonstrate that EEG measures calculated for a single EEG channel did not provide lower classification accuracies than measures calculated for multiple EEG channels in previous studies.
2. One purpose of the thesis was to identify the most sensitive EEG channel regions in the classification between MDD and healthy subjects. As a result, the highest classification accuracies were found from central, temporal, and parietal regions. As no superior EEG channel was found, a range of channels are suitable for discriminating depression.
3. The current thesis was the first study to report a negative correlation between EEG FC and SW in the alpha frequency band for MDD and healthy subjects. The relationship between FC and SW was previously unknown. Based on the results, it was proposed in the thesis that decreased small-world organization is compensated with increased alpha connectivity and the compensational mechanism works similarly for MDD and healthy subjects.
4. A specific problem was found in applying the surrogate data method to the EEG segments. It was previously known that a false detection of nonlinearity may occur in case the data are strongly cyclic for data segments with end-mismatch. However, it was unknown how the segment end-mismatch influences the surrogate data method calculated for an EEG signal and previous EEG studies have not addressed this problem. As a result of the thesis, we found that a false detection of nonlinearity occurred when the data segment did not comprise full periods of the alpha frequency component. This result shows the importance of segmenting data according to the alpha component for eyes-closed resting-state EEG when using the surrogate data method.

In the conclusion of the thesis, complicated EEG measures based on multiple EEG channels or nonlinearity are expected to provide only limited advantage in the classification between subjects with depression and healthy subjects compared to linear single-channel measures.

References

Acharya, U. R., Oh, S. L., Hagiwara, Y., Tan, J. H., Adeli, H., & Subhae, D. P. (2018). Automated EEG-based screening of depression using deep convolutional neural network. *Comput Methods Programs Biomed, 161*, 103−113. doi: 10.1016/j.cmpb.2018.04.012

Ahmadlou, M., Adeli, H., & Adeli, A. (2012). Fractality analysis of frontal brain in major depressive disorder. *Int J Psychophysiol, 85*(2), 206–211. doi: 10.1016/j.ijpsycho.2012.05.001

Alonso, J. F., Mañanas, M. A., Romero, S., Hoyer, D., Riba, J., & Barbanoj, M. J. (2010). Drug effect on EEG connectivity assessed by linear and nonlinear couplings. *Hum Brain Mapp, 31*(3), 487−497. doi: 10.1002/hbm.20881

Aragonès, E., Piñol, J. L., & Labad, A. (2006). The overdiagnosis of depression in non-depressed patients in primary care. *Fam Pract, 23*(3), 363–368. doi: 10.1093/fampra/cmi120

Babiloni, C., Lizio, R., Marzano, N., Capotosto, P., Soricelli, A., Triggiani, A. I., ... Percio, C. D. (2016). Brain neural synchronization and functional coupling in Alzheimer's disease as revealed by resting state EEG rhythms. *Int J Psychophysiol, 103*, 88−102. doi: 10.1016/j.ijpsycho.2015.02.008

Bachmann, M., Lass, J., & Hinrikus, H. (2017). Single channel EEG analysis for detection of depression. *Biomed Signal Process Control, 31*, 391−397. doi: 10.1016/j.bspc.2016.09.010

Bachmann, M., Lass, J., Suhhova, A., & Hinrikus, H. (2013). Spectral Asymmetry and Higuchi's Fractal Dimension Measures of Depression Electroencephalogram. *Comput Math Methods Med, 2013*. doi: http://dx.doi.org/10.1155/2013/251638

Bae, Y., Yoo, B. W., Lee, J. C., & Kim, H. C. (2017). Automated network analysis to measure brain effective connectivity estimated from EEG data of patients with alcoholism. *Physiol Meas, 38*, 759−773. doi: 10.1088/1361-6579/aa6b4c

Bastos, A. M., & Schoffelen, J.-M. (2016). A tutorial review of functional connectivity analysis methods and their interpretational pitfalls. *Front Syst Neurosci, 9*, 175. doi: 10.3389/fnsys.2015.00175

Bilello, J. A. (2016). Seeking an objective diagnosis of depression. *Biomark Med, 10*(8), 861−875. doi: 10.2217/bmm-2016-0076

Bilello, J. A., Thurmond, L. M., Smith, K. M., Pi, B., Rubin, R., Wright, S. M., ... Shelton, R. C. (2015). MDDScore: confirmation of a blood test to aid in the diagnosis of major depressive disorder. *J Clin Psychiatry, 76*(2), e199-206. doi: 10.4088/JCP.14m09029

Breakspear, M., & Terry, J. R. (2002). Detection and description of non-linear interdependence in normal multichannel human EEG data. *Clin Neurophysiol, 113*(5), 735−753. doi: 10.1016/S1388-2457(02)00051-2

Bäuerle, A., Teufel, M., Musche, V., Weismüller, B., Kohler, H., Hetkamp, M., ... Skoda, E. M. (2020). Increased generalized anxiety, depression and distress during the COVID-19 pandemic: a cross-sectional study in Germany. *J Public Health (Oxf), 42*(4), 672−678. doi: 10.1093/pubmed/fdaa106

Cai, H., Han, J., Chen, Y., Sha, X., Wang, Z., Hu, B., ... Gutknecht, J. (2018). A Pervasive Approach to EEG-Based Depression Detection. *Complexity, 2018*, 5238028. doi: 10.1155/2018/5238028

Chavez, M., Grosselin, F., Bussalb, A., Fallani, F. D., & Navarro-Sune, X. (2018). Surrogate-Based Artifact Removal From Single-Channel EEG. *IEEE Trans Neural Syst Rehabil Eng, 26*(3), 540−550. doi: 10.1109/TNSRE.2018.2794184

Čukić, M., López, V., & Pavón, J. (2020a). Classification of Depression Through Resting-State Electroencephalogram as a Novel Practice in Psychiatry: Review. *J Med Internet Res, 22*(11), e19548. doi: 10.2196/19548

Čukić, M., Stokić, M., Simić, S., & Pokrajac, D. (2020b). The successful discrimination of depression from EEG could be attributed to proper feature extraction and not to a particular classification method. *Cogn Neurodyn, 14*(4), 443−455. doi: 10.1007/s11571-020-09581-x

de Aguiar Neto, F. S., & G., R. J. (2019). Depression biomarkers using non-invasive EEG: A review. *Neurosci Biobehav Rev, 105*, 83−93. doi: 10.1016/j.neubiorev.2019.07.021

Di Lorenzo, G., Daverio, A., Ferrentino, F., Santarnecchi, E., Ciabattini, F., Monaco, L., ... Siracusano, A. (2015). Altered resting-state EEG source functional connectivity in schizophrenia: the effect of illness duration. *Front Hum Neurosci, 9*(234). doi: 10.3389/fnhum.2015.00234

Dimitriadis, S. I., Salis, C., Tarnanas, I., & Linden, D. E. (2017). Topological Filtering of Dynamic Functional Brain Networks Unfolds Informative Chronnectomics: A Novel Data-Driven Thresholding Scheme Based on Orthogonal Minimal Spanning Trees (OMSTs). *Front Neuroinform, 11*(28). doi: 10.3389/fninf.2017.00028

Dimitriadis, S. I., Zouridakis, G., Rezaie, R., Babajani-Feremi, A., & Papanicolaou, A. C. (2015). Functional connectivity changes detected with magnetoencephalography after mild traumatic brain injury. *NeuroImage: Clinical, 9*, 519–531. doi: 10.1016/j.nicl.2015.09.011

Ettman, C. K., Abdalla, S. M., Cohen, G. H., Sampson, L., Vivier, P. M., & Galea, S. (2020). Prevalence of Depression Symptoms in US Adults Before and During the COVID-19 Pandemic. *JAMA Netw Open, 3*(9), e2019686. doi: 10.1001/jamanetworkopen.2020.19686

Fingelkurts, A. A., Fingelkurts, A. A., Rytsälä, H., Suominen, K., Isometsä, E., & Kahkonen, S. (2007). Impaired functional connectivity at EEG alpha and theta frequency bands in major depression. *Hum Brain Mapp, 28*(3), 247–261. doi: 10.1002/hbm.20275

Fingelkurts, A. A., Fingelkurts, A. A., Rytsälä, H., Suominen, K., Isometsä, E., & Kähkönen, S. (2006). Composition of brain oscillations in ongoing EEG during major depression disorder. *Neurosci Res, 56*(2), 133–144. doi: 10.1016/j.neures.2006.06.006

Gao, S., Calhoun, V. D., & Sui, J. (2018). Machine learning in major depression: From classification to treatment outcome prediction. *CNS Neurosci Ther, 24*(11), 1037−1052. doi: 10.1111/cns.13048

Hosseinifard, B., Moradi, M. H., & Rostami, R. (2013). Classifying depression patients and normal subjects using machine learning techniques and nonlinear features from EEG signal. *Comput Methods Programs Biomed, 109*(3), 339−345. doi: 10.1016/j.cmpb.2012.10.008

Huang, Y., Zhang, J., Cui, Y., Yang, G., He, L., Liu, Q., & Yin, G. (2017). How different EEG references influence sensor level functional connectivity graphs. *Front Neurosci, 11,* 368. doi: 10.3389/fnins.2017.00368

Humphries, M., & Gurney, K. (2008). Network 'small-world-ness': a quantitative method for determining canonical network equivalence. *PLoS ONE, 3*(4), e0002051. doi: 10.1371/journal.pone.0002051

Jalili, M., & Knyazeva, M. G. (2011). EEG-based functional networks in schizophrenia. *Comput Biol Med, 41*(12), 1178−1186. doi: 10.1016/j.compbiomed.2011.05.004

Kautzky, A., James, G. M., Philippe, C., Baldinger-Melich, P., Kraus, C., Kranz, G. S., ... Lanzenberger, R. (2017). The influence of the rs6295 gene polymorphism on serotonin-1A receptor distribution investigated with PET in patients with major depression applying machine learning. *Transl Psychiatry, 7*(6), e1150. doi: 10.1038/tp.2017.108

Knott, V., Mahoney, C., Kennedy, S., & Evans, K. (2001). EEG power, frequency, asymmetry and coherence in male depression. *Psychiatry Res, 106*, 123−140. doi: 10.1016/s0925-4927(00)00080-9

Koenig, T., Prichep, L., Dierks, T., Hubl, D., Wahlund, L., John, E., & Jelic, V. (2005). Decreased EEG synchronization in Alzheimer's disease and mild cognitive impairment. *Neurobiol Aging, 26*(2), 165–171. doi: 10.1016/j.neurobiolaging. 2004.03.008

Lee, J.-S., Yang, B.-H., Lee, J.-H., Choi, J.-H., Choi, I.-G., & Kim, S.-B. (2007). Detrended fluctuation analysis of resting EEG in depressed outpatients and healthy controls. *Clin Neurophysiol, 118*(11), 2489–2496. doi: 10.1016/j.clinph.2007.08.001

Lee, P. F., Kan, D. P., Croarkin, P., Phang, C. K., & Doruk, D. (2018). Neurophysiological correlates of depressive symptoms in young adults: A quantitative EEG study. *J Clin Neurosci, 47*, 315–322. doi: 10.1016/j.jocn.2017.09.030

Lei, H., Cui, Y., Fan, J., Zhang, X., Zhong, M., Yi, J., ... Zhu, X. (2017). Abnormal small-world brain functional networks in obsessive-compulsive disorder patients with poor insight. *J Affect Disord, 219*, 119–125. doi: 10.1016/j.jad.2017.05.032

Leuchter, A. F., Cook, I. A., Hunter, A. M., Cai, C., & Horvath, S. (2012). Resting-state quantitative electroencephalography reveals increased neurophysiologic connectivity in depression. *PLoS ONE, 7*(2), e32508. doi: 10.1371/journal.pone.0032508

Li, X., Jing, Z., Hu, B., Zhu, J., Zhong, N., Li, M., ... Majoe, D. (2017). A resting-state brain functional network study in MDD based on minimum spanning tree analysis and the hierarchical clustering. *Complexity, 2017*(1), 1–11. doi: 10.1155/2017/9514369

Liao, S. C., Wu, C. T., Huang, H. C., Cheng, W. T., & Liu, Y. H. (2017). Major Depression Detection from EEG Signals Using Kernel Eigen-Filter-Bank Common Spatial Patterns. *Sensors (Basel), 17*(6), 1385. doi: 10.3390/s17061385

Lu, Q., Bi, K., Liu, C., Luo, G., Tang, H., & Yao, Z. (2013). Predicting depression based on dynamic regional connectivity: A windowed Granger causality analysis of MEG recordings. *Brain Res, 1535*, 52–60. doi: 10.1016/j.brainres.2013.08.033

Lu, Q., Jiang, H., Bi, K., Liu, C., & Yao, Z. (2014). Discriminative analysis with a limited number of MEG trials in depression. *J Affect Disord, 167*, 207–214. doi: 10.1016/j.jad.2014.06.007

Mahato, S., & Paul, S. (2020). Classification of Depression Patients and Normal Subjects Based on Electroencephalogram (EEG) Signal Using Alpha Power and Theta Asymmetry. *J Med Syst, 44*(1). doi: 10.1007/s10916-019-1486-z

Maran, M., Grent-'t-Jong, T., & Uhlhaas, P. J. (2016). Electrophysiological insights into connectivity anomalies in schizophrenia: a systematic review. *Neuropsychiatric Electrophysiology, 2,* 6. doi: 10.1186/s40810-016-0020-5

Micheloyannis, S., Pachou, E., Stam, C. J., Breakspear, M., Bitsios, P., Vourkas, M., ... Zervakis, M. (2006). Small-world networks and disturbed functional connectivity in schizophrenia. *Schizophr Res, 87*(1-3), 60–66. doi: 10.1016/j.schres.2006.06.028

Mitchell, A. J., Vaze, A., & Rao, S. (2009). Clinical diagnosis of depression in primary care: a meta-analysis. *Lancet, 374*(9690), 609–619. doi: 10.1016/S0140-6736(09)60879-5

Mohammadi, M., Al-Azab, F., Raahemi, B., Richards, G., Jaworska, N., Smith, D., ... Knott, V. (2015). Data mining EEG signals in depression for their diagnostic value. *BMC Med Inform Decis Mak, 15*(108). doi: 10.1186/s12911-015-0227-6

Mora, C., Zonca, V., Riva, M. A., & Cattaneo, A. (2018). Blood biomarkers and treatment response in major depression. *Expert Rev Mol Diagn, 18*(6), 513–529. doi: 10.1080/14737159.2018.1470927

Mumtaz, W., Ali, S. S., Yasin, M. A., & Malik, A. S. (2018). A machine learning framework involving EEG-based functional connectivity to diagnose major depressive disorder (MDD). *Med Biol Eng Comput, 56*, 233–246. doi: 10.1007/s11517-017-1685-z

Mumtaz, W., Xia, L., Ali, S. S., Yasin, M. A., Hussain, M., & Malik, A. S. (2017). Electroencephalogram (EEG)-based computer-aided technique to diagnose major depressive disorder (MDD). *Biomed Signal Process Control, 31*, 108–115. doi: 10.1016/j.bspc.2016.07.006

Natarajan, K., R., A. U., Alias, F., Tiboleng, T., & Puthusserypady, S. K. (2004). Nonlinear analysis of EEG signals at different mental states. *BioMedical Engineering Online, 3*(7). doi: 10.1186/1475-925X-3-7

Netoff, T. L., Carroll, T. L., Pecora, L. M., & Schiff, S. J. (2006). Detecting Coupling in the Presence of Noise and Nonlinearity. In B. Schelter, M. Winterhalder, & J. Timmer (Eds.), *Handbook of Time Series Analysis* (pp. 265–282). Weingeim: Wiley-VCH Berlag. doi: 10.1002/9783527609970.ch11

Nicolaou, N., Malik, A., Daly, I., Weaver, J., Hwang, F., Kirke, A., ... Nasuto, S. J. (2017). Directed Motor-Auditory EEG Connectivity Is Modulated by Music Tempo. *Front Hum Neurosci, 11*, 502. doi: 10.3389/fnhum.2017.00502

Ning, M., & Lo, E. H. (2010). Opportunities and Challenges in Omics. *Transl Stroke Res, 1*(4), 233–237. doi: 10.1007/s12975-010-0048-y

Niso, G., Bruña, R., Pereda, E., Gutiérrez, R., Bajo, R., Maestú, F., & del-Pozo, F. (2013). HERMES: towards an integrated toolbox to characterize functional and effective brain connectivity. *Neuroinformatics, 11*(4), 405–434. doi: 10.1007/s12021-013-9186-1

Olbrich, S., Tränkner, A., Chittka, T., Hegerl, U., & Schönknecht, P. (2014). Functional connectivity in major depression: Increased phase synchronization between frontal cortical EEG-source estimates. *Psychiatry Res, 222*(1-2), 91–99. doi: 10.1016/j.pscychresns.2014.02.010

Olejarczyk, E., Marzetti, L., Pizzella, V., & Zappasodi, F. (2017). Comparison of connectivity analyses for resting state EEG data. *J Neural Eng, 14*(3). doi: 10.1088/1741-2552/aa6401

Orgo, L., Bachmann, M., Kalev, K., Järvelaid, M., Raik, J., & Hinrikus, H. (2017). Resting EEG Functional Connectivity and Graph Theoretical Measures for Discrimination of Depression. *2017 IEEE EMBS International Conference on Biomedical & Health Informatics*, Orlando, FL, 389−392. doi: 10.1109/BHI.2017.7897287

Orgo, L., Bachmann M., Kalev K., Järvelaid M., Raik J., & Hinrikus H. (2018). Dependence of the EEG Nonlinear Coupling on the Frequency Bands and the Segment Lengths. In: Eskola H., Väisänen O., Viik J., Hyttinen J. (eds) EMBEC & NBC 2017. EMBEC 2017, NBC 2017. *IFMBE Proceedings, 65*. Springer, Singapore. https://doi.org/10.1007/978-981-10-5122-7_200

Papakostas, G. I., Shelton, R. C., Kinrys, G., Henry, M. E., Bakow, B. R., Lipkin, S. H., ... Bilello, J. A. (2013). Assessment of a multi-assay, serum-based biological diagnostic test for major depressive disorder: a pilot and replication study. *Mol Psychiatry, 18*(3), 332–339. doi: 10.1038/mp.2011.166

Parkkonen, L. (2015). Real-Time Magnetoencephalography for Neurofeedback and Closed-Loop Experiments. In K. Kansaku, L. Cohen, & N. Birbaumer (Eds.) Clinical Systems Neuroscience. Springer, Tokyo. doi: 10.1007/978-4-431-55037-2_17

Prichard, D., & Theiler, J. (1994). Generating Surrogate Data for Time Series with Several Simultaneously Measured Variables. *Physical Review Letters, 73*(7), 951–954. doi: 10.1103/PhysRevLett.73.951

Puthankattil, S. D. (2020). Fronto-Temporal Analysis of EEG Signals of Patients with Depression: Characterisation, Nonlinear Dynamics and Surrogate Analysis. *IntechOpen*. doi: 10.5772/intechopen.94254

Puthankattil, S. D., & Joseph, P. K. (2012). Classification of EEG signals in normal and depression conditions by ANN using RWE and signal entropy. *J Mech Med Biol 12*(4), 1240019. doi: 10.1142/S0219519412400192

Põld, T., Päeske, L., Hinrikus, H., Lass, J., & Bachmann, M. (2021). Long-term stability of resting state EEG-based linear and nonlinear measures. *Int J Psychophysiol, 159*, 83–87. doi: 10.1016/j.ijpsycho.2020.11.013

Qin, Y., Xu, P., & Yao, D. (2010). A comparative study of different references for EEG default mode network: The use of the infinity reference. *Clin Neurophysiol, 121*(12), 1981–1991. doi: 10.1016/j.clinph.2010.03.056

Rettew, D. C., Lynch, A. D., Achenbach, T. M., Dumenci, L., & Ivanova, M. Y. (2009). Meta-analyses of agreement between diagnoses made from clinical evaluations and standardized diagnostic interviews. *Int J Methods Psychiatr Res, 18*(3), 169–184. doi: 10.1002/mpr.289

Rubinov, M., & Sporns, O. (2010). Complex network measures of brain connectivity: Uses and interpretations. *NeuroImage, 52*(3), 1059–1069. doi: 10.1016/j.neuroimage.2009.10.003

Rubinov, M., Knock, S. A., Stam, C. J., Micheloyannis, S., Harris, A. W., Williams, L. M., & Breakspear, M. (2009). Small-world properties of nonlinear brain activity in schizophrenia. *Hum Brain Mapp, 30*(2), 403–416. doi: 10.1002/hbm.20517

Salari, N., Hosseinian-Far, A., Jalali, R., Vaisi-Raygani, A., Rasoulpoor, S., Mohammadi, M., ... Khaledi-Paveh, B. (2020). Prevalence of stress, anxiety, depression among the general population during the COVID-19 pandemic: a systematic review and meta-analysis. *Global Health, 16*, 57. doi: 10.1186/s12992-020-00589-w

Scarapicchia, V., Brown, C., Mayo, C., & Gawryluk, J. R. (2017). Functional Magnetic Resonance Imaging and Functional Near-Infrared Spectroscopy: Insights from Combined Recording Studies. *Front Hum Neurosci, 11*, 419. doi: 10.3389/fnhum.2017.00419

Shim, M., Im, C.-H., Kim, Y.-W., & Lee, S.-H. (2018). Altered cortical functional network in major depressive disorder: A resting state electroencephalogram study. *Neuroimage Clin, 19*, 1000–1007. doi: 10.1016/j.nicl.2018.06.012

Siu, A. L., US Preventive Services Task Force (USPSTF), Bibbins-Domingo, K., Grossman, D. C., Baumann, L. C., Davidson, K. W., … Pignone, M. P. (2016). Screening for depression in adults: US Preventive Services Task Force recommendation statement. *JAMA, 315*(4), 380–387. doi: 10.1001/jama.2015.18392

Small, M., & Tse, C. K. (2002). Applying the method of surrogate data to cyclic time series. *Physica D, 164*(3–4), 187–201. doi: 10.1016/S0167-2789(02)00382-2

Solomon, C., Valstar, M. F., Morriss, R. K., & Crowe, J. (2015). Objective methods for reliable detection of concealed depression. *Frontiers in ICT, 2*(5). doi: 10.3389/fict.2015.00005

Stam, C. J., Pijn, J. P., & Pritchard, W. S. (1998). Reliable detection of nonlinearity in experimental time series with strong periodic components. *Physica D, 112*(3–4), 361–380. doi: 10.1016/S0167-2789(97)00183-8

Sun, S., Li, X., Zhu, J., Wang, Y., La, R., Zhang, X., ... Hu, B. (2019). Graph theory analysis of functional connectivity in major depression disorder with high-density resting state EEG data. *IEEE Trans Neural Syst Rehabil Eng, 27*(3), 429–439. doi: 10.1109/TNSRE.2019.2894423

Zhang, M., Zhou, H., Liu, L., Feng, L., Yang, J., Wang, G., & Zhong, N. (2018). Randomized EEG functional brain networks in major depressive disorders with greater resilience and lower rich-club coefficient. *Clin Neurophysiol, 129*(4), 743–758. doi: 10.1016/j.clinph.2018.01.017

Zuchowicz, U., Wozniak-Kwasniewska, A., Szekely, D., Olejarczyk, E., & David, O. (2019). EEG Phase Synchronization in Persons With Depression Subjected to Transcranial Magnetic Stimulation. *Front Neurosci, 12*, 1037. doi: 10.3389/fnins.2018.01037

Theiler, J., Eubank, S., Longtin, A., Galdrikian, B., & Farmer, J. (1992). Testing for nonlinearity in time series: the method of surrogate data. *Physica D, 58*(1–4), 77–94. doi: 10.1016/0167-2789(92)90102-S

Thornhill, N. F. (2005). Finding the Source of Nonlinearity in a Process With Plant-Wide Oscillation. *IEEE Trans Control Syst Technol, 13*(3), 434–443. doi: 10.1109/TCST.2004.839570

Troyer, E. A., Kohn, J. N., & Hong, S. (2020). Are we facing a crashing wave of neuropsychiatric sequelae of COVID-19? Neuropsychiatric symptoms and potential immunologic mechanisms. *Brain Behav Immun, 87*, 34–39. doi: 10.1016/j.bbi.2020.04.027

van der Vinne, N., Vollebregt, M. A., van Putten, M. J., & Arns, M. (2017). Frontal alpha asymmetry as a diagnostic marker in depression: Fact or fiction? A meta-analysis. *Neuroimage Clin, 16*, 79–87. doi: 10.1016/j.nicl.2017.07.006

Wan, Z., Zhang, H., Huang, J., Zhou, H., Yang, J., & Zhong, N. (2019). Single-Channel EEG-Based Machine Learning Method for Prescreening Major Depressive Disorder. *Int J Inf Technol Decis Making, 18*(5), 1579–1603. doi: 10.1142/S0219622019500342

Wang, J., Zhang, L., Liu, T., Pan, W., Hu, B., & Zhu, T. (2019a). Acoustic differences between healthy and depressed people: a cross-situation study. *BMC Psychiatry, 19*(300). doi: 10.1186/s12888-019-2300-7

Wang, L., Hermens, D. F., Hickie, I. B., & Lagopoulos, J. (2012). A systematic review of resting-state functional-MRI studies in major depression. *J Affect Disord, 142*(1–3), 6–12. doi: 10.1016/j.jad.2012.04.013

Wang, R., Wang, J., Yu, H., Wei, X., Yang, C., & Deng, B. (2014). Decreased coherence and functional connectivity of electroencephalograph in Alzheimer's disease. *Chaos, 24*(3), 033136. doi: http://dx.doi.org/10.1063/1.4896095

Wang, X. W., Zhao, X. H., Li, F., Lin, Q., & Hu, Z. H. (2019b). Sample entropy and surrogate data analysis for Alzheimer's disease. *Math Biosci Eng, 16*(6), 6892–6906. doi: 10.3934/mbe.2019345

WHO. (2019). *Mental disorders.*

WHO. (2020). *Depression.*

Williamson, J. R., Quatieri, T. F., Helfer, B. S., Ciccarelli, G., & Mehta, D. D. (2014). Vocal and Facial Biomarkers of Depression Based on Motor Incoordination and Timing. *Proceedings of the 4th ACM International Workshop on Audio/Visual Emotion Challenge*, 65–72. Association for Computing Machinery. doi: 10.1145/2661806.2661809

Yao, D. (2001). A method to standardize a reference of scalp EEG recordings to a point at infinity. *Physiol Meas, 22*(4), 693–711. doi: 10.1088/0967-3334/22/4/305

Acknowledgements

I am sincerely grateful to everyone who has contributed their time or knowledge to the current thesis. My deepest gratitude goes to my supervisor Professor Maie Bachmann for the constructive guidance, good eye for detail, continuous support, and reliability. She has been my supervisor now for eight years throughout my bachelor's, master's, and doctoral studies. Another person who has always been there for me this whole time is Professor Emeritus Hiie Hinrikus. Her extensive experience has always helped me to put an emphasis on the most important aspects of my work.

I would like to thank the co-authors of my papers, who made these publications possible. Special gratitude goes to my co-supervisor Professor Jaan Raik and Jaanus Lass for practical advice and Kaia Kalev for the time spent on the EEG recordings. I am very grateful to the staff of the Centre for Biomedical Engineering for their continuous support and helpful advice on the seminars.

Most importantly, I would like to thank my husband Mats Päeske for being there for me during these difficult times and for his dedication of time and energy so I would have time to focus on the thesis. I would like to thank my son Arko Päeske for his patience, the hours of sleep, and for always putting a smile on my face, and my daughter for bringing even more love to our lives.

The research was funded partly by the Estonian Ministry of Education and Research under institutional research financing IUT 19-2 and by the Estonian Centre of Excellence in IT (EXCITE) funded by the European Regional Development Fund.

Abstract

Assessment of electroencephalographic measures applied in the detection of depression

Depression is the leading cause of disability worldwide and a major contributor to the global burden of disease. However, currently, the diagnosis of depression is based on an evaluation of the intensity of subjective symptoms using clinical interviews and psychiatric questionnaires. The general aim of the thesis is to assess different aspects of resting-state electroencephalography (EEG) measures for the purpose of an objective marker to discriminate between healthy and depressed subjects.

Firstly, the thesis aimed to compare EEG measures and EEG channel regions in depression detection (**Publication I**). Three nonlinear measures: Higuchi fractal dimension (HFD), Lempel-Ziv complexity (LZC), and detrended fluctuation analysis (DFA), and three linear measures: spectral asymmetry index (SASI), alpha power variability (APV), and relative gamma power (RGP), as well as combinations of these measures, were compared. As a result, no specific EEG measure was concluded to be superior for the discrimination of depression in resting state. Furthermore, linear EEG measures provided classification accuracies similar to nonlinear EEG measures. The results of the thesis demonstrate that the EEG measures calculated for a single EEG channel did not provide lower depression classification accuracies than the multi-channel measures used in previous studies. The highest classification accuracies were found from central, temporal, and parietal regions.

Secondly, the thesis aimed to find the relationship between EEG alpha functional connectivity (FC) and small-worldness (SW) for healthy subjects (**Publication II**) and subjects with major depressive disorder (MDD). SW describes the organization of a network by estimating the trade-off between functional integration and segregation. Pearson correlation coefficient between FC and SW was calculated for three EEG measures: magnitude-squared coherence (MSC), imaginary part of coherency (ICOH), and synchronization likelihood (SL). As a result of **Publication II**, a statistically significant negative correlation occurred for all three FC measures for healthy subjects. Furthermore, the previously unpublished results of the thesis show that the same relationship between FC and SW is maintained in MDD. Based on the results, it was proposed in the thesis that decreased small-world organization of a brain network is compensated with increased alpha connectivity and the compensational mechanism works similarly for MDD and healthy subjects.

Thirdly, the thesis aimed to clarify the impact of an EEG alpha frequency component on the results of the surrogate data method (**Publication III**). For that reason, the percentage of segments where nonlinearity was detected was calculated for gradually incremented EEG segments. As a result, the degree of nonlinearity (DEG) was statistically significantly influenced by the incrementation of the segment within one alpha period for every nonlinear statistic that indicated nonlinearity: HFD, Katz fractal dimension (KFD), and sample entropy (SampEn). This result shows the importance of segmenting data according to the alpha frequency component for eyes-closed resting-state EEG when using the surrogate data method.

The current thesis shows the feasibility of using EEG measures for an objective marker to discriminate between subjects with depression and healthy subjects. However, for a marker applicable in clinical settings, further research is needed towards sufficiently high accuracy and reproducibility.

Lühikokkuvõte
Depressiooni avastamiseks kasutatavate elektroentsefalograafilise signaali mõõdikute analüüs

Depressioon on ülemaailmselt põhiline töövõimetuse põhjustaja ning oluline tegur haiguste poolt ühiskonnale põhjustatud koormusele. Sellele vaatamata põhineb hetkel depressiooni diagnoos kliinilistes intervjuudes ning psühhiaatrilistes küsimustikes avaldunud subjektiivsetele sümptomitele. Doktoritöö üldiseks eesmärgiks on analüüsida elektroentsefalograafilise (EEG) signaali mõõdikuid eesmärgiga luua objektiivne näidik depressioonis ja tervete uuritavate eristamiseks.

Esimesteks töö eesmärkideks oli võrrelda omavahel EEG mõõdikuid ja kanalite piirkondi depressiooni tuvastamisel (**Publikatsioon I**). Selleks võrreldi omavahel kolme mittelineaarset EEG mõõdikut, Higuchi fraktaaldimensioon (*Higuchi fractal dimension* – HFD), Lempel-Ziv keerukus (*Lempel-Ziv complexity* – LZC) ja vähendatud kõikumiste analüüs (*detrended fluctuation analysis* – DFA), kolme lineaarset mõõdikut, spektraalse asümmeetria indeks (*spectral asymmetry index* – SASI), alfa võimsuse dispersioon (*alpha power variability* – APV) ja suhteline gamma võimsus (*relative gamma power* – RGP) ning nende mõõdikute kombinatsioone. Doktoritöö tulemusena järeldati, et depressiooni tuvastamiseks rahuolekus ei töötanud ükski EEG mõõdikutest teistega võrreldes oluliselt paremini. Samuti leiti, et lineaarsed EEG mõõdikud andsid sarnaseid klassifitseerimistäpsusi võrreldes mittelineaarsete mõõdikutega. Sarnaselt, ühele EEG kanalile arvutatud mõõdikud ei andnud madalamaid klassifitseerimistäpsusi võrreldes mitmele EEG kanalile arvutatud mõõdikutega depressioonis ja tervete uuritavate eristamisel. Piirkonniti leiti parim eristatavus tsentraalsetest, temporaalsetest ja parietaalsetest kanalite regioonidest.

Kolmandaks töö eesmärgiks oli leida tervete (**Publikatsioon II**) ja depressioonis uuritavate jaoks seos EEG alfa funktsionaalse ühendatavuse ja väikse maailma mõõtme vahel. Väikese maailma mõõde kirjeldab võrgustiku organiseeritust, hinnates omavahel vastandliku funktsionaalse segregatsiooni ja integratsiooni suhet. Seose leidmiseks arvutati Pearsoni korrelatsioonikordaja funktsionaalse ühendatavuse ja väikse maailma mõõtme vahel kolme erineva EEG mõõdiku korral: koherentsuse reaalosa ruut (*magnitude-squared coherence* – MSC), koherentsuse imaginaarosa (*imaginary part of coherency* – ICOH) ja sünkronisatsiooni tõenäosus (*synchronization likelihood* – SL). **Publikatsiooni II** tulemusena leiti statistiliselt oluline negatiivne korrelatsioon kõigi kolme EEG mõõdiku korral tervetel uuritavatel. Doktoritöö uudse tulemusena leiti lisaks, et negatiivne korrelatsioon esines ka depressioonis uuritavatel funktsionaalse ühendatavuse ja väikese maailma mõõtme vahel. Tulemustele tuginedes pakuti doktoritöös välja, et vähenenud väikse maailma organiseeritus kompenseeritakse ajus suurenenud alfa ühenduste tugevusega ning kompenseerimise mehhanism töötab depressioonis ja tervete uuritavate korral sarnaselt.

Neljandaks töö eesmärgiks oli selgitada EEG alfa sageduskomponendi mõju surrogaatandmete meetodile (**Publikatsioon III**). Selleks suurendati vähehaaval EEG segmentide pikkust ning arvutati iga pikkuse jaoks segmentide protsent, milles esines mittelineaarsus. Töö tulemusena leiti, et mittelineaarsuse protsent oli statistiliselt oluliselt mõjutatud segmendi pikendamisest ühe alfa perioodi ulatuses iga mittelineaarse EEG mõõdiku korral, mis näitas mittelineaarsust: HFD, Katzi fraktaaldimensioon (*Katz fractal dimension* – KFD) ja valimientroopia (*sample entropy* – SampEn). Saadud tulemus

näitab, et surrogaatandmete meetodi puhul on oluline segmenteerida rahuoleku EEG aegrida vastavalt alfa sageduskomponendile.

Käesolev doktoritöö näitab, et EEG mõõdikuid saab rakendada depressioonis ja tervete uuritavate eristamiseks vajaliku objektiivse näidiku väljatöötamiseks. Kliinilises praktikas kasutatava näidiku loomiseks on aga vajalik edasine teadustöö, et tagada näidiku piisavalt kõrge klassifitseerimistäpsus ning korratavus.

Appendix 1 – Table of EEG Studies

Table 4. Resting-state EEG studies classifying between subjects with depression (depr) and healthy controls (HC).

Ref	Subjects	Features analyzed	Best features for classification	Brain areas	Highest classif accuracy
(Mahato & Paul, 2020)	30 MDD 30 HC	Absolute power of delta, theta, alpha, alpha1, alpha2, and beta and theta asymmetry	The combination of alpha2 and theta asymmetry	Signals from all brain areas used, best results not mentioned	88%
(Čukić et al., 2020b)	21 depr 20 HC	HFD and SampEn	SampEn	Signals from all brain areas used, best results not mentioned	98%
(Sun et al., 2019)	16 MDD 16 HC	Graph theory measures L, C, edge betweenness centrality, NBC, and modularity in theta and alpha frequency bands	NBC in alpha and C in theta	All regions analyzed, best results from left central region and right temporal region	88%
(Cai et al., 2018)	92 depr 121 HC	Centroid frequency, relative and absolute centroid frequency, relative and absolute power, peak, variance, skewness, kurtosis, Hjorth parameter, power-spectrum entropy, Shannon entropy, correlation dimension, c0-complexity, Kolmogorov entropy. All these features in delta, theta, alpha, beta, gamma, and full-band frequency bands	The combination of absolute power of theta, beta, and gamma waves and absolute center frequency of beta wave	Channels Fp1, Fp2, and Fpz used. Best results with Fp1 and Fp2	77%
(Mumtaz et al., 2018)	34 MDD 30 HC	SL, interhemispheric coherence, and mutual information	SL and the combination of SL, coherence, and mutual information	All brain regions covered. Best results from frontal, temporal, and occipital regions	98%

Ref	Subjects	Features analyzed	Best features for classification	Brain areas	Highest classif accuracy
(Acharya et al., 2018)	15 depr 15 HC	EEG signal segments	No measures compared	Channels FP1-T3 and FP2-T4. Better results with FP2-T4 (right hemisphere)	96%
(Lee et al., 2018)	50 depr 50 HC	Absolute power of delta, theta, low-alpha, high-alpha, and beta frequency bands	High-alpha and beta powers	All brain regions analyzed, significant results from left central region	70%
(Mumtaz et al., 2017)	33 MDD 30 HC	Alpha interhemispheric asymmetry and absolute power of delta, theta, alpha, and beta frequency bands	Interhemispheric alpha asymmetry and the combination of power and asymmetry features	Significant results from all areas, but most results from frontal	98%
(Bachmann et al., 2017)	17 depr 17 HC	SASI and DFA	SASI	All brain areas analyzed, best results from posterior channels PZ and O2	77%
(Liao et al., 2017)	12 MDD 12 HC	KEFB-CSP in the sub-bands with the width of 4 Hz from 4 Hz to 44 Hz, absolute power of theta, alpha, beta and gamma frequency bands, and fractal dimension	KEFB-CSP and alpha power	All brain areas used, best results from temporal region	81%
(Mohammadi et al., 2015)	53 MDD 43 HC	Absolute and log power of delta, theta, alpha1, alpha2, alpha total, and beta frequency bands in EO and EC conditions	With linked mastoids as reference, EO delta power. With CZ as reference, EC alpha power. Also, the combinations of delta, theta, alpha, and beta band powers	All regions used, best results from frontal, central, and posterior regions	89%
(Bachmann et al., 2013)	17 depr 17 HC	SASI and HFD	Equal accuracy for SASI and HFD	Frontal, temporal, parietal, and occipital regions used. Best results from parietal channels	85%

Ref	Subjects	Features analyzed	Best features for classification	Brain areas	Highest classif accuracy
(Hosseinifard et al., 2013)	45 depr 45 HC	Absolute power of delta, theta, alpha and beta frequency bands, DFA, HFD, correlation dimension, and Lyapunov exponent	Combination of DFA, HFD, correlation dimension and Lyapunov exponent	All brain areas used, more significant results found from left temporal and posterior regions	90%
(Puthankattil & Joseph, 2012)	30 depr 30 HC	Relative wavelet energy in different frequency bands	Frequency range 0-4 Hz	Channels FP1-T3 and FP2-T4. Similar results for both hemispheres	98%
(Ahmadlou et al., 2012)	12 MDD 12 HC	KFD and HFD in delta, theta, alpha, beta, and gamma frequency bands	HFD in beta frequency band	Frontal channels Fp1, Fp2, F3, F4, Fz, F7, and F8. More significant results from left hemisphere	91%
(Leuchter et al., 2012)	121 MDD 37 HC	Coherence in delta, theta, alpha, and beta frequency band	Alpha coherence	All regions analyzed, best results mostly from prefrontal region	81%
(Knott et al., 2001)	69 MDD 23 HC	Absolute and relative power, inter- and intra-hemispheric power asymmetry, frequency, and coherence for delta, theta, alpha, and beta frequency bands and frequency for full-band	Relative beta power, mean total frequency, alpha inter-hemispheric asymmetry, theta intra-hemispheric asymmetry, and delta, theta, alpha, and beta inter-hemispheric coherence	Frontal, parietal and occipital brain areas used. Results found from all scalp sites with the focus on anterior sites	91%

Appendix 2 – Publication I

Publication I

Bachmann, M., **Päeske, L.**, Kalev, K., Aarma, K., Lehtmets, A., Ööpik, P., Lass, J., & Hinrikus, H. (2018). Methods for classifying depression in single channel EEG using linear and nonlinear signal analysis. *Computer Methods and Programs in Biomedicine, 155*, 11−17. doi: 10.1016/j.cmpb.2017.11.023

Computer Methods and Programs in Biomedicine 155 (2018) 11–17

Contents lists available at ScienceDirect

Computer Methods and Programs in Biomedicine

journal homepage: www.elsevier.com/locate/cmpb

Methods for classifying depression in single channel EEG using linear and nonlinear signal analysis

Maie Bachmann[a,*], Laura Päeske[a], Kaia Kalev[a], Katrin Aarma[a], Andres Lehtmets[b], Pille Ööpik[c,d], Jaanus Lass[a], Hiie Hinrikus[a]

[a] Centre for Biomedical Engineering, Department of Health Technologies, Tallinn University of Technology, Ehitajate tee 5, Tallinn 19086, Estonia
[b] Psychiatric Centre, West Tallinn Central Hospital, Paldiski mnt 68, Tallinn 10617, Estonia
[c] Ädala Family Medicine Center, Madara tn 29, Tallinn 10612, Estonia
[d] Department of Family Medicine, University of Tartu, Ülikooli 18, Tartu 50090, Estonia

ARTICLE INFO

Article history:
Received 24 October 2016
Revised 14 November 2017
Accepted 24 November 2017

Keywords:
Depression
EEG
Spectral asymmetry index
Alpha power variability
Relative gamma power
Nonlinear signal processing

ABSTRACT

Background and Objective: Depressive disorder is one of the leading causes of burden of disease today and it is presumed to take the first place in the world in 2030. Early detection of depression requires a patient-friendly inexpensive method based on easily measurable objective indicators. This study aims to compare various single-channel electroencephalographic (EEG) measures in application for detection of depression.

Methods: The EEG recordings were performed on a group of 13 medication-free depressive outpatients and 13 gender and age matched controls. The recorded 30-channel EEG signal was analysed using linear methods spectral asymmetry index, alpha power variability and relative gamma power and nonlinear methods Higuchi's fractal dimension, detrended fluctuation analysis and Lempel-Ziv complexity. Classification accuracy between depressive and control subjects was calculated using logistic regression analysis with leave-one-out cross-validation. Calculations were performed separately for each EEG channel.

Results: All calculated measures indicated increase with depression. Maximal testing accuracy using a single measure was 81% for linear and 77% for nonlinear measures. Combination of two linear measures provides the accuracy of 88% and two nonlinear measures of 85%. Maximal classification accuracy of 92% was indicated using mixed combination of three linear and three nonlinear measures.

Conclusions: The results of this preliminary study confirm that single-channel EEG analysis, employing the combination of measures, can provide discrimination of depression at the level of multichannel EEG analysis. The performed study shows that there is no single superior measure for detection of depression.

1. Introduction

Depression and other mental disorders related to the fast rhythm of life and everyday stress have a rising trend in our society. According to World Health Organization report, unipolar depressive disorder is a leading cause of burden of disease in high- and middle-income countries today and it is presumed to take the first place in the world in 2030 [1]. Nowadays, the diagnosis of depression is based mainly on evaluation of the intensity of subjective symptoms using clinical interview and psychiatric questionnaires. Detection of declinations in brain physiology before the subjective symptoms appear is crucial for early detection of depression, enabling treatment that is more effective and improving quality of mental health.

Any declinations in the brain neuronal activity and mental state are expected to be reflected in the brain bioelectrical activity. Electroencephalography (EEG) is easily available, cost-effective technique, providing high temporal resolution for evaluation of the dynamics of bioelectric activity of the brain. EEG features have been successfully applied for investigation of brain behaviour in various mental diseases [2–8]. A method distinguishing depression based on analysis of single-channel EEG can be promising to be integrated in a simple user-friendly device for regular evaluation of the state of brain.

Multichannel quantitative EEG characteristics have been under consideration for investigation of depression in many studies [6,7,9]. Specific depression EEG features have been detected using changes in EEG bands powers, coherence and interhemispheric asymmetry [6,7,10]. Resting state neurophysiologic connectivity is increased broadly across all brain regions in depression [7]. Discriminant analysis of quantitative EEG from 21 electrodes classi-

* Corresponding author.
E-mail address: maie@cb.ttu.ee (M. Bachmann).

https://doi.org/10.1016/j.cmpb.2017.11.023
0169-2607/

fied correctly 91.3% of the patients and controls whereas mainly delta and beta inter-hemispheric coherence, beta intra-hemispheric coherence and alpha intra-hemispheric power asymmetry contributed to the classification [6]. However, coherence appeared ineffective in the case of smaller number of channels [11]. In addition, there is evidence that frontal alpha asymmetry across assessment occasions was not closely linked to depression severity [10] and the validity potential as a clinical measure for depression still remains unclear [12].

Nonlinear complexity analysis of EEG is promising for obtaining additional information to that achieved by linear measures. Higuchi's fractal dimension (HFD) indicates increased complexity with depression compared to healthy controls in all brain areas [13,14]. A high accuracy of 91.3% was reported for classification of depression using enhanced probabilistic neural network and signals from 7 frontal EEG channels [13].

Detrended fluctuation analysis (DFA) has been used in resting and sleep EEG studies in depression [15,16]. The analysis of 8-channel EEG showed relatively higher values of scaling exponents of depressed patients compared to healthy controls in all brain regions [15]. Major depressive episodes are characterized by a modification in the correlation structure of the sleep EEG time series [16].

The Lempel-Ziv complexity (LZC) of multichannel resting EEG has been reported being successful in evaluation of various neuronal and mental disorders including major depression [17–19].

Machine learning algorithms combining linear (power of four EEG bands) and nonlinear (DFA, HFD, correlation dimension, Lyapunov exponent) features from 19 EEG electrodes discriminate successfully depressive and healthy groups [20]. Logistic regression classifier provided the classification accuracy of 90% using all nonlinear features as input [20]. However, comparable evaluation between various input features was not performed.

Classification of depression based on a single channel EEG signal analysis has been considered in very few studies. Spectral asymmetry index (SASI) was successfully applied for detection of depression employing single channel EEG [11,14]. The method, based on the evaluation of the balance of powers in two frequency bands selected higher and lower than the alpha band spectrum maximum in single channel EEG, provided classification accuracy of 85% comparable to that of HFD results [14].

Current study aims to identify the most sensitive EEG analysis method and channels for detection of depression based on the signal from a single EEG channel. For this purpose, the effectiveness of various linear and nonlinear EEG analysis methods was compared in each single EEG channel using statistical differences and classification accuracies as the indicators. Three linear and three nonlinear methods SASI, EEG alpha band power variability (APV), relative gamma power (RGP), HFD, DFA, and LZC, were selected. The comparisons were performed in each single EEG channel.

2. Methods

2.1. Subjects and recording protocol

The EEG data were obtained from a group of medication-free right-handed outpatients with major depressive disorder and from age, gender and handedness matched control group. Both groups consisted of 13 subjects (5 male and 8 female) with a mean age of 38.7 and standard deviation 15.8 years. All five-year subgroups between youngest 18 and oldest 66 were presented. The subjects were asked to abstain from coffee for two hours and from alcohol for 24 h before the experiment. All patients underwent a clinical interview and were diagnosed with a single (9 patients) or recurrent (4 patients) depressive episode based on ICD-10 criteria. Healthy controls completed the official Estonian self-report questionnaire (Emotional State Questionnaire – EST-Q) for depression and anxiety and the subjects without inclination to these mental disorders were selected.

The study was conducted in accordance with the Declaration of Helsinki and was formally approved by the Tallinn Medical Research Ethics Committee. All subjects signed written informed consent.

The study procedure included continuous EEG recording performed between 9 a.m. and noon – two minutes eyes open followed by 30 min eyes closed recording. During the procedure, participants were lying in relaxed position in dimly lit laboratory room; to exclude the auditory stressors, earplugs were used.

2.2. Data acquisition

The EEG signals were recorded using Neuroscan Synamps2 acquisition system (Compumedics, NC, USA). Thirty EEG channels were placed according to the International 10/20 extended system. The average of mastoids (M1, M2) was selected as reference and horizontal and vertical electro-oculograms (EOG) were recorded. Raw EEG signals were recorded with a frequency band of 0.3–200 Hz at a sampling rate of 1000 Hz. The impedance of recording electrodes was below 10 kΩ.

The raw EEG signals were digitally filtered at the cutoff frequencies of 0.5 Hz and 46 Hz. The signals were visually inspected and signal segments with artefacts were removed. The further analysis was performed on 5 min eyes-closed artefacts-free EEG signals. MATLAB software was used for EEG signal processing.

2.3. EEG analysis: linear measures

Three EEG linear measures were calculated based on signal power in different EEG frequency bands. All selected linear measures use relative combinations of powers in different EEG frequency bands to exclude dependence on the absolute values of the powers.

SASI uses subject-specific frequency bands, excluding individual alpha frequency band, while including individual theta and beta frequency bands. Compared to traditional quantitative EEG frequency bands with fixed boundary frequencies the selected individual theta and beta frequency bands are related to the central frequency F_c of EEG spectrum maximum in alpha band [11] and are calculated for each person individually. Consequently, individual modified theta band has limits from $(F_c - 6)$ Hz to $(F_c - 2)$ Hz and modified beta from $(F_c + 2)$ Hz to $(F_c + 26)$ Hz [11].

SASI was selected as a measure providing promising results in detection of depression based on single channel EEG analysis. SASI describes the asymmetry of EEG spectrum as the balance of powers in modified theta and beta bands. Powers in the frequency bands were calculated as

$$P_{\delta mn} = \sum_{f_i=F_c-6}^{f_i=F_c-2} s_{mn} \qquad and \tag{1}$$

$$P_{\beta mn} = \sum_{f_i=F_c+2}^{f_i=F_c+26} s_{mn}, \tag{2}$$

where S_{mn} is the power of the recorded EEG signal in a unit band at the frequency f_i in a channel m for a subject n. SASI in a channel m for a subject n is calculated as

$$SASI_{mn} = \frac{P_{\beta mn} - P_{\delta mn}}{P_{\beta mn} + P_{\delta mn}}. \tag{3}$$

EEG alpha band is excluded in calculation of SASI. However, alpha oscillations emerge from network properties of cortical tissue and EEG alpha rhythm is supposed to characterize fundamental brain

behaviour [21]. Biophysical model of EEG generation demonstrated that thalamo-cortical mechanisms, such as the resonance properties of feedforward, cortico-thalamo-cortical, and intra-cortical circuits, are underlying changes in amplitude and frequency of alpha oscillations [22]. Instability of the alpha rhythm amplitude and power are expected to be related to the disturbances in brain functioning.

Therefore, APV is proposed in this study as a measure to detect depression. Calculation of APV in fixed frequency bands provides indication of both, alpha power and frequency variations. Therefore, 8–12 Hz was used. APV in selected time-window was calculated in three steps. First, alpha band signal power in time-window T was calculated as

$$W_i = \frac{1}{N}\sum_{r=1}^{N}[V(r)]^2, \tag{4}$$

where $V(r)$ is the amplitude of the recorded signal in a sample r and N is the number of samples in the time-window T. In the selected time-window of 2 s N = 2000. Further, the calculated W_i values were averaged over 5 min recording and standard deviation was calculated as

$$\sigma = \frac{1}{M}\sum_{i=1}^{i=M}(W_i - W_0)^2, \tag{5}$$

where W_0 is the value of alpha band power averaged over 5 min.

Finally, APV was calculated as

$$APV = \frac{\sigma}{W_0}. \tag{6}$$

The impact of EEG gamma band power to SASI values is minimal due to low level of EEG power density in gamma band compared to beta and theta bands. Gamma band is excluded also from APV calculations. However, higher EEG frequencies in gamma band can also be affected by depression [23]. Therefore, relative gamma power (RGP) as an additional measure was introduced.

$$RGP_{mn} = \frac{P_{\gamma mn}}{P_{\Sigma mn}}, \tag{7}$$

$$\text{where } P_{\gamma mn} = \sum_{f_i=30}^{f_i=46} s_{mn} \qquad and \tag{8}$$

$$P_{\Sigma mn} = \sum_{f_i=3}^{f_i=46} s_{mn}. \tag{9}$$

2.4. EEG analysis: nonlinear measures

All nonlinear features were calculated for 10-second segments (2000 samples). A nonlinear measure was found as a median value averaged over all segments for a signal of 5 min length.

HFD algorithm calculates fractal dimension of time series directly in the time domain [24]. It is based on a measure of length $L(k)$ of the curve that represents the considered time series while using a segment of k samples as a unit if $L(k)$ scales like

$$L(k) \sim k^{-FD} \tag{10}$$

The value of fractal dimension FD with a parameter $k_{max} = 8$ was calculated according to the algorithm presented by Higuchi [24].

DFA was calculated directly in the time domain according to the steps described by Peng et al [25,26]. First, the EEG signal segment $x(i)$, where i is the length of the segment ranging from 1 to N (N = 2000), was integrated to generate a new time series $y(k)$,

$$y(k) = \sum_{i=1}^{k}[x(i) - \bar{x}] \quad k = 1, \ldots, N \tag{11}$$

where $\bar{x}$ is the average of the EEG signal $x(i)$. After that the new time series $y(k)$ is divided into n equal windows. Window length started from 4 samples up to 200 samples varying equidistantly on logarithmic scale (0.02 s up to 1.00 s). The maximum window length was selected as 1/10 of the signal segment length [27]. In each window n, the least squares line, $y_n(k)$, is fit to the data $y(k)$. The fitting range was chosen from 0.1 s, excluding the prominent alpha frequency [28], to 1.0 s, as brain often suppresses large fluctuations on longer timescales [29]. Next, the local trend $y_n(k)$ is subtracted from the data $y(k)$. The root mean square fluctuation of the demeaned, integrated and detrended signal segment is calculated as:

$$F(n) = \sqrt{\frac{1}{N}\sum_{k=1}^{N}[y(k) - y_n(k)]^2}. \tag{12}$$

Those final steps are repeated for all window sizes giving the average fluctuations as a function of window length. Those fluctuations are expected to increase with the window length. The scaling is present in case on a log-log graph of F(n) vs. n appears a linear correlation. The slope of the line, that is the scaling exponent α, relating logF(n) to logn describes the type of scaling.

For LZC calculation each signal segment is converted into binary sequence $s(n)$ as follows [30]:

$$s(n) = \begin{cases} 1, & if \quad x(n) > m \\ 0, & if \quad x(n) \le m \end{cases}, \tag{13}$$

where $x(n)$ is the signal segment, n is the segment's sample index from 1 to N (segment length) and m is the threshold value. The segment length N was chosen 2000 samples – a value for which the traditional LZC is stabilized [31]. For threshold m, signal median value was preferred considering outliers [32].

Thereafter, the resulting binary sequence s(n) is scanned from left to right counting the number of different patterns occurring. The complexity value c(n) is increased every time a new pattern is encountered. The detailed description of the algorithm can be found in [33].

It has been previously proven [32] that the upper bound of $c(n)$ is

$$\lim_{n\to\infty} c(n) = b(N) = \frac{N}{\log_a N} \tag{14}$$

where a is the number of different patterns, and N is the segment length. In order to avoid the variations due to the segment length, normalized LZC values are calculated as follows:

$$C(N) = \frac{c(N)}{b(N)} \tag{15}$$

2.5. Statistics and classification

Current study aims to identify the most sensitive EEG analysis method for detection of depression based on the signal from a single EEG channel. Therefore, a statistical analysis was performed separately in each EEG channel. The Mann-Whitney test was performed to evaluate statistical difference between depressive and control group for each of the calculated measures and channels. Logistic regression classifier (LR) with leave-one-out (LOO) cross-validation was selected as a classifier, which has previously provided highest classification accuracy between depressive and healthy subjects [20]. The classification accuracy was calculated using separate measures or their combinations as input for LOO cross-validation in each single EEG channel. The parallel testing of multiple models was taken into account by randomly permuting the labels and creating null distribution from maximum classification accuracies of each permutation.

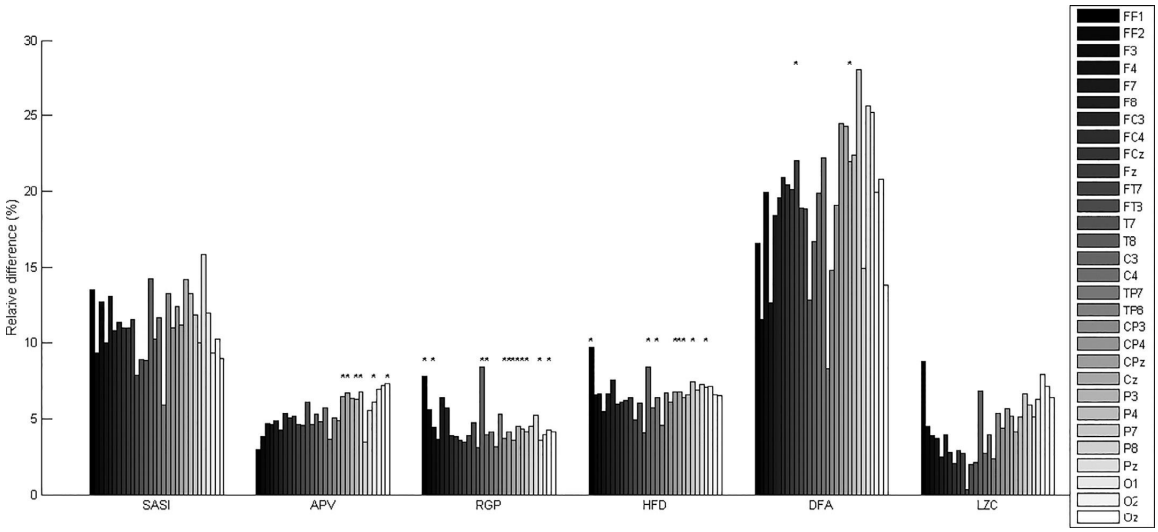

Fig. 1. Effect of depression on EEG linear (SASI, APV, RGP) and nonlinear (HFD, DFA, LZC) measures in all analysed EEG channels as relative difference between values of a measure averaged over all subjects in depressive and control group. Asterisks represent statistically significant differences after permutation testing for multiple comparisons ($p < .05$).

3. Results

Fig. 1 presents the differences between calculated measures for depressive and control group in each EEG channel. The calculated linear (SASI, APV, RGP) and nonlinear (HFD, DFA, LZC) measures are higher in depressive group compared to control group in all channels. However, the enhancement of the measures with depression is not always statistically significant. For some measures (APV, RGP and HFD) the differences between the depressive and control groups appear statistically significant in a number of EEG channels, while the differences in SASI and LZC values do not reach the level of statistical significance after considering the multiple comparisons using permutation testing.

Table 1 presents classification accuracies between depressive and healthy subjects employing linear measures in each single EEG channel. The LR classification accuracy of 81% was achieved by solely APV or RGP measures. Combining two linear measures, SASI and RGP, even higher classification accuracy of 88% was reached. Adding the third measure to the combinations did not improve the quality of classification. Considering EEG channel locations, the trend of higher classification accuracy occurs in central, temporal and parietal regions.

Results of classification based on the nonlinear measures of EEG are presented in Table 2. The best accuracy of single measure, 77%, appears in centro-parietal brain region using HFD or DFA. The best classification rate achieved by single nonlinear measure is lower than the one achieved by single linear measure (Table 1). Similar trend continues while combining two non-linear measures. The highest accuracy of 85% is achieved by combination of HFD and LZC measures. Once more, the linear measures outweigh the nonlinear ones. Nevertheless, nonlinear measures reach the trend of higher classification values more broadly, covering also the frontal brain areas. In addition, the quality of classification of nonlinear measures reaches also 88% while adding the third nonlinear measure to the combinations. The trend of higher quality of classification appears in frontal, central and temporal brain areas.

Combining all linear and nonlinear measures a classification accuracy up to 92% was achieved in central region.

4. Discussion

The experimental results presented above show that the features related to depression are evident in all EEG channels. This was reflected in the increase of linear EEG measures (SASI, APV and RGP) as well as nonlinear complexity measures (HFD, DFA and LZC) in all EEG channels due to depression (Fig. 1). Some of the measures (APV, RGP, HFD) indicate significant differences in EEG behaviour between depressive and control group for a number of EEG channels. These results are in good agreement with the earlier study which demonstrated that depression affected brain activity in nearly the whole cortex, rather than only in the frontal and/or parietal areas [9].

The Tables 1 and 2 show that higher discrimination ability between control and depressive subjects occurs in central, temporal and parietal regions for linear and in frontal, central, temporal brain areas for nonlinear measures.

Enhancement of SASI and RGP can occur if EEG power in higher frequency bands (beta and gamma) increases with depression. The conclusion about increased beta power in depression is supported by findings reported by other authors [6,8,34]. Gamma band is usually not considered in evaluation of depression because approximately 98% of spectral power lies within 0.5–30 Hz limits [9,20]. Our results for single measure indicate one of the highest accuracy for RGP. This result is in agreement with the findings that gamma power is significantly greater in depressive patients compared to healthy controls [22,33].

Instability of the alpha rhythm amplitude and frequency are expected being related to the disturbances in brain functioning [22]. Therefore, it is not surprising that APV is more informative EEG feature for detection of depression compared to traditional alpha power. To the best of our knowledge, the proposed measure, APV, is new and not used in previous depression EEG studies. Depression without cardiovascular disease has been reported being associated with reduced heart rate variability (HRV) [35]. Our experimental results indicated increased APV in depression.

The best accuracy considering nonlinear measures is achieved with HFD and DFA in current study. Similar trend of enhancement

Table 1
Classification accuracy, indicated by logistic regression analysis with leave-one-out cross-validation using linear EEG measures as input. Grey background marks statistical significance ($p < .05$) after permutation testing. MaxM indicates maximal accuracy for a measure; MaxC indicates maximal accuracy in an EEG channel.

	SASI	APV	RGP	SASI& APV	SASI& RGP	APV& RGP	SAI& APV& RGP	MaxC
FP1	0,58	0,58	0,62	0,58	0,69	0,54	0,54	**0,69**
F7	0,65	0,58	0,73	0,65	0,69	0,73	0,73	**0,73**
FP2	0,50	0,65	0,58	0,54	0,62	0,58	0,58	**0,65**
F3	0,65	0,62	0,69	0,54	0,73	0,65	0,65	**0,73**
FC3	0,58	0,62	0,73	0,62	0,73	0,62	0,62	**0,73**
FT7	0,69	0,62	0,69	0,58	0,65	0,58	0,58	**0,69**
T7	0,65	0,65	0,69	0,54	0,65	0,65	0,65	**0,69**
F8	0,54	0,54	0,69	0,50	0,62	0,69	0,69	**0,69**
F4	0,62	0,62	0,62	0,50	0,69	0,54	0,54	**0,69**
FZ	0,50	0,58	0,69	0,54	0,73	0,58	0,58	**0,73**
FCZ	0,50	0,62	0,69	0,54	**0,88**	0,65	0,65	**0,88**
C3	0,58	0,69	0,62	0,65	**0,85**	0,62	0,62	**0,85**
TP7	0,58	0,69	0,62	0,65	0,62	0,69	0,69	**0,69**
FT8	0,58	0,58	0,65	0,65	0,58	0,62	0,62	**0,65**
FC4	0,54	0,65	0,65	0,46	0,77	0,62	0,62	**0,77**
CZ	0,65	0,62	0,73	0,58	**0,81**	0,69	0,69	**0,81**
CPZ	0,62	0,73	0,73	0,69	**0,85**	0,65	0,65	**0,85**
CP3	0,65	0,58	0,69	0,65	0,77	0,73	0,73	**0,77**
P3	0,65	0,69	0,77	0,69	0,69	0,73	0,73	**0,77**
P7	0,73	0,58	0,73	0,77	0,69	0,77	0,77	**0,77**
T8	0,65	0,62	0,69	0,65	0,73	**0,81**	**0,81**	**0,81**
TP8	0,69	0,65	0,73	0,65	0,69	0,69	0,69	**0,73**
C4	0,65	0,69	0,69	0,65	**0,85**	0,65	0,65	**0,85**
P8	0,77	0,62	**0,81**	0,69	**0,81**	0,65	0,65	**0,81**
CP4	0,58	**0,81**	0,77	0,73	**0,81**	0,77	0,77	**0,81**
P4	0,58	0,77	0,73	0,65	0,73	0,73	0,73	**0,77**
PZ	0,62	0,69	0,69	0,65	0,77	0,73	0,73	**0,77**
OZ	0,65	0,65	0,69	0,65	0,65	0,65	0,65	**0,69**
O1	0,65	0,65	0,69	0,62	0,62	0,62	0,62	**0,69**
O2	0,73	0,65	0,73	0,65	0,65	0,65	0,65	**0,73**
MaxM	**0,77**	**0,81**	**0,81**	**0,77**	**0,88**	**0,81**	**0,81**	

of fractal dimension with depression has been reported also in other study [13]. Nonlinear methods HFD and DFA have demonstrated also successful classification of depression EEG [13,20].

A higher LZC in depression than control group [18] is in good agreement with our results. However, in our study the LZC differences between depressive and control groups do not reach the level of statistical significance after permutation testing. Lower detectability of LZC compared to other complexity methods is caused by the nature of the method: LZC is guided by variation of slow EEG rhythms due to higher amplitude values, overlooking the higher frequency components of lower values. EEG power measures demonstrate the importance of higher EEG frequencies to discriminate depression. Therefore, it is not surprising that LCZ has somewhat lower sensitivity compared to HFD and DFA.

The increase of all selected features with depression can provide evidence, that depression disturbs brain neurophysiology and, as a response, causes activation of compensatory processes accompanied with increased frequency of neuronal oscillations (indicated by RGP and SASI), increased instability (indicated by APV) and complexity (indicated by HFD, DFA, and LZC) of the oscillations.

The classification accuracy of depressive and healthy subjects based on linear EEG measures (Table 1) is comparable to that based on nonlinear measures (Table 2). The accuracy of 88% achieved in single channel EEG signal using two linear measures (Table 1) is higher compared to classification accuracy of 76.6% reported in the study where three linear features and signals from 19 electrodes were used [20]. Higher sensitivities of selected linear measures (SASI, APV and RGP) compared to traditional EEG frequency band powers can be explained with more specific approach used in this study taking into account the powers' balance, power variability and higher frequencies.

The results of the current study demonstrated that linear EEG methods provided comparable or even better classification accu-

Table 2
Classification accuracy indicated by logistic regression analysis with leave-one-out cross-validation using nonlinear EEG measures as input. Grey background marks statistical significance ($p < .05$) after permutation testing. MaxM indicates maximal accuracy for a measure; MaxC indicates maximal accuracy in an EEG channel.

	HFD	DFA	LZC	HFD& DFA	HFD& LZC	DFA& LZC	HFD& DFA& LZC	MaxC
FP1	0,65	0,65	0,50	0,65	0,73	0,62	0,69	0,73
F7	0,65	0,62	0,42	0,65	0,77	0,62	0,77	0,77
FP2	0,58	0,58	0,50	0,62	0,62	0,58	0,58	0,62
F3	0,65	0,69	0,46	0,77	**0,85**	0,69	**0,85**	**0,85**
FC3	0,65	0,65	0,46	0,73	**0,85**	0,73	**0,88**	**0,88**
FT7	0,69	0,65	0,27	0,65	0,77	0,62	0,77	0,77
T7	0,69	0,69	0,42	0,65	0,58	0,62	0,62	0,69
F8	0,65	0,62	0,58	0,73	0,73	0,62	**0,81**	**0,81**
F4	0,62	0,65	0,46	0,69	0,65	0,65	0,65	0,69
FZ	0,62	0,65	0,46	0,69	**0,81**	0,69	0,73	**0,81**
FCZ	0,58	0,65	0,46	0,73	0,77	0,73	0,77	0,77
C3	0,65	0,69	0,50	0,77	**0,85**	0,77	0,77	**0,85**
TP7	0,65	0,69	0,58	0,58	0,77	0,65	0,73	0,77
FT8	0,69	0,65	0,42	0,69	**0,81**	0,65	**0,81**	**0,81**
FC4	0,65	0,65	0,46	0,73	**0,81**	0,65	0,77	**0,81**
CZ	0,62	0,69	0,46	0,73	**0,81**	0,73	0,77	**0,81**
CPZ	0,69	0,65	0,46	**0,81**	0,77	0,77	0,77	**0,81**
CP3	0,69	0,69	0,50	**0,81**	**0,81**	**0,81**	0,73	**0,81**
P3	0,65	0,77	0,62	0,69	0,69	**0,81**	0,65	**0,81**
P7	0,73	0,69	0,65	0,69	0,73	0,62	0,69	0,73
T8	0,73	0,62	0,62	**0,81**	**0,85**	0,77	**0,81**	**0,85**
TP8	0,77	0,62	0,58	0,73	0,69	0,73	0,73	0,77
C4	0,62	0,65	0,46	0,77	**0,85**	0,73	**0,88**	**0,88**
P8	0,77	0,62	0,58	0,77	0,77	0,77	0,69	0,77
CP4	0,69	0,65	0,46	0,77	0,73	**0,81**	0,77	**0,81**
P4	0,62	0,62	0,58	0,73	0,77	0,73	0,77	0,77
PZ	0,65	0,65	0,62	0,69	0,73	0,73	0,65	0,73
OZ	0,62	0,50	0,58	0,62	0,65	0,58	0,62	0,65
O1	0,69	0,58	0,69	0,65	0,65	0,62	0,58	0,69
O2	0,62	0,50	0,54	0,58	0,58	0,65	0,62	0,65
MaxM	0,77	0,77	0,69	**0,81**	**0,85**	**0,81**	**0,88**	

racies compared to nonlinear EEG measures for discrimination of depression.

The maximum classification accuracy of 77%, based on a single nonlinear measure HFD (Table 2) is the same as based on a single linear measure SASI (Table 1). This is in agreement with previous results indicating comparable sensitivity of SASI and HFD in detection of small changes in brain bioelectrical activity related to depression or environmental factors [14,36]. Combination of two linear measures, SASI and RGP, shows somewhat higher accuracy of 88% (Table 1) compared to the accuracy of the best combination of two nonlinear measures HFD and LZC of 85% (Table 2). Although, the differences between depressive and control group detected by SASI or LZC do not reach the level of statistical significance after permutation testing, the methods consist valuable information improving the combined classification accuracies.

The accuracy of 92% achieved in single channel EEG using 3 linear and 3 nonlinear measures is higher compared to the accuracy of 90% achieved using 4 nonlinear features and signals from 19 channels [20]. The possible explanation is the involvement of higher EEG frequencies in current calculations. It seems likely that the impact of EEG gamma band power, despite of its relatively small value, is important for discrimination of depression.

The main purpose of the study was to find an easily measurable indicator to differentiate subjects with depression from control subjects. The selected measures are not dedicated for classification between various mental disorders but only for detection of declination in EEG for revealing major depressive disorder. Clinical diagnoses should be determined by a medical doctor.

Good ability of EEG frequency bands power has been reported for discrimination of major and bipolar depression and to predict the therapeutic response in several publications [37,38]. Further investigations are required to clarify the ability of the proposed EEG measures to detect mental disorders other than major depression or to evaluate therapeutic response.

The current preliminary study has limitations due to small number of subjects caused by the problem of finding medication-free depressive patients. Limited number of subjects in subgroups of different age and gender did not allow getting reliable data about age and gender dependencies affecting the results. Further investigations on larger groups of different age and gender are needed for the clarification of age and gender corrections necessity.

Single channel EEG analysis has an advantage compared to multichannel EEG analysis, because it is easily implementable into a patient-friendly inexpensive EEG device, applicable for screening in occupational and family medicine centres.

5. Conclusions

The results of the performed preliminary study confirm that single-channel EEG analysis, employing the combination of measures, can provide the accuracy for discrimination of depression not lower than reported in other studies where multichannel EEG signals were analysed.

The performed analysis indicates no single superior measure for detection of depression.

Conflict of interest

The authors declare no conflict of interest.

Acknowledgment

This study was financially supported by the Estonian Ministry of Education and Research under Institutional Research Financing (IUT 19-2) and by the European Union through the European Regional Development Fund. The funding sources were not involved in research and publishing.

References

[1] WHO, The Global Burden Of Disease: 2004 Update, WHO, 2014.
[2] D. Abásolo, J. Escudero, R. Hornero, C. Gómez, P. Espino, Approximate entropy and auto mutual information analysis of the electroencephalogram in Alzheimer's disease patients, Med. Biol. Eng. Comput. 46 (10) (2008) 1019–1028.
[3] D. Abásolo, R. Hornero, J. Escudero, P. Espino, A study on the possible usefulness of detrended fluctuation analysis of the electroencephalogram background activity in Alzheimer's disease, IEEE Trans. Biomed. Eng. 55 (9) (2008) 2171–2179.
[4] A.A. Fingelkurts, A.A. Fingelkurts, Altered structure of dynamic electroencephalogram oscillatory pattern in major depression, Biol. Psychiatry 77 (12) (2015) 1050–1060.
[5] P. Ghorbanian, D.M. Devilbiss, T. Hess, A. Bernstein, A.J. Simon, H. Ashrafiuon, Exploration of EEG features of Alzheimer's disease using continuous wavelet transform, Med. Biol. Eng. Comput. 53 (9) (2015) 843–855.
[6] V. Knott, C. Mahoney, S. Kennedy, K. Evans, EEG power, frequency, asymmetry and coherence in male depression, Psych. Res 106 (2) (2001) 123–140.
[7] A.F. Leuchter, I.A. Cook, A.M. Hunter, C. Cai, S. Horvath, Resting-state quantitative electroencephalography reveals increased neurophysiologic connectivity in depression, PLoS One 7 (2) (2012) e32508.
[8] H. Hinrikus, A. Suhhova, M. Bachmann, K. Aadamsoo, Ü. Vohma, H. Pehlak, J. Lass, Spectral features of EEG in depression, Biomed. Tech. 55 (3) (2010) 155–161.
[9] A.A. Fingelkurts, A.A. Fingelkurts, H. Rytsälä, K. Suominen, E. Isometsä, S. Kähkönen, Composition of brain oscillations in ongoing EEG during major depression disorder, Neurosci. Res. 56 (2) (2006) 133–144.
[10] J.J.B. Allen, H.L. Urry, S.K. Hitt, J.A. Coan, The stability of resting frontal electroencephalographic asymmetry in depression, Psychophysiology 41 (2) (2004) 269–280.
[11] H. Hinrikus, A. Suhhova, M. Bachmann, K. Aadamsoo, U. Võhma, J. Lass, V. Tuulik, Electroencephalographic spectral asymmetry index for detection of depression, Med. Biol. Eng. Comput. 47 (12) (2009) 1291–1299.
[12] C. Gold, J. Fachner, J. Erkkilä, Validity and reliability of electroencephalographic frontal alpha asymmetry and frontal midline theta as biomarkers for depression, Scand. J. Psychol. 54 (2) (2013) 118–126.
[13] M. Ahmadlou, H. Adeli, A. Adeli, Fractality analysis of frontal brain in major depressive disorder, Int. J. Psychophysiol. 85 (2) (2012) 206–211.
[14] M. Bachmann, J. Lass, A. Suhhova, H. Hinrikus, Spectral asymmetry and Higuchi's fractal dimension measures of depression electroencephalogram, Comput. Math. Methods Med. 2013 (2013) 251638.
[15] J.-S. Lee, B.-H. Yang, J.-H. Lee, J.-H. Choi, I.-G. Choi, S.-B. Kim, Detrended fluctuation analysis of resting EEG in depressed outpatients and healthy controls, Clin. Neurophysiol. 118 (11) (2007) 2489–2496.
[16] S. Leistedt, M. Dumont, J.-P. Lanquart, F. Jurysta, P. Linkowski, Characterization of the sleep EEG in acutely depressed men using detrended fluctuation analysis, Clin. Neurophysiol. 118 (4) (2007) 940–950.
[17] M. Bachmann, K. Kalev, A. Suhhova, J. Lass, H. Hinrikus, Lempel ziv complexity of EEG in depression, in: IFMBE Proceedings, 2015, pp. 58–61.
[18] Y. Li, S. Tong, D. Liu, Y. Gai, X. Wang, J. Wang, Y. Qiu, Y. Zhu, Abnormal EEG complexity in patients with schizophrenia and depression, Clin. Neurophysiol. 119 (6) (2008) 1232–1241.
[19] M.A. Méndez, P. Zuluaga, R. Hornero, C. Gómez, J. Escudero, A. Rodríguez–Palancas, T. Ortiz, A. Fernández, Complexity analysis of spontaneous brain activity: effects of depression and antidepressant treatment, J. Psychopharmacol. 26 (5) (2012) 636–643.
[20] B. Hosseinifard, M.H. Moradi, R. Rostami, Classifying depression patients and normal subjects using machine learning techniques and nonlinear features from EEG signal, Comput. Methods Programs Biomed. 109 (3) (2013) 339–345.
[21] P.L. Nunez, B.A. Cutillo, Neocortical Dynamics and Human EEG Rhythms, Oxford University Press, 1995.
[22] R. Hindriks, M.J.A.M. van Putten, Thalamo-cortical mechanisms underlying changes in amplitude and frequency of human alpha oscillations, Neuroimage 70 (2013) 150–163.
[23] J.L. Tekell, R. Hoffmann, W. Hendrickse, R.W. Greene, A.J. Rush, R. Armitage, High frequency EEG activity during sleep: characteristics in schizophrenia and depression, Clin. EEG Neurosci. 36 (1) (2005) 25–35.
[24] T. Higuchi, Approach to an irregular time series on the basis of the fractal theory, Phys. D Nonlinear Phenom. 31 (2) (1988) 277–283.
[25] C.K. Peng, S.V Buldyrev, S. Havlin, M. Simons, H.E. Stanley, A.L. Goldberger, Mosaic organization of DNA nucleotides, Phys. Rev. E. Stat. Phys. Plasmas. Fluids. Relat. Interdiscip. Topics 49 (2) (1994) 1685–1689.
[26] C.K. Peng, S. Havlin, H.E. Stanley, A.L. Goldberger, Quantification of scaling exponents and crossover phenomena in nonstationary heartbeat time series, Chaos 5 (1) (1995) 82–87.
[27] K. Hu, P.C. Ivanov, Z. Chen, P. Carpena, H.E. Stanley, Effect of trends on detrended fluctuation analysis, Phys. Rev. E. Stat. Nonlin. Soft Matter Phys. 64 (1) (2001) Pt 1, p. 11114.
[28] P.A. Robinson, Interpretation of scaling properties of electroencephalographic fluctuations via spectral analysis and underlying physiology, Phys. Rev. E 67 (3) (2003) 32902.
[29] J.W. Kim, H.-B. Shin, P.A. Robinson, Quantitative study of the sleep onset period via detrended fluctuation analysis: normal vs. narcoleptic subjects, Clin. Neurophysiol. 120 (7) (2009) 1245–1251.
[30] M. Aboy, R. Hornero, D. Abásolo, D. Alvarez, Interpretation of the Lempel-Ziv complexity measure in the context of biomedical signal analysis, IEEE Trans. Biomed. Eng. 53 (11) (2006) 2282–2288.
[31] C. Gómez, R. Hornero, D. Abásolo, A. Fernández, M. López, Complexity analysis of the magnetoencephalogram background activity in Alzheimer's disease patients, Med. Eng. Phys. 28 (9) (2006) 851–859.
[32] R. Nagarajan, Quantifying physiological data with Lempel-Ziv complexity–certain issues, IEEE Trans. Biomed. Eng. 49 (11) (2002) 1371–1373.
[33] X.S. Zhang, R.J. Roy, E.W. Jensen, EEG complexity as a measure of depth of anesthesia for patients, IEEE Trans. Biomed. Eng. 48 (12) (2001) 1424–1433.
[34] Y. Sun, Y. Li, Y. Zhu, X. Chen, S. Tong, Electroencephalographic differences between depressed and control subjects: an aspect of interdependence analysis, Brain Res. Bull. 76 (6) (2008) 559–564.
[35] A.H. Kemp, D.S. Quintana, K.L. Felmingham, S. Matthews, H.F. Jelinek, Depression, comorbid anxiety disorders, and heart rate variability in physically healthy, unmedicated patients: implications for cardiovascular risk, PLoS One 7 (2) (2012) e30777.
[36] H. Hinrikus, M. Bachmann, D. Karai, W. Klonowski, J. Lass, P. Stepien, R. Stepien, V. Tuulik, Higuchi's fractal dimension for analysis of the effect of external periodic stressor on electrical oscillations in the brain, Med. Biol. Eng. Comput. 49 (5) (2011) 585–591.
[37] AM. Al-Kaysi, A. Al-Ani, CK. Loo, TY. Powell, DM. Martin, M. Breakspear, TW. Boonstra, Predicting tDCS treatment outcomes of patients with major depressive disorder using automated EEG classification, J Affect Disord 208 (2017) 597–603.
[38] A. Woźniak-Kwaśniewska, D. Szekely, S. Harquel, T. Bougerol, O. David, Resting electroencephalographic correlates of the clinical response to repetitive transcranial magnetic stimulation: a preliminary comparison between unipolar and bipolar depression, J Affect Disord 183 (2015) 15–21.

Appendix 3 – Publication II

Publication II

Päeske, L., Hinrikus, H., Lass, J., Raik, J., & Bachmann, M. (2020). Negative correlation between functional connectivity and small-worldness in the alpha frequency band of a healthy brain. *Frontiers in Physiology, 11*, 910. doi: 10.3389/fphys.2020.00910

frontiers in Physiology

ORIGINAL RESEARCH
published: 12 August 2020
doi: 10.3389/fphys.2020.00910

Negative Correlation Between Functional Connectivity and Small-Worldness in the Alpha Frequency Band of a Healthy Brain

Laura Päeske[1], Hiie Hinrikus[1], Jaanus Lass[1], Jaan Raik[2] and Maie Bachmann[1]*

[1] *Centre for Biomedical Engineering, Department of Health Technologies, School of Information Technologies, Tallinn University of Technology, Tallinn, Estonia,* [2] *Department of Computer Systems, School of Information Technologies, Tallinn University of Technology, Tallinn, Estonia*

The aim of the study was to analyze the relationship between resting state electroencephalographic (EEG) alpha functional connectivity (FC) and small-world organization. For that purpose, Pearson correlation was calculated between FC and small-worldness (SW). Three undirected FC measures were used: magnitude-squared coherence (MSC), imaginary part of coherency (ICOH), and synchronization likelihood (SL). As a result, statistically significant negative correlation occurred between FC and SW for all three FC measures. Small-worldness of MSC and SL were mostly above 1, but lower than 1 for ICOH, suggesting that functional EEG networks did not have small-world properties. Based on the results of the current study, we suggest that decreased alpha small-world organization is compensated with increased connectivity of alpha oscillations in a healthy brain.

Keywords: electroencephalography, functional connectivity, small-world organization, network analysis, alpha frequency, coherence, imaginary part of coherency, synchronization likelihood

OPEN ACCESS

Edited by:
Plamen Ch. Ivanov, Boston University, United States

Reviewed by:
Andras Eke, Semmelweis University, Hungary
Qianli Ma, Nanjing University of Posts and Telecommunications, China

****Correspondence:***
Laura Päeske
laura.paeske@taltech.ee

Specialty section:
This article was submitted to Fractal and Network Physiology, a section of the journal Frontiers in Physiology

Received: *28 March 2020*
Accepted: *08 July 2020*
Published: *12 August 2020*

Citation:
Päeske L, Hinrikus H, Lass J, Raik J and Bachmann M (2020) Negative Correlation Between Functional Connectivity and Small-Worldness in the Alpha Frequency Band of a Healthy Brain. Front. Physiol. 11:910. doi: 10.3389/fphys.2020.00910

INTRODUCTION

Functional connectivity (FC) is highly important in physiology at various levels: from molecules to organs and physiological networks are not only of wide scientific interest, but also have high impact in medicine (Ivanov et al., 2016; Lin et al., 2016; Moorman et al., 2016). Functional connectivity is crucial also in brain physiology (Lynn and Bassett, 2019). Significant work has been done to show that neural network architecture can be adaptively reconfigured between different states of the subjects (Bassett et al., 2006; Liu et al., 2015a; Lin et al., 2020) and associate network topology to physiologic states (Bashan et al., 2012; Bartsch and Ivanov, 2014; Ivanov and Bartsch, 2014; Bartsch et al., 2015; Liu et al., 2015b).

Functional connectivity and complex network analysis have been the most widely used types of brain network analysis by providing the tools to analyze the brain as a network of interacting regions, while maintaining computational simplicity. Complex network analysis is based on classical graph theoretical analysis, but focuses on analyzing complex real-life networks (Rubinov and Sporns, 2010). Real-life neural networks are represented graphically, using electroencephalographic (EEG) channels as nodes and FC as edges between nodes. Graphs are

constructed by removing edges with lowest values. Small-world organization is one of the most frequently analyzed topological properties of functional neural networks. A network is compared to random networks and in order to have small-world properties, the network should be more clustered than a random network, but have similar characteristic path length (Watts and Strogatz, 1998; Albert and Barabási, 2002; Rubinov and Sporns, 2010; Bassett and Bullmore, 2017). In that case, functional integration and functional segregation are simultaneously high. A measure of small-worldness (SW) has been proposed to assess small-world properties of a network (Humphries and Gurney, 2008). Since then, studying small-world properties of functional brain networks has been widely used.

Changes in EEG resting state FC and small-world structure are often used for statistical analysis between two populations, generally with the aim to compare patient and control groups. Previous studies have found results in all frequency bands, but often inconsistencies between studies occur. Therefore, we will focus on frequency bands, where the most frequent and consistent results were reported. Major depressive disorder (MDD) is mostly characterized by increased FC (Fingelkurts et al., 2007; Leuchter et al., 2012; Olbrich et al., 2014; Li et al., 2017) and more random network structure (Li et al., 2017; Zhang et al., 2018; Sun et al., 2019) in theta and alpha frequency bands. However, few studies have also found a decrease in alpha FC (Shim et al., 2018; Zhang et al., 2018). Alzheimer's disease (AD) has been consistently characterized by decreased FC in alpha frequency band (Koenig et al., 2005; Wang et al., 2014; Babiloni et al., 2016). Furthermore, SW of AD subjects has been found to decrease in theta frequency band (Wang et al., 2014; Vecchio et al., 2017), and AD is characterized by more random network structure in alpha frequency band (Wang et al., 2014; Babiloni et al., 2016). In schizophrenia, most consistent FC alteration has also been the decrease of FC in alpha frequency band (Jalili and Knyazeva, 2011; Di Lorenzo et al., 2015; Maran et al., 2016). Furthermore, schizophrenia has also been associated with decreased SW in alpha, beta, and gamma frequency bands (Micheloyannis et al., 2006) and more random network architecture (Rubinov et al., 2009).

Although alterations in FC and small-world organization have been studied for diseased brain (see above), the relationship between FC and SW is unclear for healthy subjects. We have previously shown that adding graph theoretical measures to features of FC did not improve classification accuracy when classifying MDD and healthy subjects (Orgo et al., 2017). Therefore, a fundamental relationship between FC and graph theory measures can be expected and a disruption in that relationship is likely related to different mental disorders. However, only a few studies have analyzed the relationship between different graph theory measures. Lynall et al. (2010) reported a positive correlation between functional magnetic resonance imaging (fMRI) FC and SW, together with several correlations between different graph theoretical measures. However, healthy and schizophrenic subjects were analyzed together and the group contained of a small number of subjects (15 healthy and 12 schizophrenic subjects). To the best of our knowledge, the relationship between graph theory measures for EEG data has not been analyzed before.

FC has recently been shown to be a complex spatiotemporal phenomenon (Racz et al., 2018), but in the current study we apply widely used static approach of FC to construct functional networks. To ensure more reliable results, we calculate three frequently used FC measures: magnitude-squared coherence (MSC), imaginary part of coherency (ICOH), and synchronization likelihood (SL). These measures were chosen to take different EEG properties into account. Firstly, SL is calculated in time domain, while MSC and ICOH are calculated in frequency domain. Secondly, measures of FC can be divided into linear and nonlinear measures. On the one hand, EEG nonlinear time series analysis is based on the nonlinear nature of neural processes. Previous studies have reported strong nonlinear interdependences in EEG signals (Rubinov et al., 2009) and nonlinear metrics can detect nonlinear interdependencies between EEG signals that linear measures cannot. On the other hand, nonlinear measures are computationally expensive and susceptible to noise (Netoff et al., 2006). Linear measures are more robust and can perform as well as nonlinear measures in some cases (Bastos and Schoffelen, 2016; Bachmann et al., 2018). Therefore, a combination of linear and nonlinear measures should provide the most information. In the current study, SL can capture both linear and nonlinear interdependencies between signals. We have previously shown with surrogate data method that SL can detect nonlinearity in 9% of EEG segments, which cannot be detected with linear methods (Päeske et al., 2018). Therefore, SL may provide additional information to other connectivity measures. Thirdly, several FC measures such as MSC are strongly influenced by volume conduction (Bastos and Schoffelen, 2016). One solution to avoid spurious results from volume conduction would be to apply inverse method to the scalp EEG signals and then calculate FC between obtained source signals. The problem with this approach is that perfect inverse method cannot exist (Sarvas, 1987) and therefore accurate FC estimation is not guaranteed. Other option is to use FC measures that are less sensitive to volume conduction, for example ICOH (Christodoulakis et al., 2015; Bastos and Schoffelen, 2016). Imaginary part of coherency measures only phase-shifted relationship between time series, therefore minimizing connectivity between information from the same sources. At the same time, true interactions at zero-phase are also lost and for a more complete understanding, these measures can be calculated complementary to other measures.

In the current study, we analyze the relationship between alpha FC and SW in the resting state for healthy subjects. We use only alpha frequency band, because most of the alterations in FC or SW have been previously found in the alpha frequency band for MDD, AD, and schizophrenia. Furthermore, EEG alpha frequency has an important role in cognitive, sensorimotor, psycho-emotional and physiological processes (Bazanova and Vernon, 2014). It is important to note that although graphs are constructed by thresholding FC values, small-world graph theory measures are normalized. Therefore, mathematically, there is no correlation between FC and normalized graph theory measures for random graphs. If a correlation between FC and SW occurs

for a physiological network, but not for a random network, the origin of the correlation is also expected to be physiological. We will also construct random graphs for reference, using Erdös-Rényi model, to ensure that our results could not be derived mathematically.

MATERIALS AND METHODS

Subjects

The subjects were chosen for the experiment according to the following criteria: no epilepsy, no usage of psychotropic medication one month prior to the experiment, no usage of narcotics three months prior to the experiment, no history of head injury or concussion, and no psychiatric disorders at the time of the experiment. Following these criteria, the study was carried out on a group of 80 healthy volunteers from ages 19 to 75, with the mean age of 37 ± 15 years. Out of all subjects, 38 were female and 42 were male. The subjects were asked to abstain from alcohol 24 h and from coffee two hours prior to the EEG recording.

The study was conducted in accordance with the Declaration of Helsinki and was approved by the Tallinn Medical Research Ethics Committee. Informed consent was obtained from each subject before participating in the study.

Data Recordings

Electroencephalographic signals were recorded using Neuroscan Synamps2 acquisition system (Compumedics, NC, United States) from 30 electrodes (Fp1, Fp2, F7, F3, Fz, F4, F8, FT7, FC3, FCz, FC4, FT8, T7, C3, Cz, C4, T8, TP7, CP3, CPz, CP4, TP8, P7, P3, Pz, P4, P8, O1, Oz, O2). Electrodes were positioned according to the extended international 10–20 system with linked mastoids as reference. In addition, horizontal and vertical electrooculograms were recorded to monitor eye movements. To ensure good conductivity between the skin and electrodes, electrode impedances were kept below 10 kΩ.

The data were sampled at 1000 Hz. The resting state EEG was recorded for six minutes, during which the subjects were lying in a relaxed position with their eyes closed. The room of the recordings was electrically shielded and dimly lit. In addition, earplugs were used to minimize any disturbances.

Preprocessing

The data were analyzed using MATLAB (The Mathworks, Inc.). Butterworth filter was used to filter signals into alpha (8-12 Hz) frequency band. Sampling frequency was reduced to 200 Hz to reduce the computation time of FC measures and the data were divided into 20.48-s (4096 sample) segments. All segments were inspected by a studied technician and segments with ocular, muscular or other artifacts were removed. For each subject, first 10 artifact-free segments were used for further analysis.

Signals were re-referenced according to the reference electrode standardization technique (REST) (Yao, 2001), which approximately re-references scalp EEG signals to a reference point at infinity using an equivalent source model. REST has been shown to be the best reference montage to recover the real EEG FC network configuration (Qin et al., 2010; Huang et al., 2017).

FC Analysis

Three non-directed measures of FC were calculated in the current study: MSC, ICOH, and SL. An example of EEG signals in alpha frequency band for different levels of FC is shown in the **Supplementary Material**. FC measures were calculated between all channels, obtaining connectivity matrices for each subject. Median values of MSC, ICOH, and SL were obtained over segments in time.

Magnitude-Squared Coherence

Coherency estimates linear relationship between two signals at each frequency f. When time series from channels i and j are $x_i(t)$ and $x_j(t)$ and their Fourier transforms are $X_i(f)$ and $X_j(f)$, then the cross-spectrum between $X_i(f)$ and $X_j(f)$ is $S_{ij} \equiv \langle X_i(f) X_j^*(f) \rangle$, where * indicates complex conjugation and $\langle\rangle$ expectation value. Coherency is calculated as:

$$C_{ij}(f) \equiv \frac{S_{ij}(f)}{\left(S_{ii}(f) S_{jj}(f)\right)^{1/2}}, \tag{1}$$

where $S_{ii}(f)$ is the power spectrum of $X_i(f)$ and $S_{jj}(f)$ is the power spectrum of $X_j(f)$. Coherence is the absolute value of coherency:

$$COH_{ij}(f) \equiv \left|C_{ij}(f)\right| = \frac{\left|S_{ij}(f)\right|}{\left(S_{ii}(f) S_{jj}(f)\right)^{1/2}} \tag{2}$$

In the current study, the MSC (Kay, 1988) was used as a frequently used measure of FC:

$$MSC_{ij}(f) = COH_{ij}^2(f) \equiv \frac{\left|S_{ij}(f)\right|^2}{\left(S_{ii}(f) S_{jj}(f)\right)} \tag{3}$$

Symmetric Hann window with a window length of 512 samples and 50% overlap was used to calculate Fourier transform. MSC was found by averaging $MSC_{ij}(f)$ values within the alpha frequency band.

Imaginary Part of Coherency

It is often argued not to use MSC as it is strongly influenced my volume conduction. Therefore, ICOH (Nolte et al., 2004) was also used in current study as a secondary measure of FC, which is calculated as an imaginary part of coherency:

$$iCOH_{ij}(f) \equiv Imag\left(C_{ij}(f)\right) = \frac{Imag(S_{ij}(f))}{\left(S_{ii}(f) S_{jj}(f)\right)^{1/2}} \tag{4}$$

Imaginary part of coherency was found by averaging $iCOH_{ij}(f)$ values within the alpha frequency band. Imaginary part of coherency removes zero-phase interactions between time series $x_i(t)$ and $x_j(t)$, therefore minimizing the effects of volume conduction.

Synchronization Likelihood

Synchronization likelihood (Stam and Van Dijk, 2002) describes dynamical interdependencies between simultaneously

recorded signals. The definition and calculation of SL is provided by Stam and Van Dijk (2002). Briefly, time series are reconstructed in state space and the recurrences of states are detected from time-delay embedding vectors. Synchronization likelihood is the likelihood of these recurrences being simultaneous. The parameters for SL were calculated from sampling frequency, highest frequency and lowest frequency using suggestions by Montez et al. (2006). Therefore, the following parameters were used: the embedding lag L = 6, the embedding dimension m = 6, the number of recurrences nrec = 10, the fraction of recurrences pref = 0.01, window W1 = 50 and window W2 = 1049. Such selection of the parameters ensures that the state vector is long enough to sample the slowest oscillations and at the same time signal is sampled at sufficiently short intervals to take fastest oscillations into account.

Graph Theory Analysis

A connectivity matrix can be analyzed as a graph consisting of nodes (EEG channels) and edges between the nodes (FC between EEG channels). To obtain a graph, a threshold is applied on FC values: an edge exists only if the value of FC is higher than the threshold. In the current study, the sparsity of each graph was maintained by applying a different threshold to each graph. For example, network density of 40% means that 60% of all connections were removed from each graph. This ensures that differences between graph theory metrics are due to differences in graph topologies, rather than connectivity strengths. As currently there is no optimal network density used in the literature, a range of network densities are used. In the current study, the network densities from 10 to 50% with a step of 5% were used. These are one of the commonly analyzed densities, ensuring that the network is sparse enough to show small-world properties and at the same time is still fully connected (Bullmore and Bassett, 2011; Sun et al., 2019). Obtained graphs were binarized: edge values were 0 or 1, depending on whether there was a connection between two nodes or not. In other words, unweighted graphs were used in the current study. As non-directed FC measures were used, edges did not have a direction.

Brain Connectivity Toolbox (Rubinov and Sporns, 2010) was used to calculate graph theoretical measures in MATLAB. Graph theory measures calculated in the current study describe small-world properties of a network and are therefore also called small-world measures. Clustering coefficient (C) describes functional segregation, characterizing brain's ability to process information within interconnected clusters. Clustering coefficient for a given node equals with the fraction of node's nearest neighbors that are also directly connected to each other (Watts and Strogatz, 1998). Characteristic path length (L) is a measure of functional integration, characterizing brain's ability to combine information from distributed areas. Shortest path length is the smallest number of edges between two nodes. Characteristic path length is the average shortest path length of the graph (Watts and Strogatz, 1998). High functional integration is described with small L. A network has small-world properties if it is more clustered than a random network, but has similar L (Rubinov and Sporns, 2010). Small-worldness quantifies these properties and is calculated from C and L (Humphries and Gurney, 2008):

$$SW = \frac{C_{norm}}{L_{norm}} = \frac{C/C_{rand}}{L/L_{rand}}, \quad (5)$$

where C_{rand} is the clustering coefficient and L_{rand} is the characteristic path length of an equivalent random network. A network has small-world properties if SW > 1 (Wang et al., 2014). Random networks for normalization were generated according to the method of Maslov and Sneppen (Maslov and Sneppen, 2002; Rubinov and Sporns, 2010) by reshuffling the topology and maintaining the degree distribution of original networks.

Small-worldness was calculated for all three FC measures. For reference, random graphs were generated using Erdös–Rényi model – for the fixed number of nodes, the existence of each potential edge is determined by a probability p. To differentiate between graph theoretical measures calculated from different FC measures, FC measures are marked with a superscript. For example SW^{MSC} denotes small-worldness, calculated from a MSC graph.

Statistical Comparisons

For each subject, the mean values of FC and SW were calculated over all channels. The values of SW were statistically compared using Wilcoxon's ranksum test and the correlations between mean FC and SW were calculated using Pearson correlation coefficient (r). The confidence level of $p < 0.05$ was used. p-Value was adjusted according to the number of statistical tests using Bonferroni correction to address the problem of multiple comparisons. As three different measures and nine different graph densities were used, the number of statistical tests was 27 and p-value was adjusted to $p < 0.05/27 = 0.0019$. The correlations were considered statistically significant if $|r| > 0.34$, corresponding to the adjusted p-value $p < 0.0019$ and sample size of 80 subjects. If the absolute value of obtained correlation was higher than 0.34, the correlation could not have emerged randomly.

RESULTS

First, we statistically compared the values of SW calculated from different FC measures (**Figure 1**). Bonferroni correction for 27 statistical tests was applied. Small-worldness calculated from ICOH was significantly lower than SW calculated from MSC and SL for all graph densities analyzed in the current study. For MSC and SL, SW was mostly above 1 or close to 1, indicating these networks have better or similar small-world properties compared to a random network. For ICOH, most values of SW were below 1, indicating these networks have less small-world properties compared to a random network.

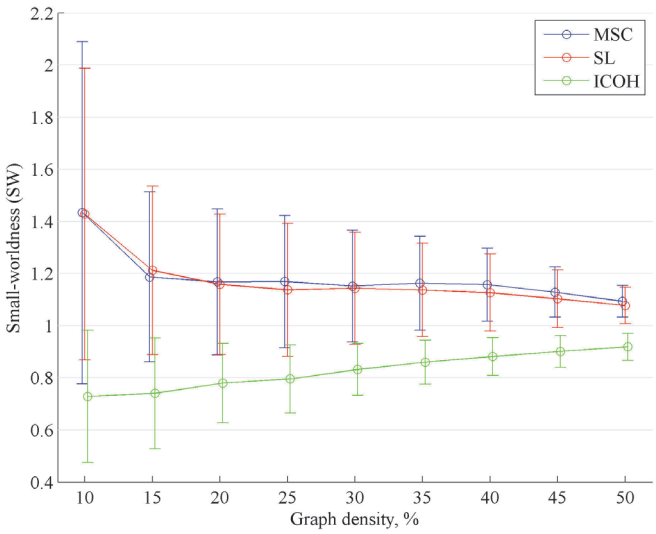

FIGURE 1 | Small-worldness (SW) depending on graph density. The mean and standard deviation values are shown for SW, calculated from MSC, SL and ICOH. SW^{ICOH} is significantly lower than SW^{MSC} and SW^{SL}.

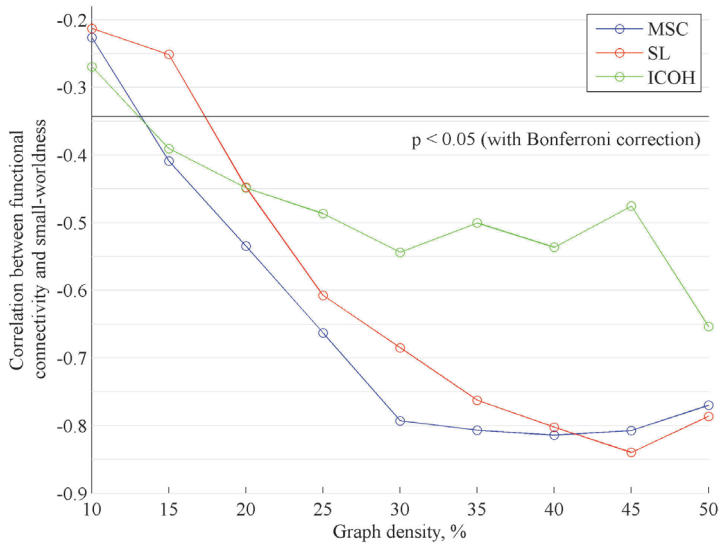

FIGURE 2 | The values of Pearson correlation coefficients (*r*) between measures of functional connectivity (MSC, SL, and ICOH) and small-worldness calculated from these measures (SW^{MSC}, SW^{SL}, and SW^{ICOH}) for different graph densities. Black horizontal line corresponds to correlation -0.34. Correlations below this line are statistically significant with confidence level of 0.05 (*p*-value is adjusted according to Bonferroni correction to $p < 0.0019$).

Secondly, Pearson correlation coefficient was calculated between SW and FC for all measures of FC (**Figure 2**). There was a statistically significant negative correlation between FC and SW for all measures of FC. For MSC and ICOH, correlations were statistically significant for graph densities 15 ... 50% and for SL 20 ... 50%. The highest correlations are plotted on **Figure 3**. The highest correlation for MSC was for graph density 40% (**Figure 3A**), for SL 45% (**Figure 3B**) and for ICOH 50%

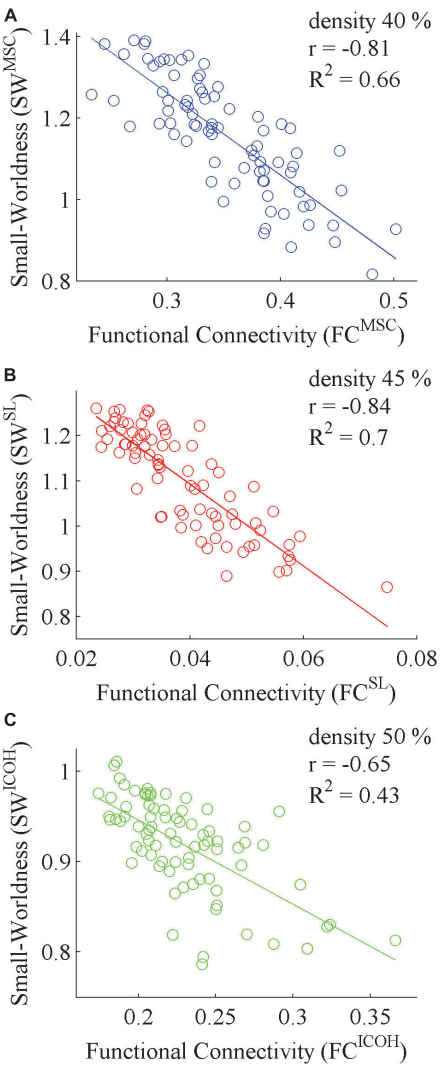

FIGURE 3 | Correlation between FC and SW for **(A)** MSC, **(B)** SL, and **(C)** ICOH. Pearson correlation coefficient (*r*) is shown in the upper right corner.

(**Figure 3C**). Pearson correlation coefficient was also found between SW and averaged edge values of random graphs. As expected, correlation for random graphs was not statistically significant for any of the analyzed graph densities.

DISCUSSION

As a result of the study, we found a negative correlation between EEG alpha FC and SW. The correlation occurred for all three measures of FC calculated in the current study. For MSC and ICOH, correlations were statistically significant for graph densities 15 ... 50% and for SL 20 ... 50%. Based on the results of the current study, we suggest a hypothesis that decreased alpha small-world organization is compensated with increased connectivity of alpha oscillations in a healthy brain. Furthermore, a correlation may indicate that a certain efficiency is maintained in the brain by balancing between alpha FC and SW: as one increases, the other decreases.

Results found in the current study may be associated with default mode network (DMN; Jann et al., 2010; Liu et al., 2017). The DMN has been the most studied of resting state networks, largely because it deactivates during demanding tasks. Furthermore, areas involved in DMN have high activity during resting state, observed with fMRI BOLD signal, and high connectivity (Hagmann et al., 2008). A recent study used high-density EEG to detect large-scale networks (Liu et al., 2017). The authors spatially overlapped obtained EEG networks with fMRI networks and found that although each resting state brain network is associated with oscillations of different frequency bands, DMN can be fully reconstructed using alpha frequency band. In the current study, alpha frequency band was also used and therefore association between the results in the current study and DMN are plausible.

Previous studies have mostly found that alpha FC is increased in MDD (Fingelkurts et al., 2007; Leuchter et al., 2012; Olbrich et al., 2014). Although changes in alpha SW in MDD are unclear, some studies have found that small-world measures of alpha EEG were decreased for subjects with MDD (Zhang et al., 2018; Sun et al., 2019). Therefore, in MDD, the relationship between FC and SW found in the current study is probably not disrupted. Fingelkurts et al. (2007) suggested that FC between short-range connections in the left hemisphere and long-range connections in the right hemisphere of subjects with MDD was increased to compensate insufficient semantic integration. However, according to the hypothesis suggested in the current study, the compensational mechanism proposed by Fingelkurts et al. (2007) may be inherent to healthy subjects as well. A compensational mechanism could be a fundamental characteristic to brain functioning. According to that theory, another possible explanation to the increase in FC for MDD is the decrease in SW, which in turn leads to an increase in FC.

Alzheimer's disease in alpha frequency band is characterized by decreased FC (Koenig et al., 2005; Wang et al., 2014; Babiloni et al., 2016), but also decreased small-world measures (Wang et al., 2014; Babiloni et al., 2016). Therefore, compensating low small-world architecture with increased FC may be disrupted in AD.

Similarly to AD, schizophrenia in alpha frequency band has also been previously described with decreased FC (Jalili and Knyazeva, 2011; Di Lorenzo et al., 2015; Maran et al., 2016) and small-world measures (Micheloyannis et al., 2006; Rubinov et al., 2009). Schizophrenia is often described with

"dysconnectivity syndrome" – impaired functional integration between and within brain areas. Considering the results of the current study, it could be presumed that "dysconnectivity syndrome" is expressed by disrupted compensational mechanism in schizophrenia.

We statistically compared the values of SW calculated from different FC measures. Small-worldness calculated from ICOH (SW^{ICOH}) was significantly lower compared to SW^{MSC} and SW^{SL}. As ICOH measures only phase-shifted relationship between time series, this result shows that MSC and SL capture a lot of information from zero-phase interactions. A lot of these interactions are due to volume conduction. Previous studies have shown that volume conduction falsely increases values of SW (Kuś et al., 2004). The same effect could also be observed in the current study, where SW^{MSC} and SW^{SL} were significantly higher compared to SW^{ICOH}. Nevertheless, the correlation between FC and SW found in the current study cannot be caused by volume conduction, because in addition to MSC and SL, the correlation was also found with ICOH, which minimizes the effects of volume conduction.

Magnitude-squared coherence is a linear measure that is calculated in a frequency domain and SL is a nonlinear measure that is calculated in a time domain. Although these measures are fundamentally different, there were no statistically significant differences between SW^{MSC} and SW^{SL}. This result shows that for robust network analysis applications, MSC can be selected instead of SL, because MSC is easier and faster to compute.

In the current study, SW^{MSC} and SW^{SL} were mostly slightly higher than 1 (**Figure 1**), indicating these networks have better or similar small-world properties compared to the random networks generated from original networks. However, SW^{ICOH} was mostly below 1 (**Figure 1**), indicating these networks have less small-world properties compared to a random network. These results are in line with previous studies: SW has been found to be above 1 for FC measures that are more influenced by volume conduction (Micheloyannis et al., 2006; Wang et al., 2014; Zhang et al., 2018) and slightly below 1 for measures that are less influenced by volume conduction (Hou et al., 2018; Zheng et al., 2018). Previous studies have found that EEG functional networks are small-world networks, but the current study shows that these results may be influenced by volume conduction, since functional ICOH networks in the current study did not show small-world properties during eyes-closed resting state.

Most studies that compare two groups of subjects, obtain values above 1 for SW. Since those metrics are obtained by comparing original networks to random networks, decrease in those values is generally interpreted as a more random network structure (Rubinov et al., 2009; Zhang et al., 2018; Sun et al., 2019). In the current study we showed that although decrease in SW^{MSC} and SW^{SL} can be interpreted as a more random network structure (**Figures 3A,B**), decrease in SW^{ICOH} resulted in a less random network structure (**Figure 3C**). Therefore, the decrease in SW does not necessarily interpret into a more random network structure, although such result can be concluded mathematically in case of certain measures. These results strengthen the argument to calculate ICOH in addition to MSC or SL.

The negative correlation obtained in the current study increased between graph densities 10 ... 25% and was more stable for graph densities 30 ... 50% (**Figure 2**). As mean FC was constant for all graph densities, this result could be more influenced by the dependence of SW on graph density. Still, one has to take into account that the dependence of SW on graph density differs for each individual network. Generally, denser networks naturally have smaller values of SW (Bassett and Bullmore, 2017). However, the same conclusion did not apply to the results of ICOH in the current study (**Figure 1**). To address the limitation of SW depending on the graph density, the small-world propensity (SWP) was introduced by Muldoon et al. (2016). However, in the current study, we chose a more common approach to calculate SW for a range of graph densities (**Figure 2**) to investigate the correlation between FC and SW depending on the graph density.

In the current study, functional networks of healthy subjects in resting state was analyzed. Further studies could also investigate the relationship between FC and SW in subjects with MDD, AD, and schizophrenia. Based on the network analysis in studies by other authors, the relationship between FC and SW found in the current study may be disrupted in AD and schizophrenia, but not in MDD.

Previous studies have shown that different physiologic states can be described with different network structure (Bartsch et al., 2015) and FC (Lin et al., 2016) within organ systems, indicating an association between network topology, FC, and physiologic function. In the more focused perspectives of the brain, the hypothesis of a compensatory mechanism between FC and SW suggested in the current study seems to be consistent with these findings in that in healthy subjects FC and SW underlying different physiologic states may well alter in an interrelated manner. This concept should be made subject of further research within a broader framework incorporating functional integration and segregation, too.

CONCLUSION

To the best of our knowledge, current study is the first to analyze the relationship between resting state EEG FC and SW. We report a negative correlation between FC and small-world organization in alpha frequency band for healthy subjects. We interpret these results as the manifestation of a compensational mechanism of the healthy brain, where lower small-world organization is compensated by higher connectivity strength. The finding is expected to be useful in the differentiation of mental and neurological disorders.

DATA AVAILABILITY STATEMENT

All datasets presented in this study are included in the article/ **Supplementary Material**.

ETHICS STATEMENT

The studies involving human participants were reviewed and approved by Tallinn Medical Research Ethics Committee, Estonia. The patients/participants provided their written informed consent to participate in this study.

AUTHOR CONTRIBUTIONS

LP designed the study and processed the data. LP and MB conducted the EEG recordings. LP, MB, and HH analyzed and interpreted the results and wrote the manuscript. JL and JR contributed to the discussion of results and writing the manuscript. All authors revised and approved the final manuscript.

FUNDING

This study was financially supported by the higher education scholarship in the growth areas of smart specialization and by the Estonian Centre of Excellence in IT (EXCITE) TAR16013 funded by the European Regional Development Fund.

SUPPLEMENTARY MATERIAL

The Supplementary Material for this article can be found online at: https://www.frontiersin.org/articles/10.3389/fphys.2020.00910/full#supplementary-material

REFERENCES

Albert, R., and Barabási, A.-L. (2002). Statistical mechanics of complex networks. *Rev. Modern Phys.* 74, 47–97.

Babiloni, C., Lizio, R., Marzano, N., Capotosto, P., Soricelli, A., Triggiani, A. I., et al. (2016). Brain neural synchronization and functional coupling in Alzheimer's disease as revealed by resting state EEG rhythms. *Int. J. Psychophysiol.* 103, 88–102. doi: 10.1016/j.ijpsycho.2015.02.008

Bachmann, M., Päeske, L., Kalev, K., Aarma, K., Lehtmets, A., Ööpik, P., et al. (2018). Methods for classifying depression in single channel EEG using linear and nonlinear signal analysis. *Comput. Methods Prog. Biomed.* 155, 11–17. doi: 10.1016/j.cmpb.2017.11.023

Bartsch, R. P., and Ivanov, P. C. (2014). Coexisting forms of coupling and phase-transitions in physiological networks. *Commun. Comp. Inform. Sci.* 438, 270–287.

Bartsch, R. P., Liu, K. K., Bashan, A., and Ivanov, P. C. (2015). Network physiology: how organ systems dynamically interact. *PLoS One* 10:e0142143. doi: 10.1371/journal.pone.0142143

Bashan, A., Bartsch, R. P., Kantelhardt, J. W., Havlin, S., and Ivanov, P. C. (2012). Network physiology reveals relations between network topology and physiological function. *Nat. Commun.* 3:702.

Bassett, D. S., and Bullmore, E. T. (2017). Small-world brain networks revisited. *Neuroscientist* 23, 499–516.

Bassett, D. S., Meyer-Lindenberg, A., Achard, S., Duke, T., and Bullmore, E. (2006). Adaptive reconfiguration of fractal small-world human brain functional networks. *Proc. Natl. Acad. Sci. U.S.A.* 103, 19518–19523.

Bastos, A. M., and Schoffelen, J.-M. (2016). A tutorial review of functional connectivity analysis methods and their interpretational pitfalls. *Front. Syst. Neurosci.* 9:175. doi: 10.3389/fnsys.2015.00175

Bazanova, O. M., and Vernon, D. (2014). Interpreting EEG alpha activity. *Neurosci. Biobehav. Rev.* 44, 94–110. doi: 10.1016/j.neubiorev.2013.05.007

Bullmore, E., and Bassett, D. S. (2011). Brain graph models: graphical models of the human brain connectome. *Annu. Rev. Clin. Psychol.* 7, 113–140. doi: 10.1146/annurev-clinpsy-040510-143934

Christodoulakis, M., Hadjipapas, A., Papathanasiou, E. S., Anastasiadou, M., Papacostas, S. S., and Mitsis, G. D. (2015). On the effect of volume conduction on graph theoretic measures of brain networks in epilepsy. *Neuromethods* 91, 103–130. doi: 10.1007/7657_2013_65

Di Lorenzo, G., Daverio, A., Ferrentino, F., Santarnecchi, E., Ciabattini, F., Monaco, L., et al. (2015). Altered resting-state EEG source functional connectivity in schizophrenia: the effect of illness duration. *Front. Hum. Neurosci.* 9:234. doi: 10.3389/fnhum.2015.00234

Fingelkurts, A. A., Fingelkurts, A. A., Rytsälä, H., Suominen, K., Isometsä, E., and Kahkonen, S. (2007). Impaired functional connectivity at EEG alpha and theta frequency bands in major depression. *Hum. Brain Mapp.* 28, 247–261. doi: 10.1002/hbm.20275

Hagmann, P., Cammoun, L., Gigandet, X., Meuli, R., Honey, C. J., Wedeen, V. J., et al. (2008). Mapping the structural core of human cerebral cortex. *PLoS Biol.* 6:e159. doi: 10.1371/journal.pbio.0060159

Hou, F., Liu, C., Yu, Z., Xu, X., and Zhang, J. (2018). Age-related alterations in electroencephalography connectivity and network topology during n-back working memory task. *Front. Hum. Neurosci.* 12:484. doi: 10.3389/fnhum.2018.00484

Huang, Y., Zhang, J., Cui, Y., Yang, G., He, L., Liu, Q., et al. (2017). How different EEG references influence sensor level functional connectivity graphs. *Front. Neurosci.* 11:368. doi: 10.3389/fnins.2017.00368

Humphries, M. D., and Gurney, K. (2008). Network 'small-world-ness': a quantitative method for determining canonical network equivalence. *PLoS One* 3:e0002051. doi: 10.1371/journal.pone.0002051

Ivanov, P. C., and Bartsch, R. P. (2014). "Network physiology: mapping interactions between networks of physiologic networks," in *Networks of Networks: the Last Frontier of Complexity*, eds G. D'Agostino and A. Scala (Cham: Springer), 203–222.

Ivanov, P. C., Liu, K. K., and Bartsch, R. P. (2016). Focus on the emerging new fields of network physiology and network medicine. *N. J. Phys.* 18:100201.

Jalili, M., and Knyazeva, M. G. (2011). EEG-based functional networks in schizophrenia. *Comput. Biol. Med.* 41, 1178–1186. doi: 10.1016/j.compbiomed.2011.05.004

Jann, K., Kottlow, M., Dierks, T., Boesch, C., and Koenig, T. (2010). Topographic electrophysiological signatures of fMRI resting state networks. *PLoS One* 5:e12945. doi: 10.1371/journal.pone.0012945

Kay, S. M. (1988). *Modern Spectral Estimation*. Englewood Cliffs, NJ: Prentice-Hall.

Koenig, T., Prichep, L., Dierks, T., Hubl, D., Wahlund, L., John, E., et al. (2005). Decreased EEG synchronization in Alzheimer's disease and mild cognitive impairment. *Neurobiol. Aging* 26, 165–171. doi: 10.1016/j.neurobiolaging.2004.03.008

Kuś, R., Kamiński, M., and Blinowska, K. (2004). Determination of EEG activity propagation: pair-wise versus multichannel estimate. *IEEE Trans. Biomed. Eng.* 51, 1501–1510. doi: 10.1109/TBME.2004.827929

Leuchter, A. F., Cook, I. A., Hunter, A. M., Cai, C., and Horvath, S. (2012). Resting-state quantitative electroencephalography reveals increased neurophysiologic connectivity in depression. *PLoS One* 7:e32508. doi: 10.1371/journal.pone.0032508

Li, X., Jing, Z., Hu, B., Zhu, J., Zhong, N., Li, M., et al. (2017). A resting-state brain functional network study in MDD based on minimum spanning tree analysis and the hierarchical clustering. *Complexity* 2017, 1–11. doi: 10.1155/2017/9514369

Lin, A., Liu, K. K., Bartsch, R. P., and Ivanov, P. C. (2016). Delay-correlation landscape reveals characteristic time delays of brain rhythms and heart interactions. *Philos. Trans. R. Soc. A* 374:20150182.

Lin, A., Liu, K. K., Bartsch, R. P., and Ivanov, P. C. (2020). Dynamic network interactions among distinct brain rhythms as a hallmark of physiologic state and function. *Commun. Biol.* 3:197.

Liu, K. K., Bartsch, R. P., Lin, A., Mantegna, R. N., and Ivanov, P. C. (2015a). Plasticity of brain wave network interactions and evolution across physiologic states. *Front. Neural Circuits* 9:62. doi: 10.3389/fncir.2015.00062

Liu, K. K., Bartsch, R. P., Ma, Q. D., and Ivanov, P. C. (2015b). Major component analysis of dynamic networks of physiologic organ interactions. *Behav. Inform. Technol.* 640:012013.

Liu, Q., Farahibozorg, S., Porcaro, C., Wenderoth, N., and Mantini, D. (2017). Detecting large-scale networks in the human brain using high-density electroencephalography. *Hum. Brain Mapp.* 38, 4631–4643. doi: 10.1002/hbm.23688

Lynall, M.-E., Bassett, D. S., Kerwin, R., McKenna, P. J., Kitzbichler, M., Müller, U., et al. (2010). Functional connectivity and brain networks in schizophrenia. *J. Neurosci.* 30, 9477–9487. doi: 10.1523/JNEUROSCI.0333-10.2010

Lynn, C. W., and Bassett, D. S. (2019). The physics of brain network structure, function, and control. *Nat. Rev. Phys.* 1, 318–332.

Maran, M., Grent-'t-Jong, T., and Uhlhaas, P. J. (2016). Electrophysiological insights into connectivity anomalies in schizophrenia: a systematic review. *Neuropsychiatr. Electrophysiol.* 2:6. doi: 10.1186/s40810-016-0020-5

Maslov, S., and Sneppen, K. (2002). Specificity and stability in topology of protein networks. *Science* 296, 910–913. doi: 10.1126/science.1065103

Micheloyannis, S., Pachou, E., Stam, C. J., Breakspear, M., Bitsios, P., Vourkas, M., et al. (2006). Small-world networks and disturbed functional connectivity in schizophrenia. *Schizophr. Res.* 87, 60–66. doi: 10.1016/j.schres.2006.06.028

Montez, T., Linkenkaer-Hansen, K., Van Dijk, B. W., and Stam, C. J. (2006). Synchronization likelihood with explicit time-frequency priors. *NeuroImage* 33, 1117–1125. doi: 10.1016/j.neuroimage.2006.06.066

Moorman, J. R., Lake, D. E., and Ivanov, P. C. (2016). Early detection of sepsis-a role for network physiology? *Crit. Care Med.* 44, e312–e313.

Muldoon, S. F., Bridgeford, E. W., and Bassett, D. S. (2016). Small-world propensity and weighted brain networks. *Sci. Rep.* 6:22057.

Netoff, T. L., Carroll, T. L., Pecora, L. M., and Schiff, S. J. (2006). "Detecting coupling in the presence of noise and nonlinearity," in *Handbook of Time Series Analysis*, eds B. Schelter, M. Winterhalder, and J. Timmer (Weingeim: Wiley-VCH Berlag), 265–282.

Nolte, G., Bai, O., Wheaton, L., Mari, Z., Vorbach, S., and Hallett, M. (2004). Identifying true brain interaction from EEG data using the imaginary part of coherency. *Clin. Neurophysiol.* 115, 2292–2307. doi: 10.1016/j.clinph.2004.04.029

Olbrich, S., Tränkner, A., Chittka, T., Hegerl, U., and Schönknecht, P. (2014). Functional connectivity in major depression: increased phase synchronization between frontal cortical EEG-source estimates. *Psychiatry. Res.* 222, 91–99. doi: 10.1016/j.pscychresns.2014.02.010

Orgo, L., Bachmann, M., Kalev, K., Järvelaid, M., Raik, J., and Hinrikus, H. (2017). "Resting EEG functional connectivity and graph theoretical measures for discrimination of depression," in *Proceedings of the 2017 IEEE EMBS International Conference on Biomedical & Health Informatics*, Orlando, FL. 389–392.

Päeske, L., Bachmann, M., Põld, T., de Oliveira, S. P., Lass, J., Raik, J., et al. (2018). Surrogate data method requires end-matched segmentation of electroencephalographic signals to estimate non-linearity. *Front. Physiol.* 9:1350. doi: 10.3389/fphys.2018.01350

Qin, Y., Xu, P., and Yao, D. (2010). A comparative study of different references for EEG default mode network: the use of the infinity reference. *Clin. Neurophysiol.* 121, 1981–1991. doi: 10.1016/j.clinph.2010.03.056

Racz, F. S., Stylianou, O., Mukli, P., and Eke, A. (2018). Multifractal dynamic functional connectivity in the resting-state brain. *Front. Physiol.* 9:1704. doi: 10.3389/fphys.2018.01704

Rubinov, M., Knock, S. A., Stam, C. J., Micheloyannis, S., Harris, A. W., Williams, L. M., et al. (2009). Small-world properties of nonlinear brain activity in schizophrenia. *Hum. Brain Mapp.* 30, 403–416. doi: 10.1002/hbm.20517

Rubinov, M., and Sporns, O. (2010). Complex network measures of brain connectivity: uses and interpretations. *NeuroImage* 52, 1059–1069. doi: 10.1016/j.neuroimage.2009.10.003

Sarvas, J. (1987). Basic mathematical and electromagnetic concepts of the biomagnetic inverse problem. *Phys. Med. Biol.* 32, 11–22. doi: 10.1088/0031-9155/32/1/004

Shim, M., Im, C.-H., Kim, Y.-W., and Lee, S.-H. (2018). Altered cortical functional network in major depressive disorder: a resting state electroencephalogram study. *Neuroimage Clin.* 19, 1000–1007. doi: 10.1016/j.nicl.2018.06.012

Stam, C. J., and Van Dijk, B. W. (2002). Synchronization likelihood: an unbiased measure of generalized synchronization in multivariate data sets. *Physica D* 163, 236–251. doi: 10.1016/S0167-2789(01)00386-4

Sun, S., Li, X., Zhu, J., Wang, Y., La, R., Zhang, X., et al. (2019). Graph theory analysis of functional connectivity in major depression disorder with high-density resting state EEG data. *IEEE Trans. Neural Syst. Rehabil. Eng.* 27, 429–439. doi: 10.1109/TNSRE.2019.2894423

Vecchio, F., Miraglia, F., and Rossini, P. M. (2017). Connectome: graph theory application in functional brain network architecture. *Clin. Neurophysiol. Pract.* 2, 206–213. doi: 10.1016/j.cnp.2017.09.003

Wang, R., Wang, J., Yu, H., Wei, X., Yang, C., and Deng, B. (2014). Decreased coherence and functional connectivity of electroencephalograph in Alzheimer's disease. *Chaos* 24:033136. doi: 10.1063/1.4896095

Watts, D. J., and Strogatz, S. H. (1998). Collective dynamics of 'small-world' networks. *Nature* 393, 440–442. doi: 10.1038/30918

Yao, D. (2001). A method to standardize a reference of scalp EEG recordings to a point at infinity. *Physiol. Meas.* 22, 693–711. doi: 10.1088/0967-3334/22/4/305

Zhang, M., Zhou, H., Liu, L., Feng, L., Yang, J., Wang, G., et al. (2018). Randomized EEG functional brain networks in major depressive disorders with greater resilience and lower rich-club coefficient. *Clin. Neurophysiol.* 129, 743–758. doi: 10.1016/j.clinph.2018.01.017

Zheng, G., Qi, X., Li, Y., Zhang, W., and Yu, Y. (2018). A comparative study of standardized infinity reference and average reference for EEG of three typical brain states. *Front. Neurosci.* 12:158. doi: 10.3389/fnins.2018.00158

Conflict of Interest: The authors declare that the research was conducted in the absence of any commercial or financial relationships that could be construed as a potential conflict of interest.

Appendix 4 – Publication III

Publication III
Päeske, L., Bachmann, M., Põld, T., de Oliveira, S. P. M., Lass, J., Raik, J., & Hinrikus, H. (2018). Surrogate Data Method Requires End-Matched Segmentation of Electroencephalographic Signals to Estimate Non-linearity. *Frontiers in Physiology, 9*, 1350. doi: 10.3389/fphys.2018.01350

frontiers in Physiology

ORIGINAL RESEARCH
published: 27 September 2018
doi: 10.3389/fphys.2018.01350

Surrogate Data Method Requires End-Matched Segmentation of Electroencephalographic Signals to Estimate Non-linearity

Laura Päeske[1], Maie Bachmann[1], Toomas Põld[1,2], Sara Pereira Mendes de Oliveira[3], Jaanus Lass[1], Jaan Raik[4] and Hiie Hinrikus[1]*

[1] Centre of Biomedical Engineering, Department of Health Technologies, Tallinn University of Technology, Tallinn, Estonia, [2] Qvalitas Medical Centre, Tallinn, Estonia, [3] Department of Electrical and Computer Engineering, Faculty of Engineering, University of Porto, Porto, Portugal, [4] Department of Computer Systems, Tallinn University of Technology, Tallinn, Estonia

The aim of the study is to clarify the impact of the strong cyclic signal component on the results of surrogate data method in the case of resting electroencephalographic (EEG) signals. In addition, the impact of segment length is analyzed. Different non-linear measures (fractality, complexity, etc.) of neural signals have been demonstrated to be useful to infer the non-linearity of brain functioning from EEG. The surrogate data method is often applied to test whether or not the non-linear structure can be captured from the data. In addition, a growing number of studies are using surrogate data method to determine the statistical threshold of connectivity values in network analysis. Current study focuses on the conventional segmentation of EEG signals, which could lead to false results of surrogate data method. More specifically, the necessity to use end-matched segments that contain an integer number of dominant frequency periods is studied. EEG recordings from 80 healthy volunteers during eyes-closed resting state were analyzed using multivariate surrogate data method. The artificial surrogate data were generated by shuffling the phase spectra of original signals. The null hypothesis that time series were generated by a linear process was rejected by statistically comparing the non-linear statistics calculated for original and surrogate data sets. Five discriminating statistics were used as non-linear estimators: Higuchi fractal dimension (HFD), Katz fractal dimension (KFD), Lempel-Ziv complexity (LZC), sample entropy (SampEn) and synchronization likelihood (SL). The results indicate that the number of segments evaluated as non-linear differs in the case of various non-linear measures and changes with the segment length. The main conclusion is that the dependence on the deviation of the segment length from full periods of dominant EEG frequency has non-monotonic character and causes misleading results in the evaluation of non-linearity. Therefore, in the case of the signals with non-monotonic spectrum and strong dominant frequency, the correct use of surrogate data method requires the signal length comprising of full periods of the spectrum dominant frequency. The study is important to understand the influence of incorrect selection of EEG signal segment length for surrogate data method to estimate non-linearity.

Keywords: EEG, dominant frequency, alpha frequency, surrogate data, Fourier transform, segment length

OPEN ACCESS

Edited by:
Sladjana Z. Spasić,
University of Belgrade, Serbia

Reviewed by:
Gonzalo Marcelo Ramírez-Avila,
Universidad Mayor de San Andrés, Bolivia
Chunhua Bian,
Nanjing University, China

****Correspondence:***
Laura Päeske
laura.paeske@ttu.ee

Specialty section:
This article was submitted to Fractal Physiology, a section of the journal Frontiers in Physiology

Received: *31 May 2018*
Accepted: *06 September 2018*
Published: *27 September 2018*

Citation:
Päeske L, Bachmann M, Põld T, de Oliveira SPM, Lass J, Raik J and Hinrikus H (2018) Surrogate Data Method Requires End-Matched Segmentation of Electroencephalographic Signals to Estimate Non-linearity. Front. Physiol. 9:1350. doi: 10.3389/fphys.2018.01350

INTRODUCTION

Non-linear dynamics is the most appropriate way to describe complex physiological systems and is therefore widely used in biomedical applications. During last decades, the interest in the theory of non-linear dynamics has increased due to raising interest in brain functioning and the necessity to understand complex dynamics of the underlying processes (Hornero et al., 2009; Rodríguez-Bermudez and Garcíia Laencin, 2015).

The brain is assumed to function as a self-organizing complex network of interacting dynamical non-linear subsystems. Despite some cellular processes may be random and characterized by probability functions, the neural systems may exhibit rather chaotic non-linear nature. Large networks of interconnected neurons behave as self-organized large systems with local non-linear interactions (Hornero et al., 2009). The question, whether EEG signals should be looked at as a non-linear deterministic process or a linear stochastic one, is still open. Therefore, before analyzing EEG signals by non-linear methods, it is required to assess whether the non-linearity exists in the data. In case non-linearity is present, the non-linear dynamics theory could also characterize the intrinsic nature of EEG, helping to understand its dynamics, underlying brain processes and search for its physiological significance, without losing or ignoring important information (Natarajan et al., 2004). The presence of non-linearity can be confirmed by hypothesis testing.

Theiler et al. (1992) described a statistical approach for identifying non-linearity in a time series, through the surrogate data method. A surrogate data is generated from the original data by shuffling the phase spectra. Null hypothesis that data were generated by a linear process is tested by comparing non-linear statistic calculated for original and surrogate data. If the value for original data is significantly different, the null hypothesis can be rejected and non-linearity concluded. The probability that the surrogate data test will reject null hypothesis depends on the non-linear statistic used (Spasic, 2010).

Surrogate data method is widely used on EEG signals for testing the null hypothesis of linearity. There are two main purposes for surrogate data testing. The first purpose is to test whether the chosen non-linear measure captures non-linear structure in the data, which cannot be detected with spectral density function (Breakspear and Terry, 2002; Natarajan et al., 2004; Spasic, 2010; Bae et al., 2017; Orgo et al., 2017). If the data does not have any non-linear structure, a linear method could be used instead. The second purpose is to determine the statistical threshold of connectivity values in network analysis (Dimitriadis et al., 2015, 2017; Olejarczyk et al., 2017), which is being used by a growing number of studies with the method of surrogate data. However, some factors can cause misleading results for EEG signal linearity estimation. Surrogate data testing for a linear stochastic system can indicate false non-linearity in case the process is non-stationary (Timmer, 1998). A specific problem has been identified that false detection of non-linearity may occur in case the data are strongly cyclic (Stam et al., 1998; Small and Tse, 2002). The problem arises when the length of the analyzed signal segment deviates from the multiple full periods of the cyclic component in the signal.

Electroencephalographic (EEG) signal has a strong alpha frequency component in the frequency range between 9 and 11 Hz. This rhythm is most pronounced in occipital region, but is also present in central, temporal or even frontal regions. Alpha rhythm is best revealed during eyes-closed resting state. Therefore, it might be expected that due to the strong cyclic alpha component of the resting eyes-closed signal, the surrogate data method may give false results.

The aim of the study is to clarify the impact of the strong cyclic signal component on the results of surrogate data method in the case of EEG signals. In addition, the impact of segment length is analyzed. For this reason, the degree of non-linearity was found in eyes-closed resting EEG signal depending on the analyzed segment length and deviation from full period of the dominant cyclic component. Five discriminating statistics were used as non-linear estimators: Higuchi fractal dimension (HFD), Katz fractal dimension (KFD), Lempel-Ziv complexity (LZC), sample entropy (SampEn), and synchronization likelihood (SL).

MATERIALS AND METHODS

Subjects

Eighty healthy volunteers (38 female and 42 male) aged 37.0 ± 14.5 years participated in the study. The experiments were approved by the Tallinn Medical Research Ethics Committee and were conducted in accordance with the Declaration of Helsinki. All subjects signed an informed consent.

EEG Recordings

The EEG was recorded using Neuroscan Synamps2 acquisition system (Compumedics, Charlotte, NC, United States) from 30 electrodes, positioned according to the extended international 10–20 system. The sampling frequency was 1,000 Hz. Linked mastoids were used as a reference and electrode impedances were kept below 10 kΩ. EEG was recorded for 6 min, during which subjects were lying in a relaxed position with their eyes closed.

Surrogate Data

Multivariate surrogate data method is used to test whether data were generated by a non-linear process (Theiler et al., 1992; Prichard and Theiler, 1994). The null-hypotheses that data were generated by a linear process and therefore data can be fully explained by a linear model, is set. Surrogate data is generated from original data. If the non-linear statistic calculated for original data significantly differs from the non-linear statistic calculated for surrogate data, null-hypothesis is rejected and non-linearity is detected.

Surrogate data is calculated from time series according to the algorithm by Prichard and Theiler (1994). Fourier transform is applied and the phase of each frequency component is independently rotated by a random degree between $(0, 2\pi)$. After that, inverse Fourier transform is performed. As a result, the power spectrum and the autocorrelation function of the time series is preserved. For multivariate time series, a fixed random sequence is used to alter the phase of each frequency, ensuring linear correlations between simultaneously recorded time series.

To determine whether the value of the non-linear statistic for the original data set significantly differs from the non-linear statistics for the surrogate data, z-test is used (Breakspear and Terry, 2002):

$$Z = \frac{Q_{data} - mean\,(Q_{surrogate})}{std\,(Q_{surrogate})} \quad (1)$$

where Q_{data} is the non-linear statistic calculated for the original data set, $mean\,(Q_{surrogate})$ is the mean and $std\,(Q_{surrogate})$ is the standard deviation of linear statistics calculated for the surrogate data. In the current study, surrogate data was calculated 20 times for each data segment and the significance level of $p < 0.05$ was used. Under the null hypothesis, z-statistic is normally distributed and when $|Z| > 1.96$ for a two-tailed test, the null hypothesis can be rejected. For data analysis, we calculated the degree of non-linearity (DEG), which we define as the percentage of segments where the null hypothesis was rejected and non-linearity was detected:

$$DEG = \frac{n_{sign}}{n} \cdot 100\% \quad (2)$$

where n is the number of segments and n_{sign} is the number of segments, where $|Z| > 1.96$.

Non-linear Statistics

The measures for estimation of non-linearity were selected based on two main criteria. Firstly, whereas different estimators detect various aspects of non-linearity, the applied measures should describe one of the specific features of the signals: self-similarity, dimension-based morphology, complexity, irregularity or functional connectivity. Secondly, less time-consuming methods currently widely used in EEG analysis should be represented. As a result, five non-linear methods were selected: HFD, KFD, LZC, SampEn, and SL. HFD and KFD are fractal dimension methods, LZC is a measure of complexity and SampEn is a measure of irregularity. As connectivity between neurons and synchronization of their spiking play crucial role in the brain functioning, functional connectivity measure SL, although computationally time consuming, was also selected.

The HFD evaluates the complexity and self-similarity of time series (Higuchi, 1988). It is calculated directly in the time domain, making it a simple and fast method. The HFD with a parameter $k_{max} = 8$ was calculated according to the algorithm presented by Higuchi (1988).

The KFD obtains fractal dimension based on morphology, measuring the roughness of the time series (Katz, 1988). The KFD is the ratio of the length of the curve (sum of distances between two successive points), divided by the maximum distance of any point under consideration from the first point. In other words, the ratio of the total length to the straight line corresponding to the maximum distance from the first point. In addition, a scaling factor, an average of the distances between two successive points is used.

Higuchi's and Katz fractal dimensions are the most common methods of estimating the fractal dimension of EEG signals directly in the time domain. Despite both, HFD and KFD describe the fractal dimension of EEG waveform, the behavior of the measures is different. HFD has been suggested being the most accurate, whereas KFD yields the most consistent results regarding discrimination between brain functional states (Esteller et al., 2001). Therefore, both are applied in this study.

The LZC evaluates the randomness of finite sequences (Lempel and Ziv, 1976). First, the EEG signal is transformed into a finite symbol sequence, according to a chosen threshold. Next, the sequence of symbols is analyzed from left to right. The LZC counts the number of times a new pattern is encountered and its recurrence rate for the given sequence. LZC is simple to calculate and does not need long data segments. Larger LZC values correspond to signals that are more complex. Still, the LZC strongly depends on the signal bandwidth (Kalev et al., 2015). In the current study, median value of the sequence was selected as threshold, as it is capable of coping with outliers. Next, the data was binarized (two symbols) according to the threshold. Due to artifact free sequences, selecting between median or mean is not expected to change the outcome considerably.

The SampEn measures the signal irregularity (Richman and Moorman, 2000). Signals that are more irregular give larger SampEn values. The method is quite independent of the signal length. It is suitable for analyzing short and noisy time series. The SampEn is the negative natural logarithm of the conditional probability that two sequences similar for $m = 2$ points remain similar at the next point. Parameters for the SampEn were chosen according to recommendations from previous studies (Richman and Moorman, 2000; Lake and Moorman, 2010): the embedding dimension $m = 2$ and the tolerance $r = 0.2\ SD$, where SD is the standard deviation of the sample.

The SL is a non-linear measure of functional connectivity (Stam and Van Dijk, 2002). The SL estimates dynamical interdependencies between simultaneously recorded time series using Takens' theorem (Takens, 1981) of reconstructing EEG signals into state space. The calculation of the SL is more thoroughly explained in the article by Stam and Van Dijk (2002). The SL parameters were calculated according to the formulas presented in the paper by Montez et al. (2006) with respect to the time-frequency content of the signal. Therefore, the following parameters were used: the embedding lag $L = 7$, the embedding dimension $m = 136$, the number of recurrences $n_{rec} = 10$, the fraction of recurrences $p_{ref} = 0.01$, window $W_1 = 2000$ and window $W_2 = 2999$. Such selection of the parameters ensures that the time-frequency characteristics of the signals are fully taken into account. Therefore, small alterations in these parameters are not expected to change the results of surrogate data method significantly.

Data Processing

Data processing was done in MATLAB (The Math-works, Inc.) using signal processing toolbox. Signals were digitally filtered (1–45 Hz) using zero-phase Butterworth filter and re-referenced according to the reference electrode standardization technique (REST) (Yao, 2001). Signals were divided into 5.3-s segments. Data were visually inspected and segments with artifacts were not analyzed.

Surrogate data method makes an assumption of stationarity. We conducted two stationarity tests: the Kwiatkowski–Phillips–Schmidt–Shin (KPSS) and the Phillips–Perron (PP) test and no non-stationarity was detected.

Dependence on the Segment Length Increment for Alpha Component

The aim of the current section was to determine how DEG depends on the segment length increment. For that purpose, the length of the segment was gradually incremented from an integer number of alpha periods by 2 ms. Therefore, the length of each segment was determined as:

$$l = kT + \Delta t,\ \Delta t = 0, 2, 4, \ldots, 108\ ms, \tag{3}$$

where k is an integer, T is the period of alpha frequency component and Δt is the segment length increment. The first segment was approximately 5 s, starting and ending at the alpha peak amplitude ($\Delta t = 0$) – consisting of an integer number of alpha periods. Therefore, the exact length of the first segment depended on the alpha period. The second segment started at the same position as the first one, but ended 2 ms later ($\Delta t = 2$). Finally, the length of the last segment ($\Delta t = 108$) was approximately 5.1 s. For most subjects, the length of the last segment corresponds to $l = (k + 1)T$ – again an integer number of alpha periods. As there were 62 data segments for a subject, we repeated the incrementation procedure for each of the 62 data segments and DEG was calculated according to formula (2) for each $\Delta t = 0, 2, 4, \ldots, 108$ ms, where $n = 62$.

Alpha peaks were found by zero-phase filtering signals into alpha frequency band (7.5–13 Hz) using Butterworth filter and peaks were indicated by local maxima. The channel O1 was chosen for processing, because of the highest average alpha power. After finding positions of alpha peaks in channel O1, whole frequency band (1–45 Hz) was used for calculating DEG. The dependence on Δt was found for five different non-linear parameters: HFD, KFD, LZC, SampEn and SL. As SL is calculated between two channels, O1 and O2 were used.

Dependence on Channel

In different channels, the amount of alpha power, the strong cyclic component, differs. This component is most pronounced in occipital region, but is also present in other regions. To analyze the dependence on the EEG channel, three channels were chosen according to average mean alpha power: O1 with the highest alpha power, C3 with average alpha power and T7 with the lowest alpha power. In addition to O1, analysis for C3 and T7 were conducted in accordance to 2.5.1, whereas HFD was used as a non-linear measure.

Dependence on the Segment Length Increment for Different Frequency Components

It is well known that alpha is the dominant frequency during eyes-closed resting state EEG recordings, especially in posterior areas. However, it is important to clarify, whether the surrogate data method is also affected by the cyclic component of other EEG frequency bands. For that purpose, the analysis in 2.5.1 was repeated using HFD, but the segments beginning and the segment length increment have been matched to the following frequencies: delta (1–1.5 Hz; $\Delta t = 0, 20, \ldots, 1000$), theta (4–8 Hz; $\Delta t = 0, 3, \ldots, 126$) and beta (13–30 Hz; $\Delta t = 0, 1, \ldots, 46$). For better comparison, the results for alpha component (7.5–13 Hz; $\Delta t = 0, 2, \ldots, 108$) are also presented.

Dependence on Segment Length

While incrementing the segment by Δt, the overall segment length was almost the same, between 5 and 5.1 s. To analyze the dependence on the segment length, the data were divided into substantially different segment lengths: around 5, 10, 15, and 20 s. Each segment started from alpha peak and ended with alpha peak, consisting of an integer number of alpha periods. Each subject had 10 segments of each segment length, whereas $n = 10$ in formula (2). DEG was calculated for each subject and segment.

Data Processing

The observations of DEG were obtained for each subject. The dependence on the Δt and the segment length were statistically evaluated using one-way analysis of variance (ANOVA) with the significance level of $p < 0.05$. To correct for the problem of multiple comparisons, Bonferroni correction was used by adjusting the p-value $p = p/m$, where m is the number of comparisons.

RESULTS

Average DEG values for end-matched segments according to alpha frequency ($\Delta t = 0$) are presented in **Table 1**. The percentage of segments where non-linearity was detected varies significantly depending on the non-linear measure. KFD indicated the highest degree of non-linearity: the KFD value was significantly changed in 99% of segments, while LZC revealed non-linearity only in 0.4% of the segments.

Dependence on the Segment Length Increment for Alpha Component

The calculated DEG values for HFD, KFD, LZC, SampEn and SL in alpha frequency band are presented in **Supplementary Datasets 1–5**. We conducted ANOVA to analyze whether the segment length increment Δt influences the results of surrogate data method. ANOVA ($p < 0.05/5$) yielded statistically significant results for every non-linear statistic that indicated non-linearity ($DEG > 5\%$): HFD DEG (**Figure 1B**), KFD DEG (**Figure 1D**) and SampEn DEG (**Figure 1H**). For example, when $\Delta t = 0$, then HFD DEG was 46.1%, but $\Delta t = 50$ (corresponding to half alpha period)

TABLE 1 | The degree of non-linearity at alpha peak.

	DEG, %
HFD	46.1
KFD	99.1
LZC	0.4
SampEn	81.5
SL	3.9

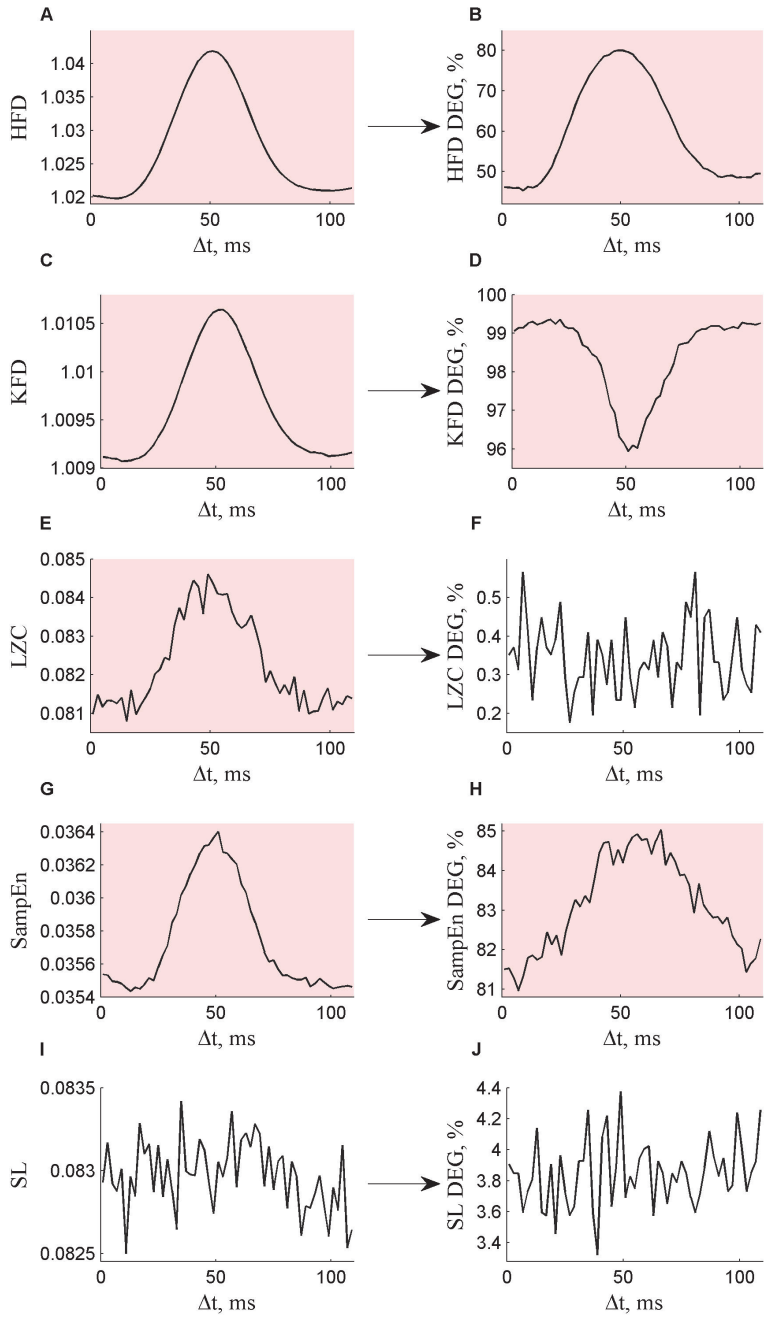

FIGURE 1 | Non-linear measures **(A)** HFD, **(C)** KFD, **(E)** LZC, **(G)** SampEn, and **(I)** SL calculated for surrogate data depending on the segment length increment Δt are presented on the left. The degree of non-linearity DEG depending on the segment length increment Δt for **(B)** HFD DEG, **(D)** KFD DEG, **(F)** LZC DEG, **(H)** SampEn DEG, and **(J)** SL DEG are presented on the right. Statistically significant results are indicated with a pink background.

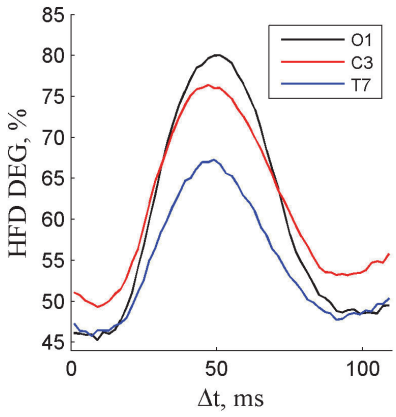

FIGURE 2 | The degree of non-linearity DEG depending on the segment length increment Δt for alpha component in channels O1, C3, and T7.

resulted in HFD DEG 80.0%. LZC DEG (**Figure 1F**) and SL DEG (**Figure 1J**) did not depend on the Δt.

In order to understand the DEG results presented in **Figure 1**, we can consider the values of non-linear measures calculated for original and surrogate data, according to which DEG was calculated. Incrementing the segment length to $\Delta t = 50$ increased the values calculated for surrogate data for all five non-linear measures, but the increase was statistically significant only for HFD (**Figure 1A**), KFD (**Figure 1C**), LZC (**Figure 1E**), and SampEn (**Figure 1G**). Since HFD and SampEn calculated for surrogate data were significantly increased compared to the values calculated for original data, this resulted in an increase also in DEG (**Figures 1B,H**). However, KDF for surrogate data was significantly decreased compared to KFD for original data, resulting in a decrease in DEG (**Figure 1D**). Although LZC calculated for surrogate data was also influenced by segment length increment (**Figure 1E**), LZC was similar for original and surrogate data, yielding low DEG values, resilient to segment length increment (**Figure 1F**).

Dependence on Channel

The calculated HFD DEG values for channels O1, C3 and T7 are presented in **Supplementary Datasets 1, 6, 7**. According to ANOVA ($p < 0.05/3$), HFD depended on the Δt for all studied channels. The deflection in DEG was the largest in channel O1, followed by C3 and T7 (**Figure 2**). These results are in accordance with the amount of spectral alpha power in those channels.

Dependence on the Segment Length Increment for Different Frequency Components

The calculated HFD DEG values for delta, theta, alpha and beta frequency components are presented in **Supplementary Datasets 1**, **8–10**. According to ANOVA ($p < 0.05/4$), HFD depended on every calculated cyclic component (**Figure 3**). The difference between maximum and minimum DEG for different Δt was the largest for alpha component (80.0% – 45.3% = 34.7%), followed by theta (63.9% − 51.4% = 12.5%), delta (61.1%−51.1% = 10.0%), and beta component (60.6% − 51.6% = 9.1%).

Dependence on Segment Length

The influence of segment length ($\Delta t = 0$) on DEG was investigated for five non-linear measures: HFD, KFD, LZC, SampEn, and SL (**Supplementary Dataset 11**). The results are presented in **Table 2**. According to ANOVA ($p < 0.05/20$), DEG depended on the segment length for HFD, SampEn, and SL (marked with * in **Table 2**). The results for 5-s segments are slightly different from the results in **Table 1**, because smaller number of segments were used.

DISCUSSION

The aim of the study was to clarify the impact of the strong cyclic EEG signal component on the results of surrogate data method

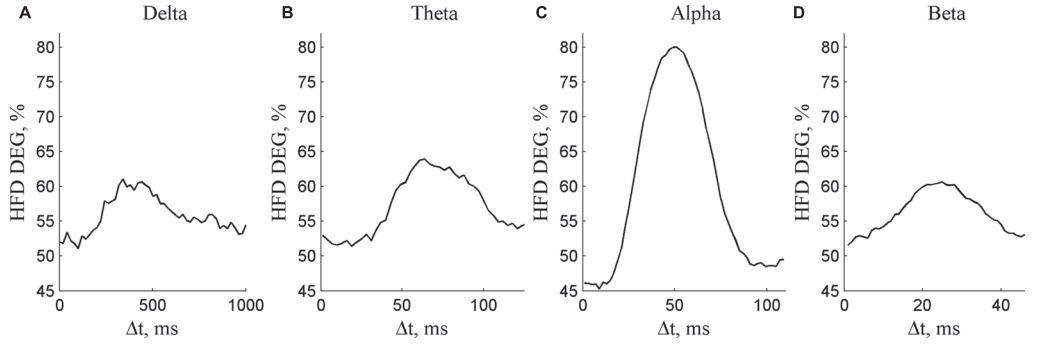

FIGURE 3 | The degree of non-linearity DEG depending on the segment length increment Δt for **(A)** delta, **(B)** theta, **(C)** alpha, and **(D)** beta frequency components.

TABLE 2 | The degree of non-linearity at different segment lengths (*$p < 0.05$).

	DEG, %			
Segment length	**5 s**	**10 s**	**15 s**	**20 s**
HFD	45.7*	41.0*	36.4*	34.0*
KFD	99.9	100	100	100
LZC	0.4	0.6	0.2	0.4
SampEn	82.0*	95.4*	98.5*	99.4*
SL	4.4*	6.5*	7.0*	9.1*

by Theiler et al. (1992). In addition, the impact of segment length was analyzed. The major finding of the study was that if the EEG segment does not contain an integer number of full alpha periods, the values calculated for surrogate data may be significantly altered, resulting in a false rejection of linearity. To the best of our knowledge, similar results have not been reported earlier.

Previous studies have shown that false detection of non-linearity may occur when the data are strongly cyclic (Stam et al., 1998; Small and Tse, 2002). However, the influence of this problem on EEG signals was not previously known. Although surrogate data method is widely used for EEG analysis (Breakspear and Terry, 2002; Natarajan et al., 2004; Spasic, 2010; Dimitriadis et al., 2015, 2017; Bae et al., 2017; Olejarczyk et al., 2017), the cyclic behavior of dominant frequency component is not considered in segmentation. The current study shows the importance of segmenting data according to the alpha component for eyes-closed resting state EEG.

Our results demonstrate remarkable non-monotonic changes in the degree of non-linearity of EEG signals with the fine tuning of the segment length within a period of dominant EEG signal frequency for every non-linear statistic that indicated non-linearity (DEG > 5%): HFD (**Figure 1B**), KFD (**Figure 1D**), and SampEn (**Figure 1H**). The changes in the degree of non-linearity are caused by the changes in the non-linear measures calculated for surrogate data (**Figures 1A,C,G**), whereas the measures calculated for original data have no remarkable dependence on so small alteration of segment length. The impact of segment length tuning on the results of surrogate data method is maximal when the segment length contains an odd number of half-periods of the dominant frequency (**Figure 1**). The phenomenon can be explained by spectral leakage in the discrete Fourier transform while deriving the surrogates, as discrete Fourier transform assumes periodic signals. Thornhill (2005) showed that even a small spectral component other than that at the dominant frequency could be interpreted as non-linearity and causes false detection of non-linearity for sine waves. However, they showed that pseudoperiodic data with weaker cyclic behavior were more robust to small end-mismatches. These results are in accordance with the results in the current study. Moreover, the current study proves that the cyclic behavior of EEG has a strong influence on non-linear measures calculated for surrogate data for large end-mismatch.

Two measures, LZC (**Figure 1F**) and SL (**Figure 1J**), did not detect significant non-linearity (DEG < 5%). In the case of LZC, the possible reason is that the measure is highly sensitive to low frequency EEG component in binarization due to its high amplitude values. The non-linearity, if contained in the low amplitude high frequency activity, gets overlooked in the process of binarization and is not detected by the measure. SL did not detect non-linear coupling, indicating that SL does not necessarily give significantly more information compared to similar linear functional connectivity measures.

The level of alterations caused by fine tuning within a period of dominant frequency differs at different non-linear discrimination measures. The degree of linearity changes about two-fold with HFD, is much lower with KDF and SampEn and becomes insignificant with LZC and SL. The different impact of fine tuning of segment length within a period of dominant frequency can be explained by different sensitivity of various non-linear measures to a small additional spectral component introduced by the deviation of the segment length from a full period. The problem can be solved by selecting the start and end of the segment by matching the period of the strong cyclic component. A segment end-matching can be performed by selecting a segment length equal to integer number of full periods of the dominant frequency (Stam et al., 1998). In addition, Small et al. (2001) suggested an alternative surrogate data method: pseudo-periodic surrogate (PPS) algorithm. However, PPS is not applicable to data where the non-linearity of interest is distortion of the periodic waveform (Thornhill, 2005).

The dependence of the degree of non-linearity on the segment length increment from full alpha periods has the maximal value for alpha frequency component (**Figure 3**). The alteration of the degree of non-linearity with the dominant frequencies in delta, theta or beta bands are less critical. The possible reason is the structure of EEG signal with a dominant alpha frequency. The minimum DEG value in **Figure 3** is the smallest for alpha frequency component. These results show that the synchronization of the fine tuning of the segment length should be performed with the dominant frequency component to decrease the amount of false positive surrogate data results.

The dependence of the degree of non-linearity on the segment length increment from full period of dominant EEG frequency is evident in various EEG channels (**Figure 2**). As expected, the impact is stronger in the EEG channels with higher alpha content (O) and weaker in channels with lower alpha content (T). The influence of segment end-mismatch on other channels also mostly depends on the spectral alpha power and lies between the obtained results of O1 and T7 (**Figure 2**). The results may also be influenced by an additional strong frequency component (channel C3 in **Figure 2**), but the dominant frequency component should be taken into account in segment end-matching.

The degree of linearity estimated at an integer number of alpha periods (**Tables 1**, **2**) shows that the degree of non-linearity varies for different non-linear measures. Different sensitivity to surrogate data method has also been reported by other author (Spasic, 2010) when comparing HFD and third order correlation. Our results suggest that HFD, KFD, and SampEn were more sensitive to non-linearity, while SL and LZC values changed significantly in less than 5% of segments for 5-s segments. In this case, SL has been calculated between O1 and O2 channels.

The results can vary for different channel pairs, but Orgo et al. (2017) found that for SL 5-s segments, the average degree of non-linearity over all channel pairs was similar to that in our current study (6.1% compared to our 4.4%). In addition, the degree of non-linearity estimated in the current study is close to the results reported by Breakspear and Terry (2002), who detected statistically significant evidence of non-linear interactions in 4.8% of the 2.048-s segments of eyes-closed resting state EEG.

The findings presented in **Table 2**, indicating changed non-linearity with increased segment length, are in principle in accordance with the results reported by other research groups (Olbrich et al., 2003; Sun et al., 2012; Orgo et al., 2017). Olbrich et al. (2003) have reported the dependence of rejection of the null hypothesis between natural and surrogate data in sleep EEG on the length of the analyzed segment. They suggested that the increase of evaluated non-linearity with the segment length might occur because of the increasing non-stationarity of the longer time series. In the current study, KPSS and PP test did not reveal any non-stationarity. Sun et al. (2012) have made a conclusion that the length of signal segment for analysis of 3–16 periods is sufficient for detecting non-linearity in the case of EEG phase synchronization. However, in the current study we showed that the results of evaluation of non-linearity vary even with the segment lengths of more than 100 periods. Orgo et al. (2017) were the first to compare the degree of EEG non-linear coupling in different frequency bands and segment lengths, during eyes-closed resting state. Their results showed that the degree of non-linear coupling increased with the length of the segment, and it was most dominant in total, alpha, beta and theta frequency bands.

CONCLUSION

The results of the performed study show that the selection of a proper segment length in evaluating non-linearity of EEG signals with surrogate data method is critical to assure the reliability of evaluation. The results of performed calculations demonstrate that false rejection of linearity occurred with surrogate data method when an EEG segment did not contain an integer number of full alpha periods using HFD, KFD, or sample entropy. LZC and SL did not detect significant non-linearity and were therefore not influenced by segment end-mismatch. The major novel finding is that the correct estimation of non-linearity with surrogate data method requires a segment length comprising of full periods of the spectrum's dominant frequency component. In addition, the degree of non-linearity estimated with HFD, sample entropy and synchronization likelihood significantly changed with the segment length.

DATA AVAILABILITY STATEMENT

The datasets analyzed in this study can be found as a xlsx file in the supplement.

AUTHOR CONTRIBUTIONS

LP and MB designed the study and conducted EEG recordings. LP processed the data. LP, MB, and HH analyzed and interpreted the results and wrote the manuscript. TP, SdO, JL, and JR contributed to discussion of results and writing the manuscript. All authors revised and approved the final manuscript.

FUNDING

This study was partly financially supported by the Estonian Ministry of Education and Research under institutional research financing IUT 19-2, by the higher education scholarship in the growth areas of smart specialization and by the Estonian Centre of Excellence in IT (EXCITE) 2014-2020.4.01.15-0018 funded by the European Regional Development Fund.

SUPPLEMENTARY MATERIAL

The Supplementary Material for this article can be found online at: https://www.frontiersin.org/articles/10.3389/fphys.2018.01350/full#supplementary-material

REFERENCES

Bae, Y., Yoo, B. W., Lee, J. C., and Kim, H. C. (2017). Automated network analysis to measure brain effective connectivity estimated from EEG data of patients with alcoholism. *Physiol. Meas.* 38, 759–773. doi: 10.1088/1361-6579/aa6b4c

Breakspear, M., and Terry, J. R. (2002). Detection and description of non-linear interdependence in normal multichannel human EEG data. *Clin. Neurophysiol.* 113, 735–753. doi: 10.1016/S1388-2457(02)00051-2

Dimitriadis, S. I., Salis, C., Tarnanas, I., and Linden, D. E. (2017). Topological filtering of dynamic functional brain networks unfolds informative chronnectomics: a novel data-driven thresholding scheme based on orthogonal minimal spanning trees (OMSTs). *Front. Neuroinform.* 11:28. doi: 10.3389/fninf.2017.00028

Dimitriadis, S. I., Zouridakis, G., Rezaie, R., Babajani-Feremi, A., and Papanicolaou, A. C. (2015). Functional connectivity changes detected with magnetoencephalography after mild traumatic brain injury. *NeuroImage Clin.* 9, 519–531. doi: 10.1016/j.nicl.2015.09.011

Esteller, R., Vachtsevanos, G., Echauz, J., and Litt, B. A. (2001). Comparison of waveform fractal dimension algorithms. *IEEE Trans. Circuits Syst. Fund. Theory Appl.* 48, 177–183. doi: 10.1109/81.904882

Higuchi, T. (1988). Approach to an irregular time series on the basis of the fractal theory. *Phys. D* 31, 277–283. doi: 10.1016/0167-2789(88)90081-4

Hornero, R., Abásolo, D., Escudero, J., and Gómez, C. (2009). Nonlinear analysis of electroencephalogram and magnetoencephalogram recordings in patients with Alzheimer's disease. *Philos. Trans. Math. Phys. Eng. Sci.* 367, 317–336. doi: 10.1098/rsta.2008.0197

Kalev, K., Bachmann, M., Orgo, L., Lass, J., and Hinrikus, H. (2015). "Lempel-Ziv and multiscale lempel-ziv complexity in depression," in *Conference Proceedins of the IEEE Engineering Medicine Biology Society* (New York, NY: IEEE), 4158–4161. doi: 10.1109/EMBC.2015.7319310

Katz, M. J. (1988). Fractals and the analysis of waveforms. *Comput. Biol. Med.* 18, 145–156. doi: 10.1016/0010-4825(88)90041-8

Lake, D. E., and Moorman, R. (2010). Accurate estimation of entropy in very short physiological time series: the problem of atrial fibrillation detection in implanted ventricular devices. *Am. J. Physiol. Heart Circ. Physiol.* 300:1. doi: 10.1152/ajpheart.00561

Lempel, A., and Ziv, J. (1976). On the complexity of finite sequences. *IEEE Trans. Inf. Theory* 22, 75–81. doi: 10.1109/TIT.1976.1055501

Montez, T., Linkenkaer-Hansen, K., van Dijk, B. W., and Stam, C. J. (2006). Synchronization likelihood with explicit time-frequency priors. *Neuroimage* 33, 1117–1125. doi: 10.1016/j.neuroimage.2006.06.066

Natarajan, K., Acharya, U. R., Alias, F., Tiboleng, T., and Puthusserypady, S. K. (2004). Nonlinear analysis of EEG signals at different mental states. *BioMedical Eng. Online* 3:7. doi: 10.1186/1475-925X-3-7

Olbrich, E., Achermann, P., and Meier, P. F. (2003). Dynamics of human sleep EEG. *Neurocomputing* 5, 857–862. doi: 10.1016/S0925-2312(02)00816-0

Olejarczyk, E., Marzetti, L., Pizzella, V., and Zappasodi, F. (2017). Comparison of connectivity analyses for resting state EEG data. *J. Neural Eng.* 14, 3. doi: 10.1088/1741-2552/aa6401

Orgo, L., Bachmann, M., Kalev, K., Järvelaid, M., Raik, J., and Hinrikus, H. (2017). Dependence of the EEG nonlinear coupling on the frequency bands and the segment lengths. *IFMBE Proc.* 65, 799–802. doi: 10.1007/978-981-10-5122-7_200

Prichard, D., and Theiler, J. (1994). Generating surrogate data for time series with several simultaneously measured variables. *Phys. Rev. Lett.* 73, 951–954. doi: 10.1103/PhysRevLett.73.951

Richman, J. S., and Moorman, J. R. (2000). Physiological time-series analysis using approximate entropy and sample entropy. *Am. J. Physiol. Heart Circ. Physiol.* 278, H2039–H2049. doi: 10.1152/ajpheart.2000.278.6.H2039

Rodríguez-Bermudez, G., and García Laencin, P. J. (2015). Analysis of EEG signals using nonlinear dynamics and chaos: a review. *Appl. Math. Inf. Sci.* 9, 1–13. doi: 10.12785/amis/090512

Small, M., and Tse, C. K. (2002). Applying the method of surrogate data to cyclic time series. *Phys. D* 164, 187–201. doi: 10.1016/S0167-2789(02)00382-2

Small, M., Yu, D., and Harrison, R. G. (2001). Surrogate test for pseudoperiodic time series data. *Phys. Rev. Lett.* 87:18. doi: 10.1103/PhysRevLett.87.188101

Spasic, S. (2010). Surrogate data test for nonlinearity of the rat cerebellar electrocorticogram in the model of brain injury. *Sig. Process.* 90, 3015–3025. doi: 10.1016/j.sigpro.2010.04.005

Stam, C. J., Pijn, J. P. M., and Pritchard, W. S. (1998). Reliable detection of nonlinearity in experimental time series with strong periodic components. *Phys. D* 112, 361–380. doi: 10.1016/S0167-2789(97)00183-8

Stam, C. J., and Van Dijk, B. W. (2002). Synchronization likelihood: an unbiased measure of generalized synchronization in multivariate data sets. *Phys. D* 163, 236–251. doi: 10.1016/S0167-2789(01)00386-4

Sun, J., Hong, X., and Tong, S. (2012). Phase synchronization analysis of eeg signals: an evaluation based on surrogate tests. *IEEE Trans. Biomed. Eng.* 59, 2254–2263. doi: 10.1109/TBME.2012.2199490

Takens, F. (1981). "Detecting strange attractors in turbulence," in *Lecture Notes in Mathematics*, eds D. A. Rand and L. -S. Young (Berlin: Springer), 366–381. doi: 10.1007/BFb0091924

Theiler, J., Eubank, S., Longtin, A., Galdrikian, B., and Farmer, J. D. (1992). Testing for nonlinearity in time series: the method of surrogate data. *Phys. D* 58, 77–94. doi: 10.1016/0167-2789(92)90102-S

Thornhill, N. F. (2005). Finding the source of nonlinearity in a process with plant-wide oscillation. *IEEE Trans. Control Syst. Technol.* 13, 434–443. doi: 10.1109/TCST.2004.839570

Timmer, J. (1998). Power of surrogate data testing with respect to nonstationarity. *Phys. Rev. E.* 58, 5153–5156. doi: 10.1103/PhysRevE.58.5153

Yao, D. (2001). A method to standardize a reference of scalp EEG recordings to a point at infinity. *Physiol. Meas.* 22, 693–711. doi: 10.1088/0967-3334/22/4/305

Conflict of Interest Statement: The authors declare that the research was conducted in the absence of any commercial or financial relationships that could be construed as a potential conflict of interest.

Curriculum vitae

Personal Information

Name:	Laura Päeske (Orgo)
Date of birth:	17.10.1990
Place of birth:	Viljandi, Estonia
Citizenship:	Estonian
E-mail:	laura.paeske@taltech.ee

Professional employment

03.2019–...	Tallinn University of Technology, Parental leave *School of Information Technologies, Department of Health Technologies*
03.2019–...	Proekspert, Parental leave
10.2018–03.2019	Proekspert, Data Scientist
09.2016–03.2019	Tallinn University of Technology, Early Stage Researcher *School of Information Technologies, Department of Health Technologies*
01.2016–03.2016	University of Bergen, Intern *Department of Biological and Medical Psychology, Bergen fMRI Group*
06.2013–08.2015	Tallinn University of Technology, Project assistant *Technomedicum, Department of Biomedical Engineering*

Education

2016–...	Tallinn University of Technology, PhD *School of Science, Engineering Physics, Biomedical Engineering and Medical Physics* *Representative of Doctoral Students at the Council of the Department of Health Technologies. Member of the Council of Biomedical Engineering and Medical Physics Master's Program.*
2014–2016	Tallinn University of Technology, MSc cum laude *Faculty of Science, Biomedical Engineering and Medical Physics*
2010–2014	Tallinn University of Technology, BSc cum laude *Faculty of Science, Engineering Physics*
1998–2010	Viljandi Carl Robert Jakobson Gymnasium, silver medal *Specialization in mathematics and physics*

Honours & awards

2010–2017	Scholarships ◦ Smart specialisation scholarship for PhD students (2017) ◦ Rotalia Foundation scholarship (2015) ◦ Scholarship in memory of Ole Golubjatnikov (2015) ◦ Scholarship for success at the five-school competition. Funded by Nortal, Skype and Viru Keemia Grupp (2010)
2016	Diploma of Estonian National Contest for University Students

Supervised theses

- Erki Arusoo, Master's Degree, 2020, (sup) Laura Päeske, Uljana Reinsalu. Describing artificial neural networks with small-worldness. Tallinn University of Technology, School of Information Technologies, Department of Health Technologies.
- Tuuli Uudeberg, Master's Degree, 2019, (sup) Laura Päeske, Maie Bachmann. Correlation Between the Spectral Asymmetry Index of the Electroencephalographic Signal and Depression: a Preliminary Study. Tallinn University of Technology, School of Information Technologies, Department of Health Technologies.
- Silver Savi, Master's Degree, 2017, (sup) Laura Päeske, Maie Bachmann. The Study of Correlation Between Heart Rate and Electroencephalographic Spectral Asymmetry Index Measured During Viewing of Affective Pictures. Tallinn University of Technology School of Information Technologies, Department of Health Technologies.

Elulookirjeldus

Isiklik informatsioon

Nimi:	Laura Päeske (Orgo)
Sünniaeg:	17.10.1990
Sünnikoht:	Viljandi, Eesti
Kodakondsus:	Eestlane
E-mail:	laura.paeske@taltech.ee

Teenistuskäik

03.2019–...	Tallinna Tehnikaülikool, Lapsehoolduspuhkus *Infotehnoloogia teaduskond, Tervisetehnoloogiate instituut*
03.2019–...	Proekspert, Lapsehoolduspuhkus
10.2018–03.2019	Proekspert, Andmeteadlane
09.2016–03.2019	Tallinna Tehnikaülikool, Nooremteadur *Infotehnoloogia teaduskond, Tervisetehnoloogiate instituut*
01.2016–03.2016	Bergeni Ülikool, Praktikant *Bioloogilise ja meditsiinilise psühholoogia instituut, Bergen fMRI Group*
06.2013–08.2015	Tallinna Tehnikaülikool, Projekti assistent *Tehnomeedikum, Biomeditsiinitehnika keskus*

Hariduskäik

2016–...	Tallinna Tehnikaülikool, PhD *Loodusteaduskond, Tehniline füüsika, Biomeditsiinitehnoloogia* *Doktorantide esindaja TalTech Tervisetehnoloogiate instituudi nõukogus. TalTech biomeditsiinitehnika ja meditsiinifüüsika magistrikava programminõukoja liige.*
2014–2016	Tallinna Tehnikaülikool, MSc cum laude *Matemaatika-loodusteaduskond, Biomeditsiinitehnika ja meditsiinifüüsika*
2010–2014	Tallinna Tehnikaülikool, BSc cum laude *Matemaatika-loodusteaduskond, Tehniline füüsika*
1998–2010	Carl Robert Jakobsoni Gümnaasium, hõbemedal *Matemaatika-füüsika süvaklass*

Tunnustused

2010–2017	Stipendiumid ◦ Nutika spetsialiseerumise erialastipendium (2017) ◦ Rotalia Foundation stipendium (2015) ◦ Ole Golubjatnikovi mälestusstipendium (2015) ◦ Viie kooli võistlusel reaalainetes edukalt esinenud õpilaste stipendium. Rahastajad Nortal, Skype ja Viru Keemia Grupp (2010).
2016	Üliõpilaste teadustööde riikliku konkursi diplom

Juhendatud magistritööd

- Erki Arusoo, magistrikraad, 2020, (juh) Laura Päeske, Uljana Reinsalu. Tehisnärvivõrkude kirjeldamine väikese maailma omaduse abil. Tallinna Tehnikaülikool, Infotehnoloogia teaduskond, Tervisetehnoloogiate instituut.
- Tuuli Uudeberg, magistrikraad, 2019, (juh) Laura Päeske, Maie Bachmann. Elektroentsefalograafilise signaali spektraalse asümmeetria indeksi ja depressiooni korrelatsioon: eeluuring. Tallinna Tehnikaülikool, Infotehnoloogia teaduskond, Tervisetehnoloogiate instituut.
- Silver Savi, magistrikraad, 2017, (juh) Laura Päeske, Maie Bachmann. Emotsionaalsete piltide vaatamisel mõõdetud südame löögisageduse ja elektroentsefalograafilise spektraalse asümmeetria indeksi vahelise korrelatsiooni uurimine. Tallinna Tehnikaülikool, Infotehnoloogia teaduskond, Tervisetehnoloogiate instituut.

ISSN 2585-6901 (PDF)
ISBN 978-9949-83-677-2 (PDF)